

Anna Regoutz

# **Evaluation of Decapsulation Methods for Semiconductor Devices**

## **MASTER THESIS**

zur Erlangung des akademischen Grades einer Diplom-Ingenieurin  
der Studienrichtung Technische Chemie  
erreicht an der

Technischen Universität Graz

in Zusammenarbeit mit Infineon Technologies Austria AG

Ao.Univ.-Prof. Dipl.-Ing. Dr.techn. tit.Univ.-Prof. Ernst Lankmayr  
Institut für Analytische Chemie und Lebensmittelchemie  
Technische Universität Graz  
2010



## STATUTORY DECLARATION

I declare that I have authored this thesis independently, that I have not used other than the declared sources / resources, and that I have explicitly marked all material which has been quoted either literally or by content from the used sources.

.....  
date

.....  
Anna Regoutz

# Acknowledgements

I greatly appreciate the guidance of my advisers Ao.Univ.-Prof. Dipl.-Ing. Dr.techn. tit.Univ.-Prof. Ernst Lankmayr of the Institute of Analytical Chemistry and Food Chemistry at the Graz University of Technology and Dr. Josef Maynollo at Infineon Technologies Austria AG in Villach through the entire process of completing this thesis. I want to thank my managers at Infineon Technologies Dipl.-Ing. Harald Kowald, Dipl.-Ing. (FH) Oliver Ayoub, and Dipl.-Ing. Josef Moser for making this project possible.

Thanks to the staff members of the Internal Physical Inspection Group at the Failure Analysis Department for making my time there entertaining and interesting. Every single one of them had a part in this thesis, but I want to state special thanks to Michael for helping me with graphic issues, to Ferdinand for his inspiring ideas and critical input, and to Mario for helping with the experimental work. I wish to thank the other staff of the Failure Analysis Department as well.

I'm also thankful for the support of the staff at the Institute of Analytical Chemistry and Food Chemistry.

Finally I wish to express my gratitude to my friends and family for their support and encouragement during my years of education and this master thesis. Especially my parents, without whom this thesis would not exist in various respects.

Anna Regoutz  
Graz, June 2010

# Abstract

During failure analysis of semiconductor devices inorganic acids are used to remove or open the polymer package covering the electronic circuit. However these methods can cause damage of the metallic components of the device. The purpose of this work is the evaluation of methods which do not employ inorganic acids, but are based on organic solvents and reagents and thereby preparation artefacts should be avoided. A systematic study of potentially suitable solvent systems based on semi empirical considerations is included.

**Keywords:** semiconductor, failure analysis, decapsulation, solubility, solvolysis, hydrogenolysis, subcritical solvents, aminolysis, mould compound

# Kurzfassung

Während der Fehleranalyse von Halbleiterbauelementen werden anorganische Säuren zum Entfernen oder Öffnen des Polymergehäuses, welches die elektronische Schaltung umschließt, verwendet. Diese Methoden können Beschädigung an den metallischen Komponenten des Bauelementes verursachen. Der Zweck der vorliegenden Arbeit ist die Evaluierung von Methoden, die keine anorganischen Säuren verwenden, sondern auf organischen Lösungsmitteln und Reagenzien basieren, wodurch Präparationsartefakte vermieden werden sollen. Eine systematische Studie von potentiellen Lösungsmittelsystemen basierend auf semiempirischen Betrachtungen wurde durchgeführt.

**Stichwörter:** Halbleiter, Fehleranalyse, Dekapsulierung, Löslichkeit, Solvolyse, Hydrogenolyse, Subkritische Lösungsmittel, Aminolyse, Pressmasse

# Contents

<b>Acknowledgements</b>	<b>iii</b>
<b>Abstract</b>	<b>iv</b>
<b>List of Tables</b>	<b>viii</b>
<b>List of Figures</b>	<b>xi</b>
<b>1. Introduction</b>	<b>1</b>
1.1. Motivation . . . . .	1
1.2. Integrated Circuits and their Failure Analysis . . . . .	2
<b>2. Fundamental Considerations</b>	<b>4</b>
2.1. Decapsulation Methods in the Failure Analysis of Integrated Circuits	4
2.2. Moulding Compounds . . . . .	6
<b>3. Theoretical Approach</b>	<b>9</b>
3.1. Solvolysis . . . . .	9
3.1.1. Solubility Parameters . . . . .	9
3.1.1.1. Thermodynamics and the Hildebrand Solubility Parameter . . . . .	9
3.1.1.2. Molecular Interactions and the Hansen Solubility Parameters . . . . .	11
3.1.1.3. The Solubility of Polymers . . . . .	16
3.1.1.4. Comparison of Polymer and Solvent Solubilities . . . . .	17
3.1.2. Solvent Functionalities . . . . .	19
3.2. Transfer Hydrogenolysis and Aminolysis . . . . .	21
3.3. Sub- and Supercritical Solvents . . . . .	22
3.3.1. Catalysts for Sub- and Supercritical Water . . . . .	24
3.3.2. Supercritical Water Oxidation . . . . .	24
3.4. Glycolysis . . . . .	25
<b>4. Experimental Setup and Results</b>	<b>26</b>
4.1. Tool Setup . . . . .	26
4.1.1. Reflux Equipment . . . . .	26
4.1.2. High Pressure Asher . . . . .	27

4.1.3.	Pressure Vessel System . . . . .	28
4.1.3.1.	Estimation of Work Pressure in the Parr Pressure Vessel . . . . .	30
4.2.	Devices . . . . .	34
4.2.1.	Device Preparations . . . . .	36
4.2.1.1.	Laser Ablation . . . . .	37
4.2.1.2.	Manual Grinding . . . . .	37
4.2.1.3.	Parallel Polishing . . . . .	37
4.3.	Reaction Types . . . . .	38
4.3.1.	Solvolysis . . . . .	38
4.3.1.1.	Primary Solvent Screening . . . . .	38
4.3.1.2.	High Pressure Asher . . . . .	41
4.3.1.3.	Parr Pressure Vessel . . . . .	42
4.3.2.	Transfer Hydrogenolysis and Aminolysis . . . . .	47
4.3.2.1.	Primary Screening of the Hydrogen Donors . . . . .	47
4.3.2.2.	High Pressure Asher . . . . .	48
4.3.2.3.	Parr Pressure Vessel . . . . .	48
4.3.3.	Sub- and Supercritical Solvents . . . . .	53
4.3.3.1.	Parr Pressure Vessel . . . . .	53
4.3.4.	Glycolysis . . . . .	60
4.3.4.1.	Parr Pressure Vessel . . . . .	60
4.4.	Analytical Methods . . . . .	61
4.4.1.	Analysis of Devices . . . . .	61
4.4.1.1.	Optical Microscopy . . . . .	61
4.4.1.2.	Scanning Electron Microscopy . . . . .	61
4.4.1.3.	Focused Ion Beam . . . . .	61
4.4.1.4.	Scanning Acoustic Microscopy . . . . .	62
4.4.2.	Analysis of the Reaction Solutions . . . . .	62
4.4.2.1.	UV-Vis Spectroscopy . . . . .	62
4.4.2.2.	High Performance Liquid Chromatography . . . . .	64
4.4.2.3.	Gas Chromatography coupled with a Mass Spectroscopy Detector . . . . .	64
4.4.2.4.	Fourier Transformation Infrared Spectroscopy . . . . .	65
<b>5.</b>	<b>Case Studies</b>	<b>66</b>
5.1.	Devices with Bare Copper Metallisation and Soldered Top Die . . . . .	66
5.2.	Devices with Sputtered Bare Copper Metallisation . . . . .	70
5.3.	Next Generation Packages . . . . .	73
5.4.	Devices with Power Copper Metallisation . . . . .	76
<b>6.</b>	<b>Conclusion</b>	<b>82</b>
<b>A.</b>	<b>Appendix</b>	<b>84</b>

## *Contents*

<b>Glossary</b>	<b>96</b>
<b>Acronyms</b>	<b>98</b>
<b>List of Symbols</b>	<b>100</b>
<b>Bibliography</b>	<b>108</b>

# List of Tables

3.1.	Hansen solubility parameters for the solvents chosen for the primary screening series . . . . .	15
3.2.	Group molar contributions $F$ and internal energy $U$ compiled by Beer-bower [1] and the calculated partial HSPs of N,N-dimethyl-m-toluamide . . . . .	15
3.3.	HSPs for crosslinked epoxies published by Bellenger and Launay . . . . .	16
3.4.	Fractional HSPs $f_i$ for the used solvents and the epoxy data given in table 3.3 . . . . .	18
3.5.	Structures and functionalities of the selected solvents for the primary screening . . . . .	20
4.1.	Parameter settings for the experimental series using the HPA . . . . .	27
4.2.	Qualitative categories chosen to classify the results of all Parr pressure vessel series . . . . .	30
4.3.	Equations of state used to calculate the nitrogen pressure increase . . . . .	31
4.4.	Equations for the calculations or data of the parameters used in each equation of state . . . . .	32
4.5.	Estimated pressures using several equations of state in comparison to a pressure test result (estimated failure 1%) . . . . .	33
4.6.	Estimated pressure values for several solvents in use calculated using the Antoine equation . . . . .	34
4.7.	Package and mould compound information of the devices for the experimental series. . . . .	35
4.8.	Technology and application information of the devices for the experimental series. . . . .	36
4.9.	HPLC method information . . . . .	64
A.1.	Characteristics of the solvents for the primary screening . . . . .	84
A.2.	Characteristics of the hydrogen donors . . . . .	84
A.3.	Antoine constants (A,B,C) and their temperature range for different solvents in use (taken from the NIST Chemistry WebBook [2]) . . . . .	85

# List of Figures

1.1. General outline of a surface mounted device . . . . .	2
1.2. Detail of the surface area around a bond pad including important layers . . . . .	2
2.1. Structures of main epoxy resin groups . . . . .	7
3.1. $\delta_v$ - $\delta_h$ diagram for the selected solvents and various epoxy resins . . . . .	17
3.2. Ternary diagram for the chosen solvents and the available data for epoxy resins . . . . .	19
3.3. Proposed reaction mechanism for the hydrogenolytic degradation of an epoxy resin . . . . .	22
4.1. Final installation of the Parr pressure vessel with all accompanying parts . . . . .	28
4.2. Cross section of a Parr 4760 series pressure vessel showing the sealing system [3]. . . . .	29
4.3. Stereoscopic micrograph of the devices in use . . . . .	35
4.4. Reflected-light micrographs of the die after decapsulation with PYR using the reflux equipment. Both the aluminium metallisation and the polyimide layer are completely unharmed. . . . .	39
4.5. Reflected-light micrographs of the die after decapsulation with DMSO using the reflux equipment. Severe damage of the metallisation can be observed. . . . .	39
4.6. SEM micrographs of a device treated with DETA and a reference device . . . . .	40
4.7. Reflected-light micrographs of the die after decapsulation with BAL using the HPA. The aluminium metallisation is in perfect condition and the polyimide has been removed. . . . .	41
4.8. Effects Pareto charts for the HPA solvolysis series . . . . .	42
4.9. Comparison of the results of solvolysis runs at 473 and 523 K . . . . .	43
4.10. Reflected-light micrographs of a device decapsulated using BAL. . . . .	44
4.11. Reflected-light micrographs of an IC device decapsulated using PYR. The orange colour of the surface is caused by the polyimide. Some mould compound residues are present. . . . .	45
4.12. Results of the DETA combination runs at 523 K . . . . .	46



## List of Figures

4.13. Reflected-light micrographs of a device after preparation with DETA-NMP. The metallisation is in perfect shape and the polyimide is already partially removed and has no adhesion to the underlying metal any more. . . . .	47
4.14. Effects Pareto charts for the HPA hydrogenolysis and aminolysis series	48
4.15. Results of the transfer hydrogenolysis and aminolysis combination runs at 523 K . . . . .	49
4.16. Reflected-light micrographs of a device decapsulated with pure IND. The polyimide shows a giraffe like structures, which is due to temperature caused tightening. . . . .	50
4.17. Reflected-light micrographs of a device decapsulated with TET in combination with EA. Attack of the aluminium metallisation is visible.	50
4.18. Reflected-light micrographs of devices decapsulated with a mixture of TET and ANI. The metallisation is in perfect shape and only little mould compound residues can be seen. . . . .	51
4.19. Results of the indoline combination runs at 523 K . . . . .	52
4.20. Reflected-light micrographs after preparation with IND-DMF or IND-DETA/DMF. . . . .	53
4.21. Results of the subcritical water runs in combination with salt or hydrogen peroxide at 523 K (except for one H <sub>2</sub> O run at 623 K) . . . . .	54
4.22. Reflected-light micrographs of a device decapsulated with a mixture of deionised water with 1 w% Na <sub>2</sub> CO <sub>3</sub> . . . . .	55
4.23. Reflected-light micrographs of a decapsulated device using deionised water with 10 w% hydrogen peroxide. . . . .	56
4.24. Results of the subcritical water runs in combination with other solvents/reagents at 523 K (except for H <sub>2</sub> O+IND at 473 K) . . . . .	57
4.25. Reflected-light micrographs of a device decapsulated using a mixture of deionised water and BAL. The polyimide remained on the die surface.	58
4.26. Reflected-light micrographs of two devices decapsulated with a mixture of deionised water and indoline at 473 K. . . . .	58
4.27. Results of the subcritical methanol runs in combination with other solvents/reagents at 523 K . . . . .	59
4.28. Reflected-light micrograph of a device decapsulated using a mixture of MeOH and DETA. The polyimide layer remained on the die surface.	60
4.29. UV-Vis spectra of a HPA DETA sample and a pure solvent reference	63
4.30. UV-Vis spectra of a HPA MOE sample and a pure solvent reference .	63
5.1. Package Outline of a PG-TO220-3-1 . . . . .	67
5.2. Bare copper devices after preparation prior to solvolysis experiment using N-diethyl-m-toluamide . . . . .	68
5.3. SEM micrographs of the copper metallisation at the base die . . . . .	69
5.4. EDX result at the copper metallisation of the base die (excitation energy: 2 kV). The carbon peak results from organic contaminations.	69

## List of Figures

5.5. Comparison of decapsulated dies using two different methods, namely laser ablation combined with wet chemical etch and solvolysis . . . .	70
5.6. Reflected-light micrographs of the die surface after solvolysis treatment with DETA-NMP . . . . .	71
5.7. Surface at the gate pad area of a SFET5 device after decapsulation with DETA-NMP . . . . .	72
5.8. Scanning electron micrographs of a non-moulded reference device before temperature storage . . . . .	72
5.9. Scanning electron micrographs of the gate pad on non-moulded devices after HTS . . . . .	73
5.10. Schematic cross section of a next generation package . . . . .	74
5.11. Stereo micrographs of different stages of NGP preparation . . . . .	75
5.12. Reflected-light micrograph of a SMART6 die decapsulated using ANI (A... electrically stressed DMOS, B... unstressed DMOS, C... logic part) . . . . .	76
5.13. Reflected light micrographs of decapsulated devices using different methods . . . . .	77
5.14. Scanning acoustic micrographs of partly stressed SMART6 devices (mirrored images). . . . .	77
5.15. Stereoscopic micrograph of a partly stressed device after parallel grinding. . . . .	78
5.16. Reflected light micrograph of a SMART6 device after preparation with ANI . . . . .	78
5.17. SEM micrographs of a SMART6 device after preparation with ANI .	79
5.18. Micrographs showing the FIB cutting positions on the stressed transistor of a SMART6 device . . . . .	80
5.19. FIB cuts . . . . .	81
A.1. Workflow of the Parr pressure vessel series . . . . .	86
A.2. HPLC chromatogram of HPA run R3 using 9,10-dihydroanthracene .	87
A.3. HPLC chromatogram of HPA run R3 using indoline . . . . .	87
A.4. HPLC chromatogram of HPA run R3 using tetralin . . . . .	88
A.5. HPLC chromatogram of HPA run R3 using a mixture of tetralin and ethanolamine (1:1 v/v, upper phase) . . . . .	88
A.6. HPLC chromatogram of HPA run R5 using aniline . . . . .	89
A.7. HPLC chromatogram of HPA run R5 using benzyl alcohol . . . . .	89
A.8. HPLC chromatogram of HPA run R5 using N,N-diethyl-m-toluamide	90
A.9. HPLC chromatogram of HPA run R5 using 2-methoxyethanol . . . .	90
A.10. HPLC chromatogram of HPA run R5 using 2-pyrrolidone . . . . .	91
A.11. Background of the wafer used as substrate for the FT-IR analysis . .	91

# 1. Introduction

“Thermosetting plastics are the group that causes the greatest problem to the failure analyst.”

Mike Jacques, 1979

## 1.1. Motivation

Before starting this master thesis I already worked at Infineon Technologies Austria AG in Villach for four years as an industrial student. Out of my engagement in failure analysis the idea for this work originated. I already encountered the difficulties of wet chemical decapsulation of semiconductor devices during the standard failure analysis process. For the failure analysis of semiconductor devices it is vital that no artefacts are generated during the decapsulation process to assess failures properly. This was not guaranteed with the methods used before, which involved pure inorganic acids like sulphuric and nitric acid at high concentrations (see section 2.1 for further explanation).

The goal of this work should be to formulate a method, which does not employ inorganic acids, and therefore to avoid any artefacts and damages on the semiconductor devices. Furthermore following requirements should be fulfilled:

- suitable for routine failure analysis
- applicability to all common moulding compounds and package types
- reaction temperature  $\leq 473$  K (maximum acceptable change of device properties)
- least possible mechanical forces on the devices
- safe and non toxic reaction environment
- little preparative effort

## 1.2. Integrated Circuits and their Failure Analysis

An integrated circuit (IC) is a very small electronic circuit manufactured most commonly on a thin silicon wafer. Today the most common packaging for ICs are surface mounted polymer packages, like the basic example in figure 1.1. The schematic layout shows important components of a semiconductor device (for further explanation of the components see the glossary).

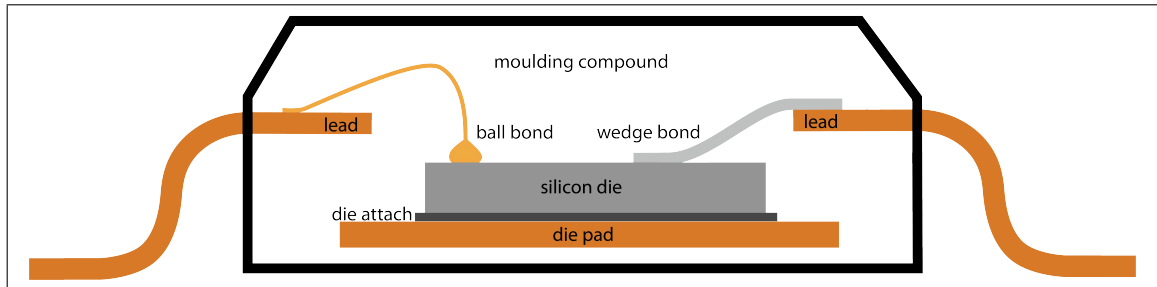


Figure 1.1.: General outline of a surface mounted device

Figure 1.2 shows a more detailed sketch of a bond connection on an IC surface. It shows all structural elements, which are important during the decapsulation of a package.

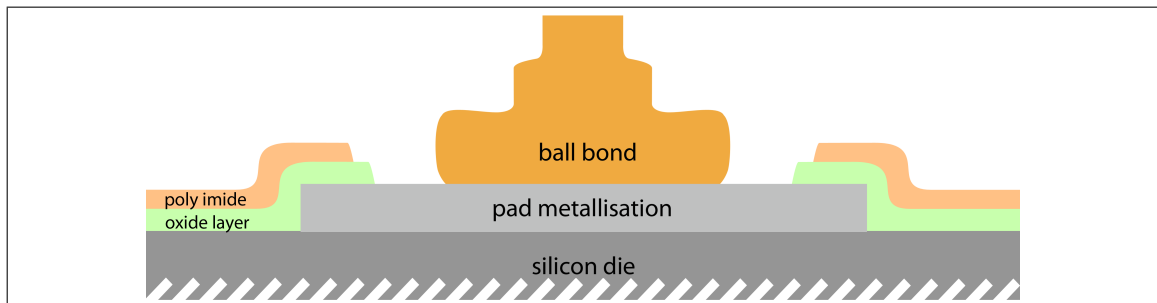


Figure 1.2.: Detail of the surface area around a bond pad including important layers

Failure analysis (FA) of integrated circuits became a vital part for semiconductor manufacturing. It is important during the design of new products, production support, product qualification, and customer returns. The goal of failure analysis is to localise and characterise the failure (electrical FA) and to detect the underlying defect (physical FA). The performed analysis flow depends on the given problem and can range from simple to very complicated and complex setups. Several different techniques are involved, like x-ray, scanning acoustic microscopy, optical and

## *1. Introduction*

electron microscopy, electrical measurements, and chemical preparations.

Modern failure analysis is changing very quickly due to the rapid changes in the technologies in use and the overall complexity of the devices. Today the demands towards the used methods are at a very high level.

During failure analysis of semiconductor devices an important step is the removal of the polymer package surrounding the components, i.e. package decapsulation or simply decapsulation. This preparation step is necessary in order to be able to perform optical or electron microscopy, or FIB cross sections at the die surface. Different techniques are used to remove or partially open the package to inspect the surface of the die, the wires, or the lead frame. Until present the most widespread preparation techniques are laser decapsulation and wet chemical etching.

The next chapter will take a look at existing decapsulation methods, their characteristics, and limitations.

## 2. Fundamental Considerations

### 2.1. Decapsulation Methods in the Failure Analysis of Integrated Circuits

The first decapsulation methods in use during failure analysis were mechanical processes, e.g. "milling or cracking open" [4], which often led to severe damage of the electronic device and therefore are no longer used today. They were replaced by chemical methods involving inorganic acids, sometimes coupled with laser ablation beforehand.

Laser ablation is a quite new process, which is by now used in the standard analysis flow of the FA Villach. The mould compound can be removed to a certain extent by this method (approximately 50-100  $\mu\text{m}$  above the die), but further removal is not possible, because the laser will cause damage to the surface of the die. Several work groups did research on such laser techniques, their problems, and possible improvements [5–10]. Laser ablation is used as the first preparation step during package opening, but is then followed by manual wet chemical removal, where damages can not be completely excluded. Advantages of the engagement of laser techniques are the possibility to decapsulate very small packages, a uniform abrasion, a clearly defined opening cavity, and reduction of preparation time. Although it has many positive characteristics, laser ablation of the mould compound is not always possible, as some resin blends tend to char, and it becomes more difficult to remove or swell the epoxide with chemical decapsulation methods afterwards. Another fact that complicates the wet chemical etching after laser ablation is that the wires mask the underlying mould compound, which can only be removed when etch times are increased. This leads to over etching and artefacts of the metallisation.

The next step in standard FA decapsulation is manual chemical wet etching. Mainly fuming nitric acid ( $\text{HNO}_3$ ) or 98% sulfuric acid ( $\text{H}_2\text{SO}_4$ ) and mixtures of these are used. The first methods caused major destruction and were often not repeatable [11–15]. For aluminium and gold metallisations pure fuming nitric acid was used, because both metallisations are stable against the attack of this acid, and

## 2. Fundamental Considerations

the acid is capable of removing the highly crosslinked epoxy resin very easily and rather fast. The method encountered several limits, when copper became popular as metall part of the devices (metallisation, wires, lead frame).  $\text{HNO}_3$  attacks copper and  $\text{H}_2\text{SO}_4$  had to be added to the etching mixture. This gave way for a new problem, because aluminium is attacked by sulfuric acid, and even with low concentrations discolorations are inevitable. This is the reason why during the last years, these methods were improved at Infineon Technologies as to temperature reduction, variation of composition, water content of the acids, and general handling during preparation. This reduced the number and severity of the artefacts, but still several limitations and problems exist. Copper is favoured over gold or aluminium, and in more and more technologies it replaces aluminium as well as gold, because of several positive characteristics: it has a lower electrical resistance, a higher mechanical strength, a high thermal conductivity, and has an important economic advantage. Also mono metallic connections between copper wires and pads are possible. This is advantageous because problems resulting from the formation of intermetallic phases, for example between gold and aluminium, are avoided. For this reasons copper will become an inevitable part of ICs and acids are not the best choice as decapsulation reagents.

Automatic etching tools (like Nisene Jet Etch) were invented, which are able to control temperature, mix ratio, and pressure of the used acids [16]. They use rubber or polytetrafluoroethylene (PTFE) gaskets to specify the area and size of opening of the device, but widening of the recess can not be completely avoided. Furthermore this method needs manual wet etching afterwards to obtain a satisfactory result and avoid over etching of the metallic components.

Another new approach to the problem are dry etching techniques, where a plasma (mostly  $\text{O}_2/\text{CF}_4$ ) is used to remove the resin. Their advantage is the high selectivity to metals, but they are not used for standard analysis due to high expenditure of time, problems in removing filler particles, and not completely developed systems [4, 17, 18]. The main and most problematic disadvantage is the lack of selectivity to dielectrics.

All possible methods are facing one main problem, which is a lack of selectivity towards a fraction of vital components of the device. Very often copper is attacked and as an increasing number of new technologies employs copper as part of the metallisation, the wires, and other components of the device, the urge to develop a new decapsulation technique increases rapidly.

## 2.2. Moulding Compounds

Today semiconductor circuits are encapsulated in so-called moulding compounds, which replaced ceramic and metallic packages. They consist of a highly cross-linked thermoset, where epoxy resins are most common to use, filler materials, and several different additives. These polymer packages are cost-effective, easily handled during manufacturing, and very robust. Their task is to protect the integrated circuit from environmental influences and mechanical stress, enhance the reliability, and provide easy handling for the customer.

The exact composition of the mould compound blends is kept secret by the supplier and varies enormously between different blends, although mostly the same basic polymer systems are used. The main suppliers for moulding compounds in case of Infineon Technologies are Shin Etsu, Hitachi, Sumitomo, Nitto, Henkel, and KCC. The mould compounds are supplied as pellets, already containing all components, which makes analysis a challenge due to the intricacy of the mixture. Even to analyse the polymer itself is very difficult due to the complexity of the repeating units (oligomers), the multitude of possible co-monomers, the number and type of initiators, the variety of polymer reactions, and their insolubility and inhomogeneity [19]. For this reasons the following information is only a rough guideline.

Besides the actual resin (including hardener), which only accounts for 10 - 20 weight per cent, several other components are integrated in the moulding compounds. The largest part (between 80 and 90 weight per cent) are fillers, which are mainly fused silica ( $\text{SiO}_2$ ) particles. The filler decreases the thermal expansion coefficient of the epoxy resin, reduces the costs, and can improve the abrasion resistance of the device [19]. Various additives account for under 5 weight per cent of the compound. They include:

- catalyst:  
in some cases needed for initiation of the polyaddition between base-resin and hardener, e.g. substituted triphenylphosphines
- flame retardants:  
e.g. low phosphorous compounds, polyphosphazenes or bismut compounds
- adhesion promoters:  
improve adhesion of the epoxide to metals, e.g. silanes
- wax/releasing agent:  
act as mould release agents, e.g. carnauba wax, polyethylene wax



## 2. Fundamental Considerations

- stress modifier/flexibiliser:  
relieving internal stress of the package, e.g. epoxidised vegetable oils
- carbon black:  
colouring and dissipation of electrostatic charges of the package

In general the epoxy resins are synthesized from oligomeric, end-functional epoxides, and multifunctional curing agents/hardeners under catalytic conditions. The most commonly used epoxy resins for mould compounds can be classified according to the type of oligomer, structures see figure 2.1:

- BER: Biphenyl Epoxy Resin
- DCPD: Dicyclopentadienyl Resin
- ECN/OCN: Epoxy Cresole Novolak / Ortho Cresole Novolak
- EPN: Epoxy Phenol Novolak and its modifications  
(MAR: Multiaromatic Resin, LMW: Low Molecular Weight Resin, MFR: Multi Functional Resin)

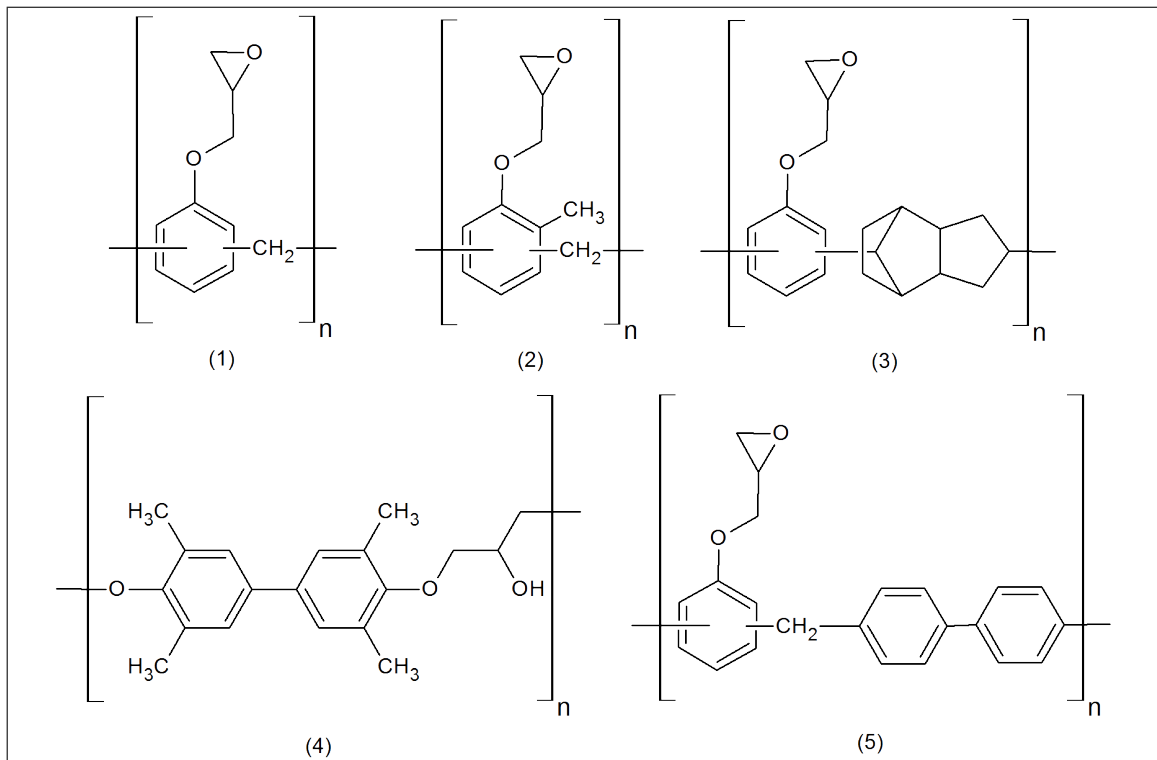


Figure 2.1.: Structures of main epoxy resin groups. (1) Epoxy Phenol Novolak (2) Ortho Cresole Novolak (3) Dicyclopentadienyl Resin (4) Biphenyl Epoxy Resin (5) Low Molecular Weight Resin

## 2. Fundamental Considerations

The curing reactions typically consist of two steps, of which the first is always the opening of the epoxide ring. The second step can be the homopolymerisation with another epoxy oligomer or the addition of another species. The curing agents used to gain high crosslinking densities can be basic (e.g. Lewis bases, inorganic bases, primary or secondary amines/amides) or acidic (e.g. carboxylic acid anhydrides, polybasic organic acids, phenols, Lewis acids) [19]. They can also be divided due to the sort of interaction they provide. There are catalytically functioning ones that promote reactions between epoxy groups or real coupling agents, which have two different functionalities at opposite ends and are build in the polymer network. The quality of the coupling agents depends on their molecular weight, the multifunctionality, and the degree in which they are able to form covalent bonds to the epoxy oligomers [19].

The properties of the cured epoxy resins do not only depend on the type of resin and curing agent (hardener), but also on the exact amounts employed (which affects the crosslinking density), the temperature and time of cure (which is important for the degree of curing), the curing mechanism (depending on the kind of functional groups of the used hardeners), the crosslinking density (depending on the amount of functional groups in both resin and hardeners), and the type of bridges/bonds between the functional groups of resin/hardener [20, 21].

It is possible to synthesize tailor-made epoxy polymers to fit nearly every requirement. Epoxy resins in general have perfect properties for use as mould compounds. They can be cured over a wide temperature range with varying speed, have a low shrinkage during cure, excellent chemical and corrosion resistance, good electrical insulation, and good mechanical properties [19, 21].

## 3. Theoretical Approach

### 3.1. Solvolysis

The first approach to the given problem was to select solvents, which are potentially capable of dissolving or swelling the moulding compound, which covers the die and other components of the semiconductor device. The goal was to establish a certain number of different solvents for the primary screening. Besides practical considerations, like stability and boiling point, two main criteria were used in order to achieve a great variety and different solvent features, namely the Hansen solubility parameters and the functional groups of the solvents.

#### 3.1.1. Solubility Parameters

##### 3.1.1.1. Thermodynamics and the Hildebrand Solubility Parameter

To understand the concept of solubility parameters one has to start with the thermodynamic considerations, which are basic to that concept. The cohesion energy is defined as the negative molar internal energy  $U$ . This energy term is associated with the work required to separate a condensed phase into its constituents or, equivalently, the amount by which the energy of the condensed state is lower than that of the isolated constituents.

The cohesive effect in a condensed phase is represented by the so called cohesive energy density  $ced$ , defined by equation 3.1.

$$ced = -\frac{U}{V_m} \quad (3.1)$$

where  $U$  = molar internal energy and  $V_m$  = molar volume.

### 3. Theoretical Approach

This was the basis of the original definition of the first solubility parameter, which was defined by Hildebrand as the square root of the *ced* (see equation 3.2). This origin of solubility parameters explains why they are also called cohesion parameters, especially in case of solids. The molar internal energy  $U$  can be exchanged with the molar vaporisation energy  ${}_l\Delta_g U$  (sometimes also expressed in terms of the enthalpy of vaporisation  ${}_l\Delta_g H$ ). This approach to solubility behaviour is applicable, as the same intermolecular forces have to be overcome to vaporise or to dissolve a substance.

$$\delta = (ced)^{1/2} = \left[ -\frac{U}{V_m} \right]^{1/2} \approx \left[ \frac{{}_l\Delta_g U}{V_m} \right]^{1/2} = \left[ \frac{{}_l\Delta_g H - RT}{V_m} \right]^{1/2} \quad (3.2)$$

where  $\delta$  = solubility parameter,  $U$  = molar internal energy,  $V_m$  = molar volume,  ${}_l\Delta_g U$  = energy of vaporisation,  ${}_l\Delta_g H$  = enthalpy of vaporisation,  $R$  = universal gas constant, and  $T$  = temperature.

Solubility parameters are always given for a standard temperature of 298 K. The SI unit for all solubility parameters is  $\text{Pa}^{1/2}$ , but most common is the use of  $\text{MPa}^{1/2}$ . To understand why the solubility parameters have a pressure unit again thermodynamic considerations have to be taken into account.

The internal pressure  $\pi_p$  of a system is defined as

$$\pi_p = \left( \frac{\partial U}{\partial V_m} \right)_T \quad (3.3)$$

where  $U$  = molar internal energy,  $V_m$  = molar volume, and  $T$  = temperature.

There is obviously a connection between the internal pressure  $\pi_p$  and the before mentioned cohesive energy density *ced*. But the *ced* is the total molecular cohesion per volume (integral quantity), whereas  $\pi_p$  is a derivative of the internal energy (a differential quantity). Both terms are connected via equation 3.4.

$$\pi_p = w \cdot ced \quad (3.4)$$

where  $w$  = empirical parameter.

### 3. Theoretical Approach

Therefore the internal pressure  $\pi_p$  and the  $ced$  have the same unit, namely the Pascal in the SI-system. In the past the unit  $\text{cal}^{1/2} \text{ cm}^{-3/2}$  has often been used for solubility parameters. The conversion to SI units is  $1 \text{ cal}^{1/2} \text{ cm}^{-3/2} = 2,0455 \text{ MPa}^{1/2}$ .

#### 3.1.1.2. Molecular Interactions and the Hansen Solubility Parameters

The Hansen solubility parameters (HSPs) are often summed up into one main general statement: if  $\delta_{t,solvent} \cong \delta_{t,polymer}$  good solubility can be expected. As we will see this is a rather sketchy approach to this complex concept.

The traditional Hildebrand solubility parameter mentioned above disregards polar and specific interactions as hydrogen bonding. Hansen proposed that the solubility depends on the type of bonding between the material to be dissolved and the solvent and not only on the strength of these interactions. In 1967 [22] he stated that the cohesive energy  $U_{coh}$  is the sum of three different contributions namely the dispersive ( $U_d$ ), the polar ( $U_p$ ), and the hydrogen bonding ( $U_h$ ) energy (see equation 3.5).

$$-U_{coh} = -U_d - U_p - U_h \quad (3.5)$$

To understand this division in three different contributions one has to understand the types of molecular interactions.

Dispersion or London forces are induced dipole-induced dipole interactions between adjacent pairs of molecules and are the weakest intermolecular forces. They occur in all molecules whether they are polar or not. The origin of dispersion forces is that the electrons of a molecule polarise the electron clouds of adjacent molecules and induce a temporary dipole which has opposite polarity. The resulting attractive forces are symmetrical as each molecule interacts due to the same characteristic, namely the polarisability  $\alpha_i$ . A reasonable but rough approximation for the dispersion cohesive energy  $-U_d$  is the so called London formula given in equation 3.6.

$$-U_d = \frac{3\alpha_1\alpha_2}{2(4\pi\epsilon_0)^2 r^6} \frac{I_1 I_2}{I_1 + I_2} \quad (3.6)$$

### 3. Theoretical Approach

where  $\alpha_i$  = polarisability for each molecule,  $\varepsilon_0$  = vacuum permittivity [=  $8,854 \cdot 10^{-12} F/m$ ],  $r$  = separation distance between two interacting molecules, and  $I_i$  = ionisation potential for each molecule.

Polar interactions can be divided into orientation and induction effects. Therefore also the polar energy  $U_p$  is divided into two parts. Orientation effects result from dipole-dipole interactions which are also called Keesom interactions. They occur only between molecules which have permanent dipole moments. The resulting attractive forces are again symmetrical as each molecule interacts because of the same characteristic, namely the dipole moment  $\mu_i$ . A good approximation for the orientation energy  $-U_o$  is given in equation 3.7 which was stated by Keesom.

$$-U_o = \frac{2\mu_1^2\mu_2^2}{3(4\pi\varepsilon_0)^2k_BTr^6} \quad (3.7)$$

where  $\mu_i$  = permanent dipole moment for each molecule,  $\varepsilon_0$  = vacuum permittivity [=  $8,854 \cdot 10^{-12} F/m$ ],  $k_B$  = Boltzmann constant [=  $1,381 \cdot 10^{-23} J/K$ ],  $T$  = temperature, and  $r$  = separation distance between two interacting molecules.

The second contribution to the polar interactions are the dipole-induced dipole or Debye interactions. They occur between a molecule with permanent dipole and a neighbouring molecule, which can be polar or not. This interactions are unsymmetrical as different characteristics influence the interaction for each molecule. For the molecule with the permanent dipole it is its dipole moment  $\mu_i$  and for the other one its polarisability  $\alpha_i$ . A good approximation can be given by equation 3.8.

$$-U_i = \frac{\mu_1^2\alpha_2 + \mu_2^2\alpha_1}{(4\pi\varepsilon_0)^2r^6} \quad (3.8)$$

where  $\mu_i$  = dipole moment for each molecule,  $\alpha_i$  = polarisability for each molecule,  $\varepsilon_0$  = vacuum permittivity [=  $8,854 \cdot 10^{-12} F/m$ ], and  $r$  = separation distance between two interacting molecules.

Hydrogen bonding occurs between a hydrogen atom covalently bound to an electronegative atom like oxygen or nitrogen and a second electronegative atom. They

### 3. Theoretical Approach

can be described using the Lewis acid-base mechanism, but giving a formula as for the other interactions is impossible. To determine the hydrogen bond energy  $U_h$  experimental data is necessary to a great extent. Fundamental problems of Hansen solubility parameters are often closely connected to this bond type.

The respective energy terms of all intermolecular forces are used to calculate the Hansen solubility parameter of a substance. As  $-\frac{U}{V_m} = \delta^2$  (see equation 3.2), the total Hansen solubility parameter  $\delta_t$  is composed of three terms representing different bond types, as there are:  $\delta_d$  for dispersion bonds,  $\delta_p$  for polar bonds, and  $\delta_h$  for hydrogen bonds. The mathematical correlation between the different solubility parameters is given in equation 3.9.

$$\delta_t = \sqrt{\delta_d^2 + \delta_p^2 + \delta_h^2} \quad (3.9)$$

The three Hansen solubility parameters of a solute define a solubility sphere in the Hansen room, which has the three HSPs as axes and the scale on the axis of the dispersion parameter  $\delta_d$  is doubled to gain spherical volumes.  $R_1$  is the radius of the solute sphere of solubility. A solubility parameter distance  $R_{1,2}$  between a solvent and a solute can be calculated using equation 3.10. The factor "4", which is connected to the dispersion term, results from the doubling of the  $\delta_d$  scale in the Hansen room.

$$(R_{1,2})^2 = 4(\delta_{d_2} - \delta_{d_1})^2 + (\delta_{p_2} - \delta_{p_1})^2 + (\delta_{h_2} - \delta_{h_1})^2 \quad (3.10)$$

where index "2" indicates the HSP of the solvent, and index "1" indicates the HSP of the solute.

The distance  $R_{1,2}$  can be compared with the solubility radius  $R_1$  using equation 3.11, where the outcome is called the relative energy difference  $RED$ , which is a characteristic value often given when talking about HSP.  $RED < 1$  indicates high affinity,  $RED = 1$  is a boundary condition, and  $RED > 1$  means low or none affinity between the two materials in question.

### 3. Theoretical Approach

$$RED = \frac{R_{1,2}}{R_1} \quad (3.11)$$

The Hansen parameters are primarily used in polymer-solvent interactions. Before Hansen's approach, Hildebrand parameters were used, which can only give a qualitative information on the behaviour of polymers in solvents and got some severe limitations. Hansen's theory still has some constraints, but is a good tool for practical considerations. The reason is the possibility to predict the properties of a system using the properties of its components. No knowledge of the system properties is necessary.

Especially when it comes to smaller molecular species there can be major exceptions to Hansens theory. Although smaller solvents might not be in reach according to their solubility parameters, they can be able to dissolve a solute. Also mixing of non-solvents can lead to solvents. Fundamental problems are associated with the solubility parameter for hydrogen bonding  $\delta_h$ , because it is not capable of completely describing the present bond quality. It would be better to use separated parameters for Lewis acid and base interactions, but that would be way more complicated and not applicable for practical usage.

The Hansen solubility parameters of the selected solvents for the different bond types as well as the total Hansen solubility parameter are given in table 3.1. The given values can vary according to the methods used for their determination.



### 3. Theoretical Approach

Table 3.1.: Hansen solubility parameters (HSP) for the solvents chosen for the primary screening series ( $\delta_t$ : total HSP,  $\delta_d$ : dispersion bond HSP,  $\delta_p$ : polar bond HSP,  $\delta_h$ : hydrogen bond HSP)

Solvent	$\delta_d$ [MPa <sup>1/2</sup> ]	$\delta_p$ [MPa <sup>1/2</sup> ]	$\delta_h$ [MPa <sup>1/2</sup> ]	$\delta_t$ [MPa <sup>1/2</sup> ]
N,N-Dimethyl-m-formamide <sup>[23]</sup>	17,4	13,7	11,3	24,9
1,1,2-Trichloroethylene <sup>[1]</sup>	18,0	3,1	5,3	19,0
Chlorobenzene <sup>[23]</sup>	19,0	4,3	2,0	19,6
Aniline <sup>[1]</sup>	19,4	5,1	10,0	22,6
Tetrahydrofuran <sup>[24]</sup>	16,8	5,7	8,0	19,5
Dimethyl sulfoxide <sup>[24]</sup>	18,4	16,4	10,2	26,7
Benzyl alcohol <sup>[1]</sup>	18,4	6,3	13,7	23,8
2-Pyrrolidone <sup>[25]</sup>	19,5	17,4	11,3	28,5
2-Methoxyethanol <sup>[25]</sup>	16,2	9,2	16,4	24,8
N-Methyl-2-pyrrolidone <sup>[1]</sup>	18,0	12,3	7,2	23,0

As it was not possible to find any data on the HSPs of N,N-diethyl-m-toluamide (DETA), a rough estimation using the group contribution method and Beerbower data [1] was done. The HSPs were calculated using the three equations given below (equation 3.12). All data necessary for the calculations and the results for the partial HSPs are given in table 3.2. The total HSP for DETA was calculated using equation 3.9 and a  $\delta_t$  of 19,6 MPa<sup>1/2</sup> was obtained.

$$\delta_d = \frac{\sum F_d}{V_m} \quad \delta_p = \frac{(\sum F_p^2)^{1/2}}{V_m} \quad \delta_h = \left( \frac{\sum U_h}{V_m} \right)^{1/2} \quad (3.12)$$

Table 3.2.: Group molar contributions  $F$  and internal energy  $U$  compiled by Beerbower [1] and the calculated partial HSPs of N,N-dimethyl-m-toluamide

Group	Quantity	$F_d(= V_m \delta_d)$ [J <sup>1/2</sup> cm <sup>3/2</sup> mol <sup>-1</sup> ]	$F_p(= V_m \delta_p)$ [J <sup>1/2</sup> cm <sup>3/2</sup> mol <sup>-1</sup> ]	$U_h(= V_m \delta_h^2)$ [Jmol <sup>-1</sup> ]
CH <sub>3</sub>	3	419	0	0
CH <sub>2</sub>	2	270	0	0
-CON<	1	301	1229	4772
Phenyl<	1	1319	133	205
		$\delta_d = 17,8 \text{ MPa}^{1/2}$	$\delta_p = 6,4 \text{ MPa}^{1/2}$	$\delta_h = 5,1 \text{ MPa}^{1/2}$
$M=191,28 \text{ g/mol}, \rho=0,996 \text{ g/cm}^3, V_m=192,1 \text{ cm}^3\text{mol}^{-1}$				

### 3.1.1.3. The Solubility of Polymers

A general statement which gives the major problem in case of the solubility of polymers is, that the solubility decreases as the molecular mass of the solute increases. Certainly the structure and physical state of the polymers have major influence on the solubility as well. Hydrogen bonds (and in general all significant donor-acceptor interactions) have an exceptionally strong influence on the solubility. The solubility parameters are strictly applicable only to amorphous polymers. In case of epoxy resins, which are highly crystalline, no solubility but only swelling behaviour can be observed at room temperature. At elevated temperatures the solubility parameters are applicable as epoxy resins dissolve. The HSPs are estimated by using the swelling behaviour of the polymers (especially in case of cross-linked polymers). As mentioned above it is generally preferred to use the term cohesion parameter instead of solubility parameter whenever solids are concerned.

Little information can be found on the cohesion parameters of thermosets, especially crosslinked epoxy resins. Bellenger et al. [25] were one of the few to determine the parameters of amine-crosslinked aromatic epoxies by calculation using additive laws and elemental group contribution, and by an experimental approach. They postulated that the values for the total Hansen solubility parameters  $\delta_t$  range from 20 MPa<sup>1/2</sup> to 27 MPa<sup>1/2</sup>. In another publication a solubility parameter of 18,8 MPa<sup>1/2</sup> was given for an epoxy resin [20]. Launay et al. [26] investigated carbon fibre/epoxy composites and therefore calculated an HSP of 23,7 MPa<sup>1/2</sup> for the epoxy resin in use. These rough estimates were used to compare them with the Hansen parameters of the solvents (see table 3.3 for the estimated numbers).

Table 3.3.: HSPs for crosslinked epoxies published by Bellenger and Launay

	$\delta_h$	$\delta_p$	$\delta_d$	$\delta_t$
DGEBA-DDM <sub>e</sub> [25]	9,54	8,76	15,64	20,31
DGEBA-DDM [25]	9,39	10,11	17,36	22,18
TGAP-DDM <sub>e</sub> [25]	10,41	10,41	15,88	21,65
TGAP-ANI [25]	13,70	13,01	16,33	24,97
TGAP-DDM [25]	13,02	15,38	16,40	25,98
TGAP-DDS [25]	14,43	15,36	16,39	26,70
Launay et al. [26]	8,0	10,0	20,0	20,0

DGEBA... diglycidyl ether of bisphenol A, TGAP... triglycidyl derivative of amino phenol, DDM... diamino diphenyl methane, DDM<sub>e</sub>... tetraethyl derivate of DDM, DDS... diamino diphenyl sulfone, ANI... aniline

### 3.1.1.4. Comparison of Polymer and Solvent Solubilities

As it is difficult to compare possible solvents with polymers by using plain data various plots are used. As three dimensional graphs of all Hansen solubility parameters can be quite complicated, two dimensional plots are widely used. Several different types of polymer maps have been postulated as useful tools (see [1] for a summary). In the present thesis a two dimensional diagram according to Bagley and a ternary diagram for the selected solvents and the data for the epoxy resins given in table 3.3 were used.

Bagley merged the cohesion parameters for dispersive and polar interactions according to equation 3.13. The reason for this is, that the two interactions have often a close similarity, whereas the hydrogen bonding has a different effect.

$$\delta_v = \sqrt{(\delta_d^2 + \delta_p^2)} \quad (3.13)$$

The new parameter  $\delta_v$  was plotted against  $\delta_h$  in a two dimensional diagram shown in figure 3.1. The data given in tables 3.1 and 3.3 was used.

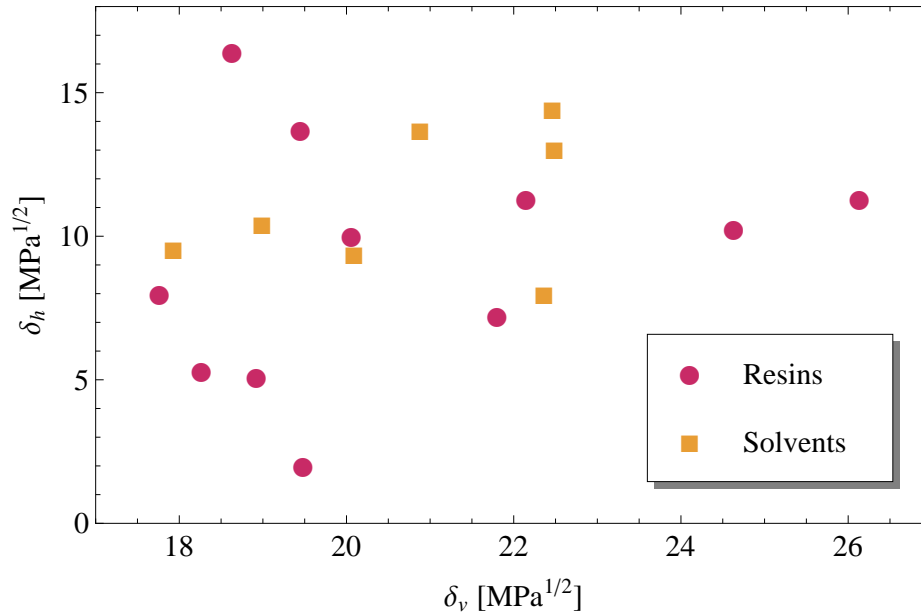


Figure 3.1.:  $\delta_v$ - $\delta_h$  diagram for the selected solvents and various epoxy resins

Ternary diagrams are a good possibility to show three variables in a two dimensional plot. To use them for solubility parameters the partial HSPs have to be converted

### 3. Theoretical Approach

into fractional HSPs using equation 3.14. The calculated data is given in table 3.4.

$$f_i = \frac{\delta_i}{\delta_d + \delta_p + \delta_h} \quad \text{for } i = d, p, h \quad (3.14)$$

Table 3.4.: Fractional HSPs  $f_i$  for the used solvents and the epoxy data given in table 3.3

Solvent	$f_d$	$f_p$	$f_h$	Polymer	$f_d$	$f_p$	$f_h$
N,N-Diethyl-m-toluamide	0,61	0,22	0,17	DGEBA-DDMe	0,46	0,26	0,28
N,N-Dimethylformamide	0,41	0,32	0,27	DGEBA-DDM	0,47	0,27	0,25
1,1,2-Trichloroethylene	0,68	0,12	0,20	TGAP-DDMe	0,43	0,28	0,28
Chlorobenzene	0,75	0,17	0,08	TGAP-ANI	0,38	0,30	0,32
Aniline	0,56	0,15	0,29	TGAP-DDM	0,37	0,34	0,29
Tetrahydrofuran	0,55	0,19	0,26	TGAP-DDS	0,35	0,33	0,31
Dimethyl sulfoxide	0,41	0,36	0,23	Launay et al	0,53	0,26	0,21
Benzyl alcohol	0,48	0,16	0,36				
2-Pyrrolidone	0,40	0,36	0,23				
2-Methoxyethanol	0,39	0,22	0,39				

### 3. Theoretical Approach

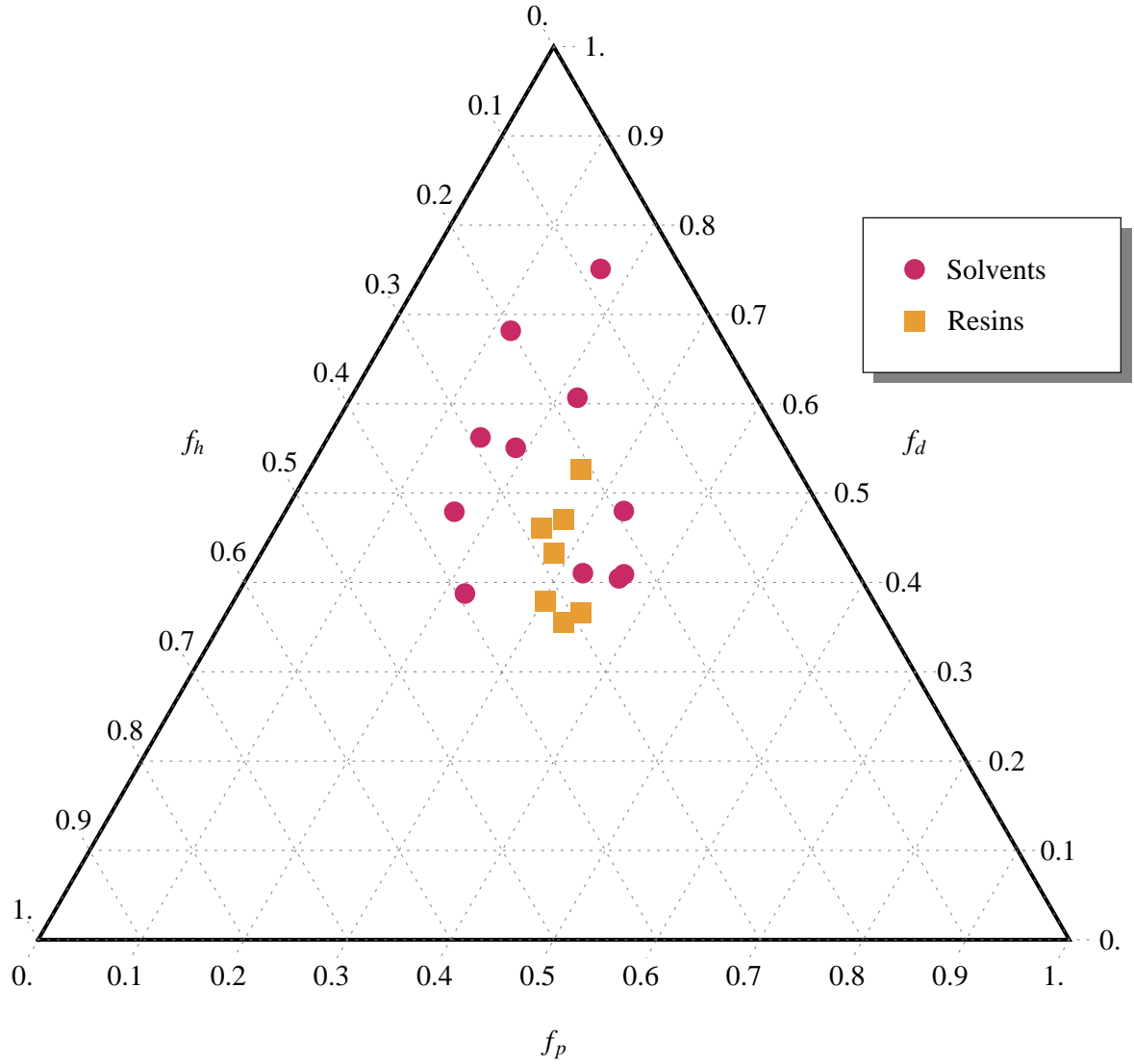


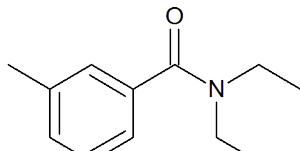
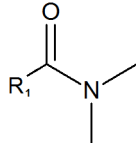
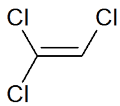
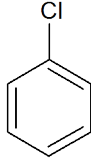
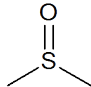
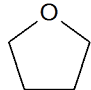
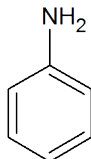
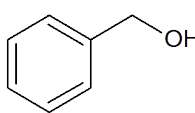
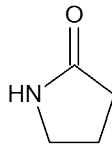
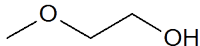
Figure 3.2.: Ternary diagram for the chosen solvents and the available data for epoxy resins

#### 3.1.2. Solvent Functionalities

The functionalities of the solvents were considered insofar as to have a wide spread variety. The structure and functionalities of the chosen solvents are given in table 3.5.

### 3. Theoretical Approach

Table 3.5.: Structures and functionalities of the selected solvents for the primary screening

Solvent	Functionalities	Structure
N,N-Diethyl-m-toluamide	carboxamide, aromatic	
N,N-Dimethylformamide	carboxamide with $R_1=H$	
1,1,2-Trichloroethylene	halogenated, alkene	
Chlorobenzene	halogenated, aromatic (benzene derivative)	
Dimethyl sulfoxide	sulfoxide	
Tetrahydrofuran	cyclic ether	
Aniline	primary amine, aromatic (benzene derivative)	
Benzyl alcohol	alcohol, aromatic (toluene derivative)	
2-Pyrrolidone	cyclic amide (lactam)	
2-Methoxyethanol	alcohol, ether	

## 3.2. Transfer Hydrogenolysis and Aminolysis

Hydrogenolysis in general is a reaction in which a single bond is cleaved by hydrogen. Transfer hydrogenolysis is a special type, where partially hydrogenated aromatics are used as hydrogen sources instead of gaseous hydrogen. They allow milder reaction conditions in terms of temperature, pressure, and reaction time. Tetralin is the most popular hydrogen source used in several applications like the liquification of coal [27], and liquid-phase cracking of thermosetting resins [28].

Rudolf [29] did an extensive PhD-thesis on a method for hydrogenolytic degradation to liquefy thermosets for recycling, wherein the experimental conditions for the methods are described in detail. An outline was published in 2000 [30]. Tetralin, indoline, and 9,10-dihydroanthracene were used as hydrogen donors.

In his work Rudolf also postulated a possible reaction mechanism for an epoxy resin, which consisted of three steps (see figure 3.3). The first step is the elimination of water at higher temperatures from the secondary alcohol group, followed by homolysis of the allylic bonds. The free radicals formed are then saturated by hydrogen abstraction from the donor. It was concluded that the rate determining step is the homolysis and not the hydrogen transfer to the resin.

### 3. Theoretical Approach

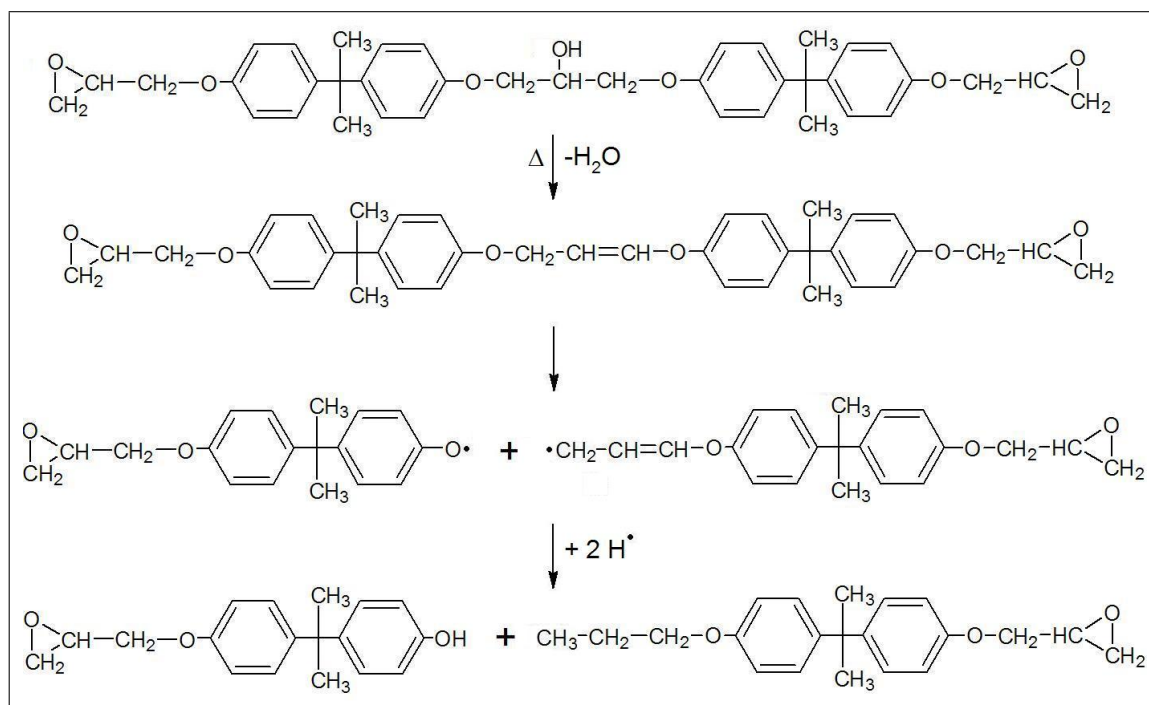


Figure 3.3.: Proposed reaction mechanism for the hydrogenolytic degradation of an epoxy resin

He also investigated a combination of tetraline with ethanolamine, which helped to reduce the necessary temperature and reaction time. The reaction now depended on aminolysis instead of hydrogenolysis. Also some of the solvents used during the solvolysis experiments, e.g. aniline, could incorporate aminolysis reactions.

### 3.3. Sub- and Supercritical Solvents

Sub- and supercritical solvents have been of great popularity in the past years and a wide range of applications has been discovered. A main field of use, which is connected to thermosetting resins, is the chemical recycling of polymer wastes. Especially sub- and supercritical water (SCW) have great potential for recycling purposes because water is inexpensive, recyclable, non-toxic, and relatively easy to handle [31]. Lately water has been used in the treatment of several compounds containing highly-crosslinked, thermosetting resins, like carbon fibre reinforced epoxy composites [31], moulding epoxy resins [32], phenolic resins [33], model compounds with ether linkages [34], and printed circuit boards [35]. Besides recycling purposes supercritical fluids are getting more popular in organic synthesis.



### 3. Theoretical Approach

The critical point of a substance in general is determined by a certain combination of temperature and pressure. In case of water the critical point lies at 647 K and 22,1 MPa [32]. Water changes its characteristics even before the critical point is reached. High-temperature water (HTW), which is defined as water above 473 K, is very useful as a solvent to enhance many chemical reactions (see the review by Akiya et al. [36] and the references therein). When the temperature of water is increased, the hydrogen bonds get fewer and weaker, the tetrahedral coordination is lost, and the solubility of organic compounds and gases increases with the temperature, whereas the solubility of inorganic salts decreases. Due to the loss in binding strength of the hydrogen bonds, only small clusters of hydrogen-bonded water molecules exist in HTW. In SCW the number of hydrogen bonds per water molecule is about one third the number at ambient conditions [37].

Due to the change in its structure, SCW has low viscosity, high mass transport coefficients, high diffusivity, and solvation power [31]. It can influence reactions in many different ways depending on the type of the present reaction, for example ionic, polar non-ionic, and free-radical. The water molecules act as active participants, like reactants or as catalysts, and not just as an inert medium. HTW can also influence reactions by phase behaviour, solute-solvent collisions, solvent reorganization, and diffusion limitations [36].

For example, HTW can catalyse hydrogen transfer reactions by participating in the transition state and reducing its energy. This has been shown for smaller model compounds, like nitroaniline [38] and acetic acid derivatives [39], but to my knowledge not for polymeric materials.

Besides water also lower alcohols have been used in the recycling of thermosetting resins. The main advantage of supercritical methanol over SCW is the fact that the critical point is lower and more easy to achieve under laboratory conditions, namely 515 K and 8,09 MPa [40]. It has been used mainly for depolymerisation of polymers, e.g. PET [41] and phenolic resin [40]. N-propanol (critical point 514 K and 5,2 MPa [42]) was used in the same manner including carbon fibre composites. Although both alcohols have favourable reaction conditions, the focus still lies on supercritical water for the treatment of highly crosslinked polymers.

#### 3.3.1. Catalysts for Sub- and Supercritical Water

The most effective way to enhance the reaction rate in SCW is to increase the reaction temperature. As this means high energy consumption and in the present case also problems with the specifications for the semiconductor devices, the maximum temperature was limited to 523 K and catalysts had to be found. In the literature different catalyst types for reactions in HTW have been described.

A popular alkaline catalyst is potassium hydroxide KOH, which is often used in recycling processes [31,43]. It can not be used in the present decapsulation process, as it would severely damage the metallisation of the die.

A second possible catalyst is sodium carbonate  $\text{Na}_2\text{CO}_3$ , which is also effective in promoting decomposition reactions of resins [32–34,44]. The catalysis mechanism is not clearly devised, but it is believed that the positive effect of  $\text{Na}_2\text{CO}_3$  can be attributed to an acceleration of ionic reactions. In combination increased amounts of water were effective.

Salt effects, like in case of sodium chloride, have been discussed to improve the hydrolysis rate in supercritical water [32,45,46], but the results were very inconsistent and not promising, always depending largely on the resin sample in question.

Acid catalysts as well as the addition of a hydrogen donor (tetralin) showed no observable difference in any of the published reactions [33,44].

#### 3.3.2. Supercritical Water Oxidation

In supercritical water oxidation (SCWO) an oxygen source like air, oxygen, or hydrogen peroxide is used to at least partially oxidise a solute. The governing mechanism is free radical and the most effective oxidant is the hydroxyl radical ( $\text{OH}^\bullet$ ). Hydrogen peroxide subsequently dissociates to add two OH-radicals to the overall reaction, which increases the reaction rates significantly [47].

SCWO has been used in recycling of waste polymer compounds, e.g. for printed circuit boards [35,48], carbon fibre reinforced epoxy composites [31], and model thermosetting resin compounds [49].

A point of concern is the corrosion of stainless steel reactors used in SCWO. It occurs whenever the temperature is increased up to the critical temperature, but nevertheless stainless steels can be used for thousands of hours without significant damage [50–52].

### 3.4. Glycolysis

In glycolysis the active reagent is a glycol/diol. Therefore it can be regarded as an alcoholysis reaction. A combination of diethyleneglycol (DEG) and titanium(IV)*n*-butoxide (TBT) as catalyst was shown to be applicable for the depolymerisation of polymers. It was studied intensively for the cases of polyethylene terephthalate [53–55] and of epoxy resins [56–58].

The reaction depends strongly on the reaction settings like solvent/resin/catalyst ratio and temperature. As the reaction mechanism is not completely understood it is difficult to predict the influences. Therefore vast experimental series are necessary to gain knowledge and optimise the conditions.

## 4. Experimental Setup and Results

### 4.1. Tool Setup

As the requirements for the different solvolysis reactions were not clear at the beginning and only little information was available, an evaluation to gain a usable tool had to be done. The starting point was a simple reflux equipment, which was replaced by a tool capable of pressure adjustment. The last tool, which proved to be the most suitable, was a pressure vessel.

#### 4.1.1. Reflux Equipment

A standard reflux equipment was used for the primary screenings of the solvents and hydrogen donors. It consisted of a three-neck round-bottom flask with an intensive condenser. The flask was heated with a LabHeat KM-ME heating mantle and the temperature of the reagent was controlled using a digital thermometer.

For all runs the chosen devices were immersed in a total volume of 50 mL of reagent and heated till reflux (boiling points see table A.1 in the appendix). The reagent was kept at this temperature for 9 hours. Due to safety reasons it was not possible to keep the reaction running over night. After 9 hours on the first day the devices were left in the solvent without further heating over night. On the second day the solvent was reheated and refluxed for another 9 hours, in order to obtain a total of 18 hours reflux time. Thereafter the devices were shortly rinsed with acetone and dried with a stream of nitrogen.

### 4.1.2. High Pressure Asher

The *High Pressure Asher* (HPA) enables experimental settings under added nitrogen pressure and automated temperature control. Pressure addition allows to heat solvents to desired temperatures (above the boiling point at atmospheric pressure) under exclusion of air/oxygen.

The chosen devices and the solvents were placed in 50 mL test tubes, which are made out of fused quartz glass. In general 25 mL of the organic solvents or hydrogen donors were used. The tubes were closed with a glass lid and then sealed with PTFE tape. The rack which could contain five test tubes was immersed into the reaction chamber. The settings of the experimental series are given in table 4.1. The series were planned and analysed using Ceda, which is a statistical software tool for design of experiments based on a Cornerstone architecture. For this purpose three categorical responses were defined, namely quality of polyimide, quality of metallisation, and number of decapsulated devices.

Table 4.1.: Parameter settings for the experimental series using the HPA

run no.	T [K]	t [h]	p [bar]	solvent group
R1	423	5	124	organic solvents <sup>a)</sup>
R2	423	5	109	hydrogen donors <sup>b)</sup>
R3	523	5	108	hydrogen donors <sup>b)</sup>
R4	523	5	104	organic solvents <sup>a)</sup>
R5	523	10	112	organic solvents <sup>a)</sup>
R6	523	10	114	hydrogen donors <sup>b)</sup>
R7	423	10	126	organic solvents <sup>a)</sup>
R8	423	10	- *	hydrogen donors <sup>b)</sup>

<sup>a)</sup> ANI, BAL, DETA, MOE, PYR; <sup>b)</sup> DHA, IND, TET, TEA

\* Run R8 was not performed due to leakage of the HPA

Run R8 could not be performed due to severe leakage of the HPA. Although the results had been promising, the tool could not be used for the device preparation with organic solvents, because the incorporated rubber gaskets did not withstand the chemical attack. The exchange of the rubber gaskets with more sturdy materials is not possible.

### 4.1.3. Pressure Vessel System

After the HPA turned out not to be a suitable tool, an alternative was found in pressure vessels by Parr. The system consisted of the pressure vessel itself, a gas supply and safety system, and a heating system coupled with a temperature controller. Figure 4.1 shows a photograph of the final installation as present in the failure analysis laboratory in Villach.

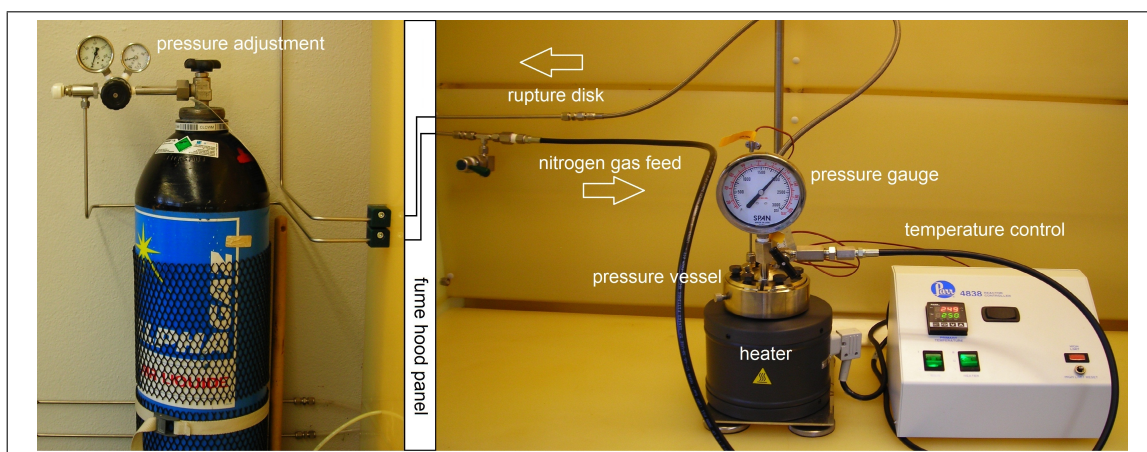


Figure 4.1.: Final installation of the Parr pressure vessel with all accompanying parts

A simple setup consisting of a 300 mL reactor with a pressure gauge, one valve, a safety rupture disc, and a temperature probe was chosen (Parr pressure vessel 4766). To preserve the stainless steel 316 vessel a glass liner was used in which the chosen devices and the solvents were immersed. The decomposition products of the devices and the solvent remained inside this liner to a great extent. The vessel was sealed using a PTFE gasket and a so called split ring system, where the compressive force to seal the system was provided by six cap screws (see figure 4.2).

#### 4. Experimental Setup and Results

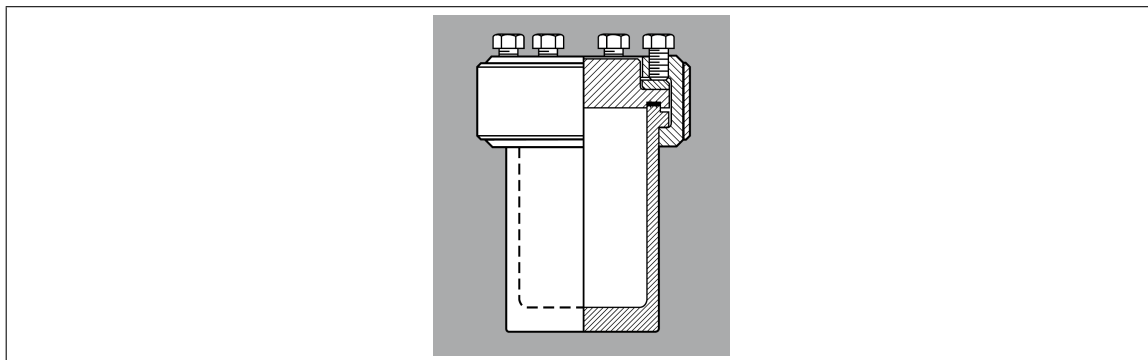


Figure 4.2.: Cross section of a Parr 4760 series pressure vessel showing the sealing system [3].

The pressure vessel system allowed a flexible setup for all reaction types analysed during this thesis. The pressure was adjusted before starting the heating cycle over a feed line using a standard nitrogen gas bottle as source. After applying the desired nitrogen load the feed line was detached for safety reasons. The complete work flow is given in figure A.1 in the appendix.

The security specifications stated a maximum pressure of 200 bar and a maximum operating temperature of 633 K. Practically the pressure was kept below 180 bar and the temperature never exceeded a maximum of 523 K. The maximum allowable water loading (MAWL) at 523 K was about 200 mL, but the volume was only varied to a maximum of 100 mL. For the exact experimental settings used see the appropriate reaction type in section 4.3.

For easier comparison of the results of all Parr experiments three categories were defined, namely the condition of metallisation and polyimide, and the percentage of decapsulated devices. The condition of metallisation and polyimide were purely qualitative categories, which were defined according to operating experience (see table 4.2). For the metallisation category number 3 was the goal, and in case of polyimide either 3 or 1 were favourable. The reason is, that the polyimide layer is sometimes needed to assess a specific failure (category 3), but it can also complicate further investigation in other cases (category 1). The resulting diagrams are shown in the appropriate reaction sections (see section 4.3).

#### 4. Experimental Setup and Results

Table 4.2.: Qualitative categories chosen to classify the results of all Parr pressure vessel series

category	metallisation	polyimide
3	unharmd	unharmd
2	discolourations on parts of the surface	partially removed/damaged/thinned
1	severe discolourations or attack	severely removed/damaged/thinned

##### 4.1.3.1. Estimation of Work Pressure in the Parr Pressure Vessel

To estimate the pressure inside the vessel beforehand, different approaches were used. The main contribution to the overall pressure comes from the nitrogen added to adjust the reaction pressure and only a small percentage is due to vapour pressure of the solvents in use. The calculations serve as estimations for the pressure inside the vessel with non-quantifiable errors. Any contributions of reactions going on inside the vessel were not taken into account. Hence a safety margin is necessary at all times.

For the pressure calculation of nitrogen an evaluation of several different equations of state (EOS) was done. The evaluation included the EOS postulated by Van der Waals, Clausius, Berthelot, Dieterici, Wohl, Redlich-Kwong, Redlich-Kwong-Soave, Peng-Robinson, and Benedict-Webb-Rubin (see table 4.3 for the general formulations).



#### 4. Experimental Setup and Results

Table 4.3.: Equations of state used to calculate the nitrogen pressure increase

Van der Waals [59]	$p = \frac{nRT}{V-nb} - a \cdot \frac{n^2}{V^2}$
Clausius [60]	$p = \frac{RT}{V_m-b} - \frac{a}{T(V_m+c)^2}$
Berthelot [60]	$p = \frac{RT}{V_m-b} - \frac{a}{TV_m^2}$
Dieterici [60]	$p = \frac{RT}{V_m-b} e^{-\left(\frac{a}{RTV_m}\right)}$
Wohl	$p = \frac{RT}{V_m-b} - \frac{a}{TV_m(V_m-b)} + \frac{c}{T^2V_m^3}$
Redlich-Kwong [61]	$p = \frac{RT}{V_m-b} - \frac{a}{T^{0,5}V_m(V_m-b)}$
Redlich-Kwong-Soave [61]	$p = \frac{RT}{V_m-b} - \frac{a\alpha}{V_m(V_m-b)}$
Peng-Robinson [62]	$p = \frac{RT}{V_m-b} - \frac{a}{V_m(V_m+b)+b(V_m-b)}$
Benedict-Webb-Rubin [63]	$p = RT\rho + (B_0RT - A_0 - \frac{C_0}{T^2})\rho^2 + (bRT - a)\rho^3 + a\alpha\rho^6 + \frac{c\rho^2}{T^2} e^{-\gamma\rho^2}$

---

$p$  = pressure [bar],  $n$  = amount of substance [mol],  $V$  = volume [L],  $V_m$  = molar volume [L mol<sup>-1</sup>],  $T$  = temperature [K],  $R$  = universal gas constant [= 0,08314 bar L mol<sup>-1</sup> K<sup>-1</sup>],  $\rho$  = molar density [mol L<sup>-1</sup>],  $e$  = Euler's constant, and  $a, b, c, A_0, B_0, C_0, \alpha, \gamma$  = equation specific parameters

Each equation of state needs a certain number of parameters. They were calculated using the equations in table 4.4. For the critical point of nitrogen the same values were used as chosen by Span et al. [64], who did an extensive comparison of the experimental data available, namely the data acquired by Nowak et al. [65, 66]:

- critical temperature  $T_c = 126,192 \pm 0,010$  K
- critical pressure  $p_c = 33,958 \pm 0,0017$  bar
- critical density  $\rho_c = 313,3 \pm 0,4$  kg m<sup>-3</sup>
- critical molar volume  $V_{m,c} = 0,08941$  L mol<sup>-1</sup> (calculated from  $\rho_c$ )

#### 4. Experimental Setup and Results

For the acentric factor  $\omega$  of nitrogen a value of 0,0377 was used [67].

Table 4.4.: Equations for the calculations or data of the parameters used in each equation of state

equation of state	parameters
Van der Waals	$a = \frac{27R^2T_c^2}{64p_c} \quad b = \frac{RT_c}{8p_c}$
Clausius	$a = V_c - \frac{RT_c}{4p_c} \quad b = \frac{3RT_c}{8p_c} - V_c \quad c = \frac{27R^2T_c^3}{64p_c}$
Berthelot	$a = \frac{27R^2T_c^3}{64p_c} \quad b = \frac{RT_c}{8p_c}$
Dieterici	$a = \frac{4R^2T_c^2}{p_c e^2} \quad b = \frac{RT_c}{p_c e^2}$
Wohl	$a = 6p_c T_c V_c^2 \quad b = \frac{V_c}{4} \quad c = 4p_c T_c^2 V_c^3$
Redlich-Kwong	$a = \frac{0,4278R^2T_c^{2,5}}{p_c} \quad b = \frac{0,0867RT_c}{p_c}$
Redlich-Kwong-Soave	$a = \frac{0,42747R^2T_c^2}{p_c} \quad b = \frac{0,08664RT_c}{p_c}$ $\alpha^{0,5} = 1 + m(1 - T_R^{0,5})$ $m = 0,480 + 1,574\omega - 0,176\omega^2$
Peng-Robinson	$a = 0.45724 \frac{R^2T_c^2}{p_c} \quad b = 0.07780 \frac{RT_c}{p_c}$
Benedict-Webb-Rubin	$a = 0.0312319 \quad b = 0.0032351$ $c = 547.364 \quad A_0 = 0.872086$ $B_0 = 0.0281066 \quad C_0 = 7813.75$ $\alpha = 7.09232 \cdot 10^{-5} \quad \gamma = 4.5 \cdot 10^{-3}$

$p_c$  = critical pressure [bar],  $T_c$  = critical temperature [K],  $V_c$  = critical volume [L],  $R$  = universal gas constant [= 0,08314 bar L mol<sup>-1</sup> K<sup>-1</sup>],  $T_R$  = reduced temperature [-],  $m$  = slope of  $\alpha^{0,5}$  vs.  $T_R^{0,5}$  [-],  $\omega$  = acentric factor [-],  $e$  = Euler's constant, and a,b,c,A<sub>0</sub>,B<sub>0</sub>,C<sub>0</sub>, $\alpha$ , $\gamma$  = equation specific parameters

#### 4. Experimental Setup and Results

In each case the first step was to calculate the amount of substance  $n$  of nitrogen inside the vessel at room temperature, when a certain pressure load was added. For this purpose the equations were solved for  $n$  (the calculation program in use was Mathematica 7.0).

Using the calculated values for the amount of substance  $n$  and all necessary parameters the pressure could be estimated for the reaction temperatures using the same equations of state, but this time solved for pressure  $p$  (see table 4.3 for the general equations). To evaluate the results a pressure test without solvent or glass liner (total volume of 300 mL) and 70 bar nitrogen load was performed, and the result was compared to the estimations from the equations of state (see table 4.5). The Redlich-Kwong-Soave turned out to be the best fitted for the present experimental conditions and was used for further estimations.

Table 4.5.: Estimated pressures using several equations of state in comparison to a pressure test result (estimated failure 1%)

method	resulting pressure [bar]	n [mol]
measured	127,0	-
Van der Waals	135,0	0,899
Clausius	125,3	0,803
Berthelot	130,8	0,822
Dieterici	138,6	0,942
Wohl	133,7	0,882
Redlich-Kwong	132,9	0,855
Redlich-Kwong-Soave	129,7	0,861
Peng-Robinson	135,5	0,946
Benedict-Webb-Rubin	133,0	0,879

To estimate the contribution of the solvents to the overall pressure increase the so called Antoine equation for vapour pressure (see equation 4.1) was used. The Antoine constants  $A$ ,  $B$ , and  $C$  were taken from the NIST Chemistry WebBook [2] (if available) and are given in table A.3 in the appendix. As these constants are only valid in certain temperature ranges, which are in most of the cases below the present reaction temperature of 523 K, deviations are inevitable. But as the contribution of most solvents to the overall pressure is small, those deviations are acceptable in practice (see the calculated values for the available solvents at 523 K in table 4.6).

$$\log p = A - \frac{B}{C + T} \quad (4.1)$$

Table 4.6.: Estimated pressure values for several solvents in use calculated using the Antoine equation

solvent	pressure [bar]
ANI	4,4
BAL	2,9
MOE	19,9
DMF	7,8
THF	39,4
TCE	21,1
CLB	11,0
TET	2,5
H <sub>2</sub> O	38,0

For practical purposes it was sufficient to simply sum up the contributions of nitrogen and solvent to the overall pressure instead of using more complicated laws for mixtures.

## 4.2. Devices

The different types of devices used for the various experimental series were chosen according to a row of characteristic features. The most important were the mould compound type, the package, and the process group. Figure 4.3 shows a stereoscopic micrograph of the different devices. The numbers refer to the information tables 4.7 and 4.8 in which the most important features are listed.

#### 4. Experimental Setup and Results

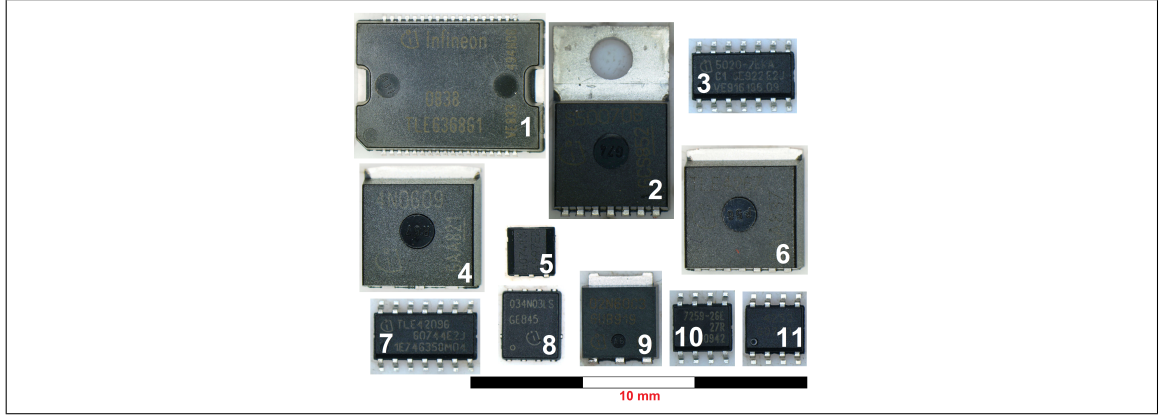


Figure 4.3.: Stereoscopic micrograph of the devices in use. For more information see tables 4.7 and 4.8.

Table 4.7.: Package and mould compound information of the devices for the experimental series.

No.	Package	MC	MC type	Hardener type
1	P-DSO-36-12	EME 6710 LX	ECN	PN
2	PG-TO220-7-12	KMC 2110 G-7	modified ECN	PN
3	PG-DSO-14-40	CEL 9220 HF10	_*	_*
4	PG-TO263-3-2	KMC 2110-(G)7	modified ECN	PN
5	PG-SSO-3-10	KMC 2110 G-3	modified ECN	PN
6	PG-TO263-7-1	CEL 9220 HF10 KM	_*	_*
7	PG-DSO-14-22	CEL 9220 HF10 V83	LMW-2	LWA-1
8	PG-TDSON-8-5	CEL 1772 HF9-SS	OCN/LMW-1/BER	LWA-1
9	PG-TO251-3-11	EME 6300 SR	ECN	_*
10	PG-DSO-8-16	CEL 9220 HF10 V83	LMW-2	LWA-1
11	PG-DSO-8-10	EME G700 LX	_*	_*

MC... mould compound, for further information see section 2.2 or the glossary

\_\*... no information available

## 4. Experimental Setup and Results

Table 4.8.: Technology and application information of the devices for the experimental series.

No.	Sales Code	Basic Type	Process Group	Used in
1	TLE6368G1	S0978W	SPT4_90V_8	C,D
2	BTS50070-1TMB	U0169C/D	SSMART_8	D
3	BTS5020-2EKA	L8300C	SMART6_8	C,D
4	IPB45N06S4-09	L8954O	SFET4MV_8	B,C,D
5	TLE4997E2	M4997M	B6CA_S8	B,C,D
6	TLE4267G	S0770J	DOPL_6	B,C,D
7	TLE4209G	S1787A/B	DOPL4_8	B,C,D
8	BSC034N03LS G	L8941S	SFET4LV_8	A,B,C,D
9	SPS02N60C3	L5923T	EHAT_8	D
10	TLE7259-2GE	S1229A	SPT5_60V_8	D
11	TLE4253GS	S1719A	DOPL_6	D

A... Reflux, B... HPA, C... Parr solvolysis/transfer hydrogenolysis/aminolysis

D... Parr hydrogenolysis, glycolysis

### 4.2.1. Device Preparations

For some experiments preparations prior to the actual tests had to be done. They can be divided into general preparations and thinning.

A general preparation was done for each experimental run to allow easier handling. In case of a heat sink or an exposed pad (device no. 1, 2, 3, 4, 6, 8, 9) the tin plating was removed by manual grinding. If the leads were too spacious and would have led to catching of the devices inside the test tubes, they were removed mechanically (device no. 1, 2, 4, 5, 6, 9).

Thinning was used in some special cases to reduce the reaction time and facilitate the solvent preparation. Three different methods were used, namely laser ablation, manual grinding, and parallel polishing. As each of them means a significantly higher effort and time consumption they were not used in general.

### 4.2.1.1. Laser Ablation

For the removal of mould compound by laser ablation a decapsulation system by LCL (Las Consult Leitner) was used. This is the standard tool for partial decapsulation during failure analysis in Villach. It contains a Nd:YAG (neodymium-doped yttrium aluminium garnet) class 4 laser with an emitting wavelength of 1064 nm, a pulse frequency of 0-50 kHz, and a pulse peak power of 35-250 kW.

### 4.2.1.2. Manual Grinding

Manuel grinding is a very easy and rather fast way to thin a device, but has several disadvantages over parallel polishing. The devices experience a non-uniform stress and rather high mechanical forces, and it is not possible to grind to an exact position above the die.

A RotoPol-35/PdM-Force-20 grinding and polishing machine by Struers was used for mechanical removal of mould compound above the die. Three different silicon carbide abrasive discs with P-180, P-1200, and P-4000 grit by Allied were used in this order.

### 4.2.1.3. Parallel Polishing

Parallel polishing is a complex and time intensive preparation method, but it is well controlled. It is even possible to remove the mould compound to the point where it gets transparent (at about 50  $\mu\text{m}$  above the die surface) and one can see the outline and structure of the die [68].

It was used only in special cases and in case of standard plastic packaging did not help to reduce the reaction time in combination with solvolysis. In case of so called *Next Generation Packages* it proved to be a successful device preparation prior to solvolysis (see section 5.3).

## 4.3. Reaction Types

### 4.3.1. Solvolysis

#### 4.3.1.1. Primary Solvent Screening

The primary solvent screening was conducted in a simple reflux equipment (see section 4.1.1 for more information). 50 mL of the solvents, which were chosen according to the solubility parameter approach, were used. Informations about the solvents in use (suppliers and physical properties) are listed in table A.1 in the appendix.

Five pieces of device number 8 (see tables 4.7 and 4.8 for further information) were chosen for the primary screening. This package is very thin and easy to handle, which made it a perfect sample for the first investigations.

Aniline (ANI), benzyl alcohol (BAL), and 2-methoxyethanol (MOE) showed similar results after 18 hours of reflux. The moulding compound became soft and could be removed from the die and the lead frame with little effort. N,N-Diethyl-m-toluamide (DETA) and 2-pyrrolidone (PYR) showed an apparent colour change from yellow to orange and then to a dark reddish brown most possibly due to oxidation and extraction of mould compound additives. The moulding compound of the packages became extremely soft and fragmented and it came off during the removal of the devices from the solvent. In all mentioned solvents the metallic components were completely unharmed and in case of DETA and PYR even the polyimide layer, which covers the die surface, was completely unharmed (see figure 4.4 for an example). Due to the mechanical stress during removal of the moulding compound the bond wire in all packages broke.



#### 4. Experimental Setup and Results

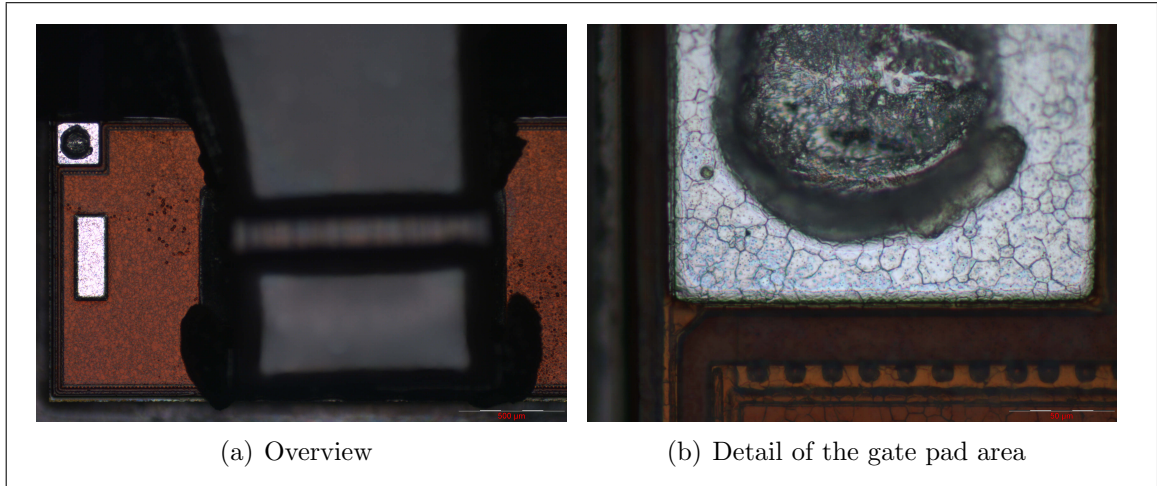


Figure 4.4.: Reflected-light micrographs of the die after decapsulation with PYR using the reflux equipment. Both the aluminium metallisation and the polyimide layer are completely unharmed.

The run with dimethyl sulfoxide (DMSO) was quitted after the first 9 hours due to damage of the aluminium metallization of the die. A possible explanation is that the solvent decomposes and sulphur compounds react with the aluminium metallisation (see figure 4.5). For that reason DMSO was excluded from all following experiments.

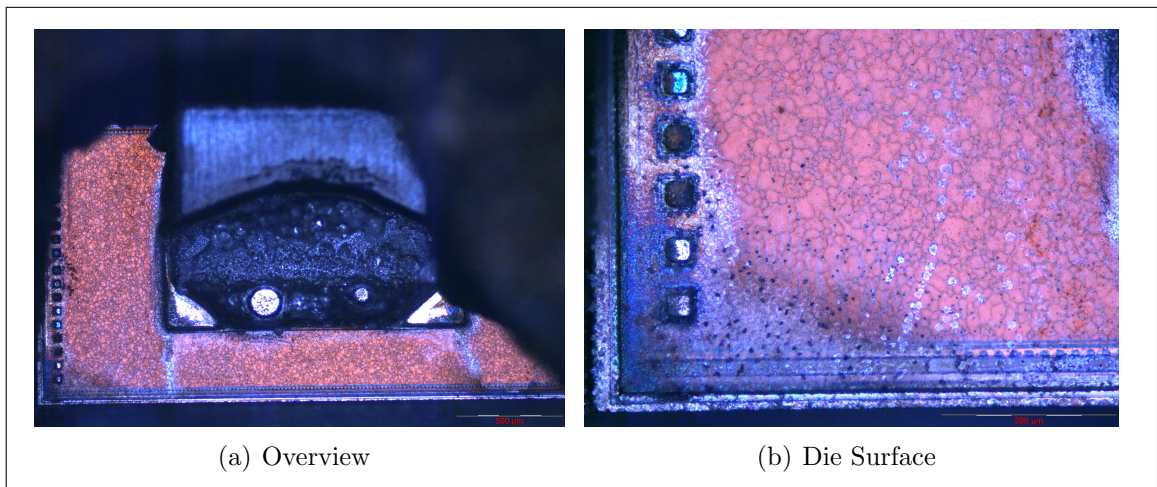


Figure 4.5.: Reflected-light micrographs of the die after decapsulation with DMSO using the reflux equipment. Severe damage of the metallisation can be observed.

1,1,2-Trichloroethylene (TCE) was the second solvent to be excluded, because the exposed copper lead frame of the device suffered severe damage. Although the die could not be decapsulated, it was concluded that the more fragile metallisation of

#### 4. Experimental Setup and Results

the die would suffer attack in a similar if not even more severe way.

The other three of the chosen solvents, namely N,N-dimethylformamide (DMF), tetrahydrofuran (THF), and chlorobenzene (CLB), did not show any observable interaction with the mould compound in this experiments. They were not excluded at this point as their boiling points at atmospheric pressure are considerably low.

In order to gain some understanding of the changes in the mould compound, embedded cross sections of a device after preparation with DETA and a reference part were done, and analysed using scanning electron microscopy (SEM) (see figure 4.6).

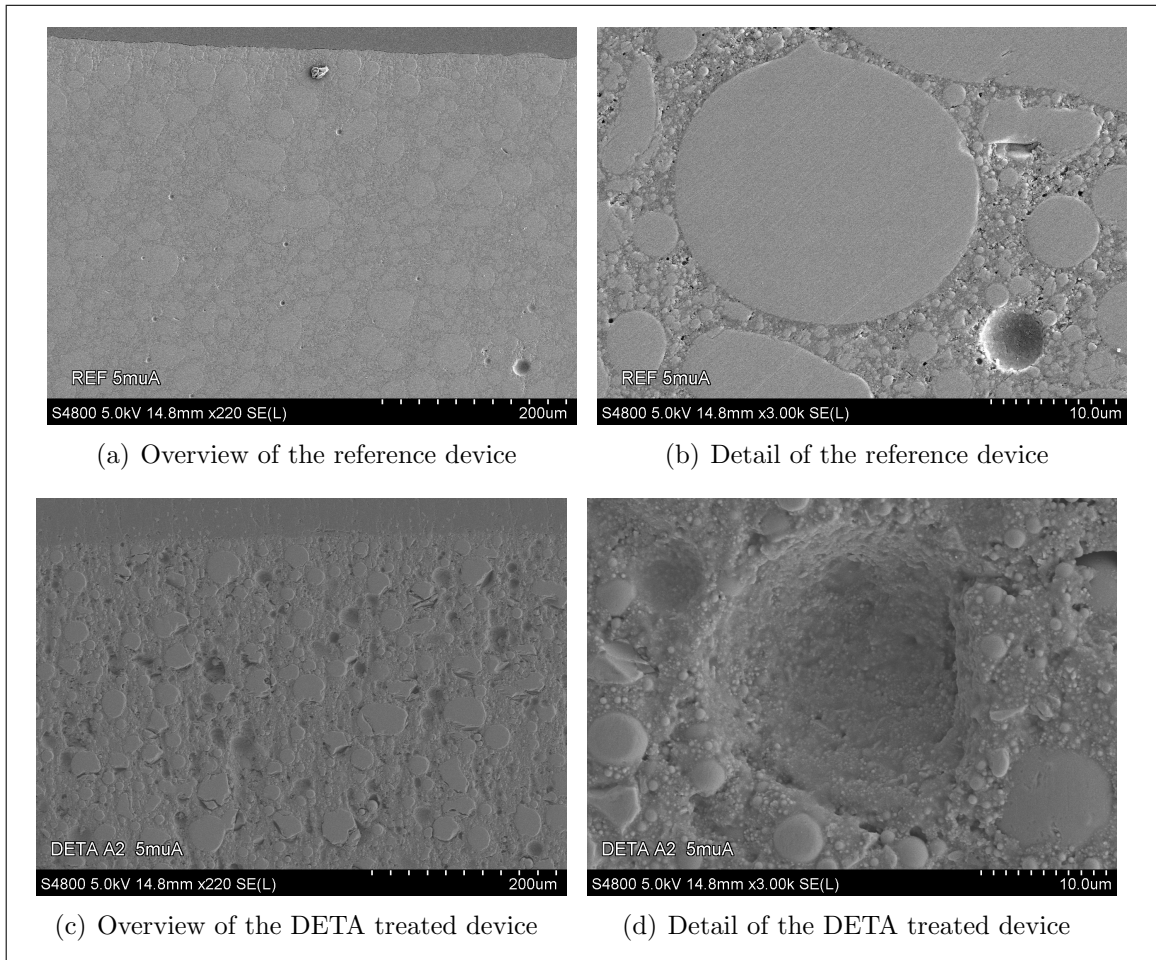


Figure 4.6.: SEM micrographs of a device treated with DETA and a reference device

The micrographs show that in the reference device the mould compound is quite dense and that only a few filler particles are missing due to preparation (see fig-

ures 4.6(a) and 4.6(b)). In the device prepared with DETA it is apparent that the filler particles have no sufficient hold inside the mould compound any more, which causes them to be partially or completely removed out of the composite (see figures 4.6(c) and 4.6(d)). The same investigation was undertaken for some of the other solvents as well (ANI, BAL, DMSO, MOE, and PYR) and the results were comparable.

### 4.3.1.2. High Pressure Asher

For the solvolysis experiments with the High Pressure Asher (HPA) the five solvents, which showed interaction with the mould compound during the primary screening, were chosen, namely aniline (ANI), N,N-diethyl-m-toluamide (DETA), 2-methoxyethanol (MOE), 2-pyrrolidone (PYR), and benzyl alcohol (BAL).

In general the same results for the device number 8 (see tables 4.7 and 4.8 for further information) were obtained as in the primary screening (see figure 4.7 for an example after treatment with BAL). It could be demonstrated that under the addition of pressure, the reaction time could be reduced from 18 to 10 hours, still giving the same results.

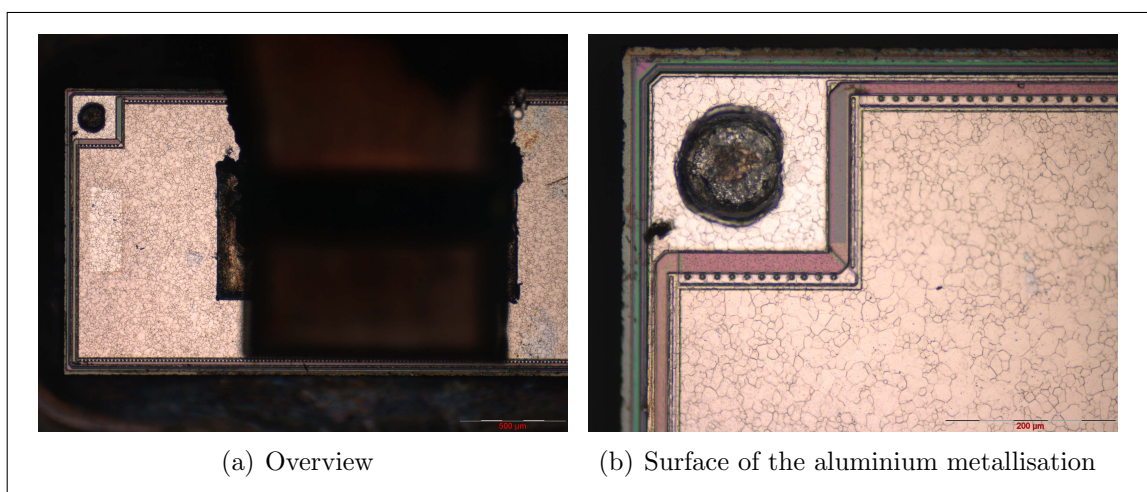


Figure 4.7.: Reflected-light micrographs of the die after decapsulation with BAL using the HPA. The aluminium metallisation is in perfect condition and the polyimide has been removed.

As the number of different devices was raised to five (device number 4-8, see tables 4.7 and 4.8 for further information) for the HPA experiments to ensure a better

#### 4. Experimental Setup and Results

technology coverage, the results for device number 8 could be compared to the other four. It seemed that this package was a good choice for the primary screening, because it turned out to be the most easily swellable. Only with BAL or PYR all five different devices could be decapsulated.

The analysis of the DOE showed clearly that the main influence is the solvent, as expected. For the number of decapsulated devices the temperature has a very strong positive influence and the polyimide tends to be removed more readily. The time has not such a huge impact, but still it seems favourable to use 10 hours of preparation time. The effects Pareto charts for the number of devices and the polyimide are given in figure 4.8. For the metallisation the Pareto chart did not show any influences, because the metallisation always stayed unharmed no matter what experimental setups were chosen.

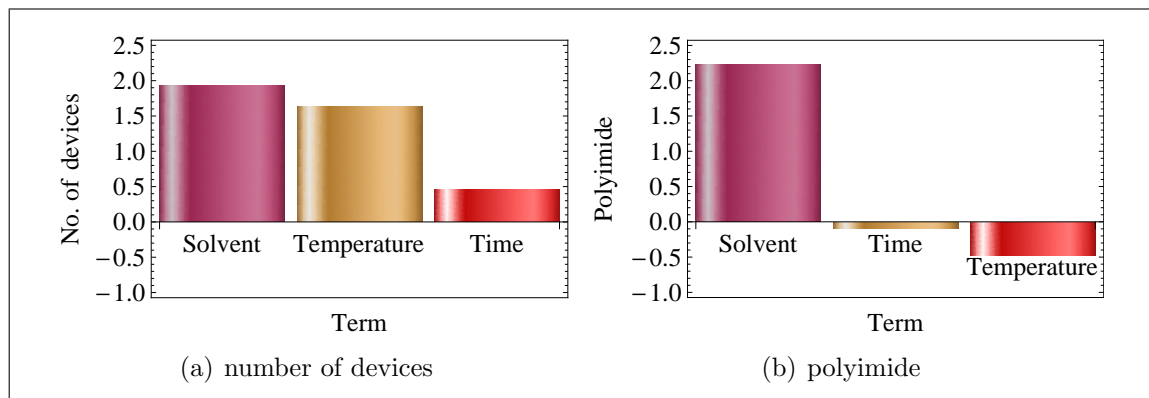


Figure 4.8.: Effects Pareto charts for the HPA solvolysis series

##### 4.3.1.3. Parr Pressure Vessel

For the solvolysis series with pure solvents two different reaction temperatures were investigated, namely 473 and 523 K. The added nitrogen pressure was 100 bar for the 473 K series and 70 bar for the 523 K series. The pressure load was chosen after a series of experiments using benzyl alcohol (BAL) to obtain a reasonable work pressure. In this series it could be shown that the favourable pressure range at 523 K lies between 50 and 70 bar and at about 100 bar at 473 K. The total solvent volume was 50 mL and the reaction time was 10 h for both series.

After completion of the reaction time, the tool was cooled down to room temperature. The swollen mould compound was removed from the device manually using

#### 4. Experimental Setup and Results

tweezers. The necessary mechanical force varied greatly between the different solvents in use. In some cases the mould compound stuck very tightly to the devices, but in other it came off by itself. After this the devices were cleaned using the solvent itself and acetone followed by drying with a stream of nitrogen. All devices, which could be decapsulated, were inspected using reflected light microscopy. The devices were assessed according to the systematic approach detailed in subsection 4.1.3. The result is given in figure 4.9. The main finding is, that a reaction temperature of 523 K is absolutely necessary in order to achieve a sufficient decapsulation of the devices.

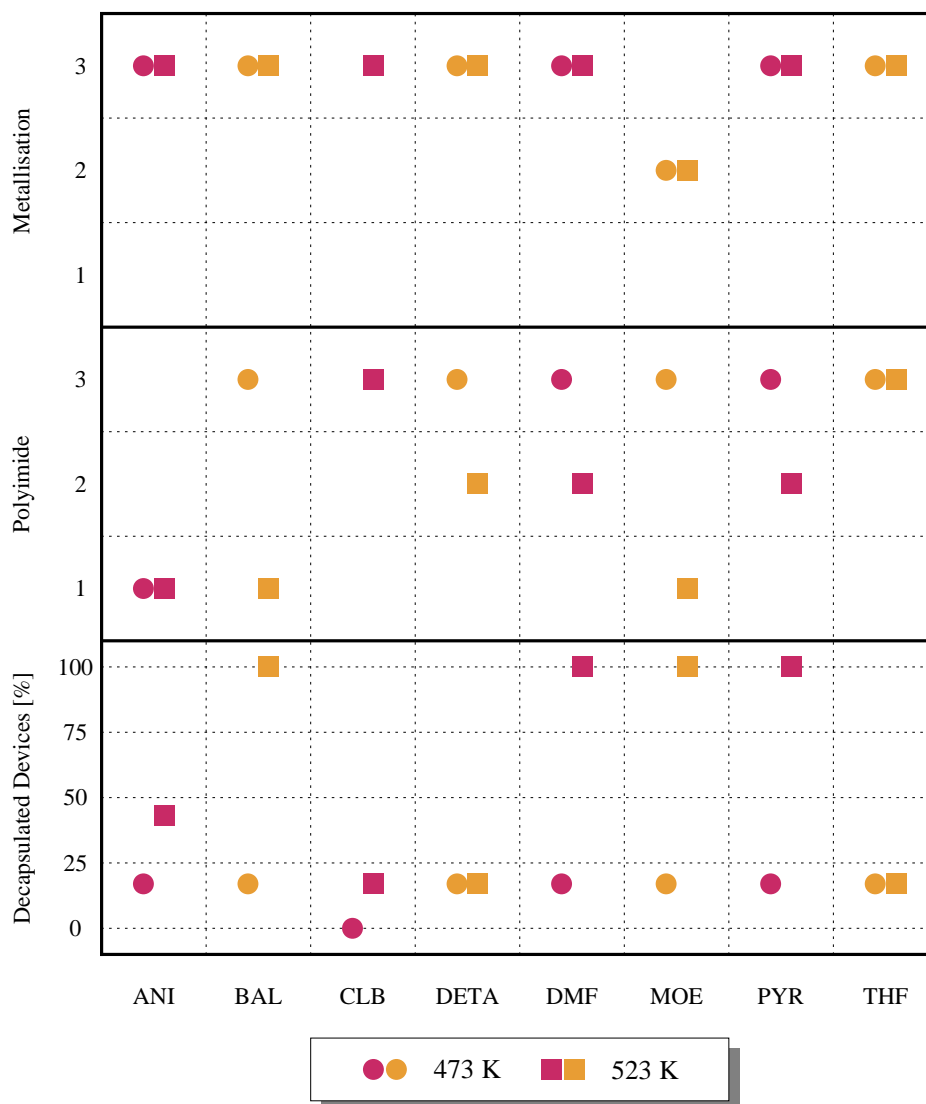


Figure 4.9.: Comparison of the results of solvolysis runs at 473 and 523 K

BAL worked really well at 523 K and figure 4.10 shows device number 1 (see tables



#### 4. Experimental Setup and Results

4.7 and 4.8) after decapsulation. This is an extremely good result, as this device has a high surface roughness and the mould compound tends to stick tightly to the die.

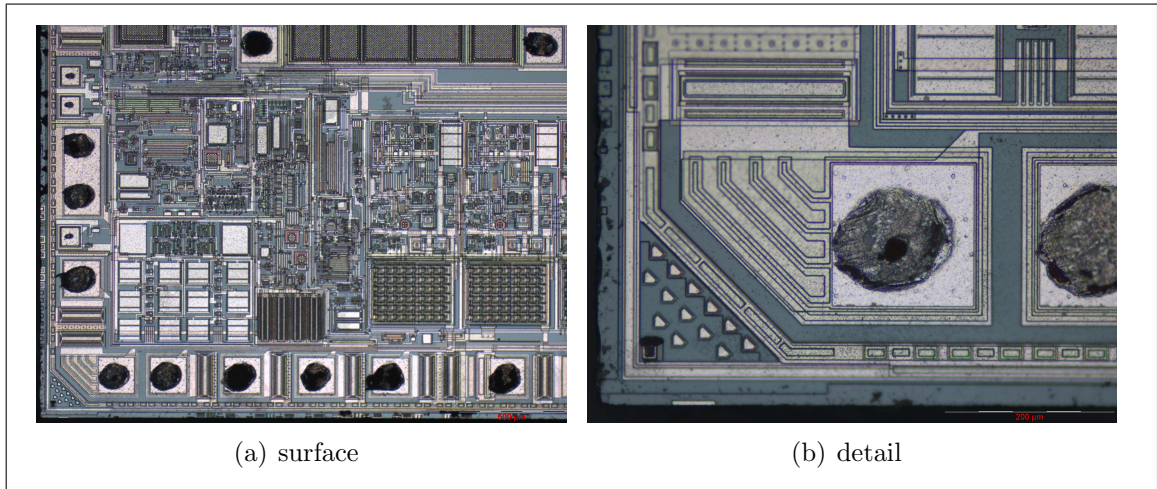


Figure 4.10.: Reflected-light micrographs of a device decapsulated using BAL.

2-Methoxyethanol (MOE) was the only solvent which led to slight discolourations on some of the metallisations. Only with 50 per cent of the solvents it was possible to decapsulate all different devices in use.

After these two series 2-pyrrolidone (PYR) was substituted with N-methyl-2-pyrrolidone (NMP), because it was solid at room temperature and therefore caused problems as it sublimated inside the valves and feeds. See figure 4.11 for one of the decapsulated devices using PYR.

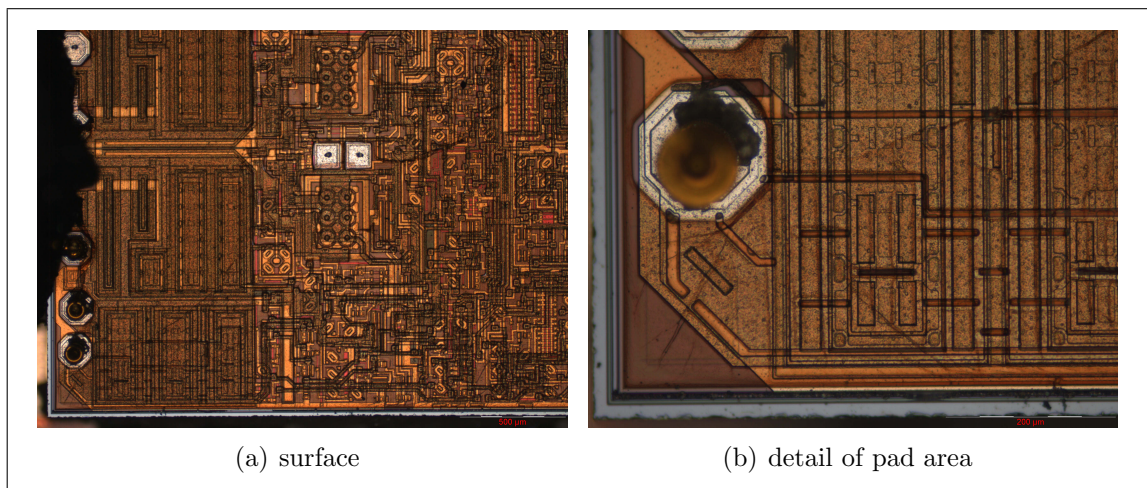


Figure 4.11.: Reflected-light micrographs of an IC device decapsulated using PYR. The orange colour of the surface is caused by the polyimide. Some mould compound residues are present.

N,N-diethyl-m-toluamide (DETA) had a different effect on the devices in comparison with the other solvents, as it seemed to diffuse into the weakest interface inside the device instead of swelling it evenly. It was suspected that in combination with another solvent the effect could be increased and hence a series of DETA combinations was performed.

The total solvent volume for this series was 50 mL and the two reagents were mixed in a ratio of 50:50 volume per cent. 70 bar nitrogen load was added before heating to 523 K. After 10 h and cooling over night the mould compound was manually removed, which required a higher force than in comparison with the pure solvents. This was attributed to a decreased swelling of the mould compound, and the diffusion of DETA into weak interfaces was not able to compensate these losses. The devices were cleaned with a freshly prepared amount of the solvent mixture in use and acetone, and dried with a stream of nitrogen.

#### 4. Experimental Setup and Results

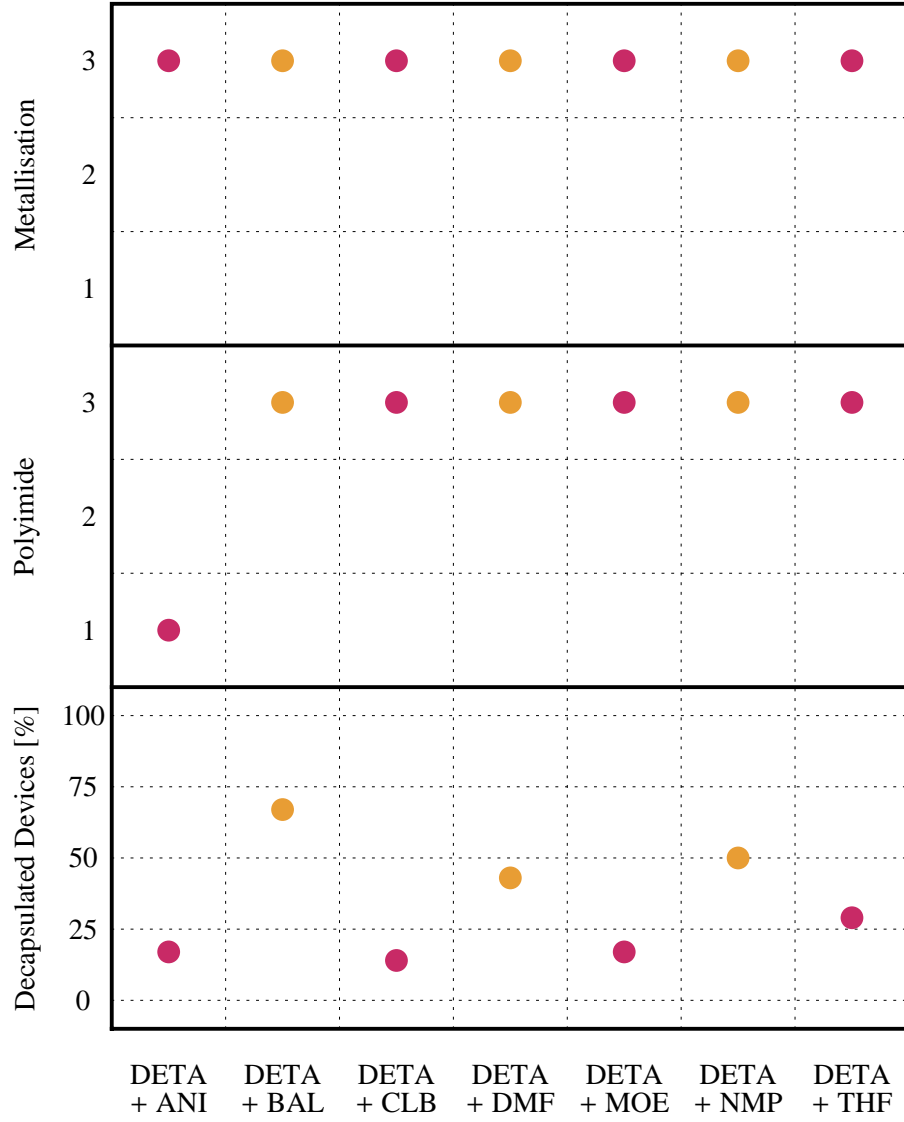


Figure 4.12.: Results of the DETA combination runs at 523 K

In case of BAL, DMF, and NMP the percentage of decapsulated devices could be at least doubled, but the outcome compared with the pure solvents was worse in respect to the percentage of decapsulated devices (see figure 4.12). Figure 4.13 shows one of the devices, which could be decapsulated using the combination of DETA and NMP. The wished-for magnifying effect could only be shown for few solvents and did not match the expectations.



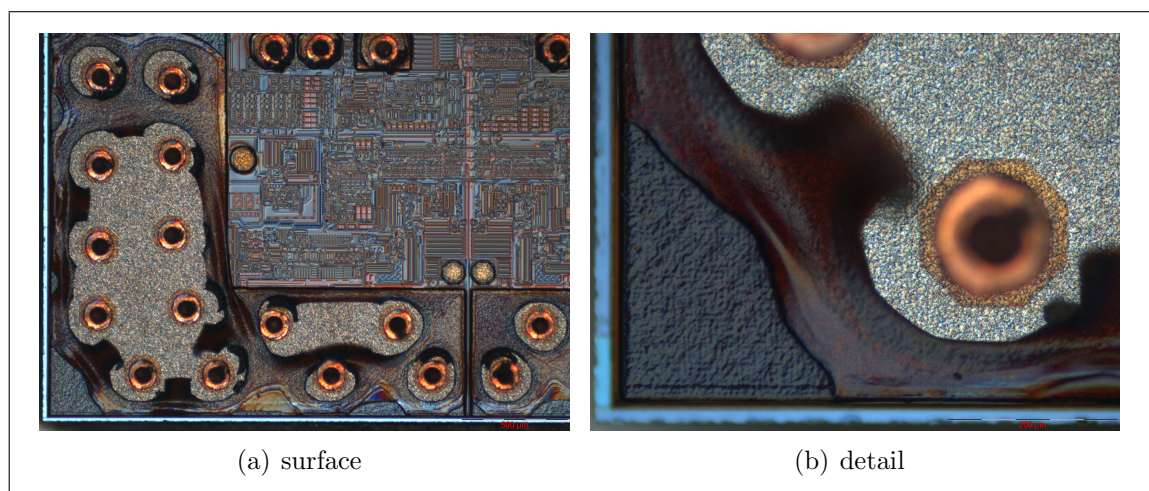


Figure 4.13.: Reflected-light micrographs of a device after preparation with DETA-NMP. The metallisation is in perfect shape and the polyimide is already partially removed and has no adhesion to the underlying metal any more.

### 4.3.2. Transfer Hydrogenolysis and Aminolysis

#### 4.3.2.1. Primary Screening of the Hydrogen Donors

For the primary screening of the three hydrogen donors, tetralin, indoline, and dihydroanthracene, the reflux equipment was used (see section 4.1.1). More informations about the reagents (suppliers and physical properties) are listed in table A.2 in the appendix.

Of the three hydrogen donors tetralin did not cause any observable changes in the semiconductor package. This may be connected to the low boiling point at ambient pressure. Indoline was difficult to handle without applying pressure because it showed severe retardations of boiling when refluxed. This occurred although the solvent was boiling constantly at reflux. Due to this problem the temperature had to be reduced so that the solvent was just lightly boiling at 501 K. The mould compound became soft and could be easily removed. 9,10-Dihydroanthracene, which is solid at room temperature, had a different effect on the devices. The moulding compound became brittle, instead of the swelling effect of the other two hydrogen donors had.

None of the hydrogen donors showed the expected reaction with the devices.

#### 4.3.2.2. High Pressure Asher

All three hydrogen donors and the tetralin-ethanolamine mixture were tested. In case of 9,10-dihydroanthracene 20 g were used for the experiments. For the mixture of tetraline and ethanolamine 12 mL of each reagent were mixed in the test tube.

The effect on the moulding compound was the same as after the reflux series. The reaction time could be reduced from 18 to 10 hours. The effects Pareto charts for the three responses (number of devices, polyimide, and metallisation) are shown in figure 4.14.

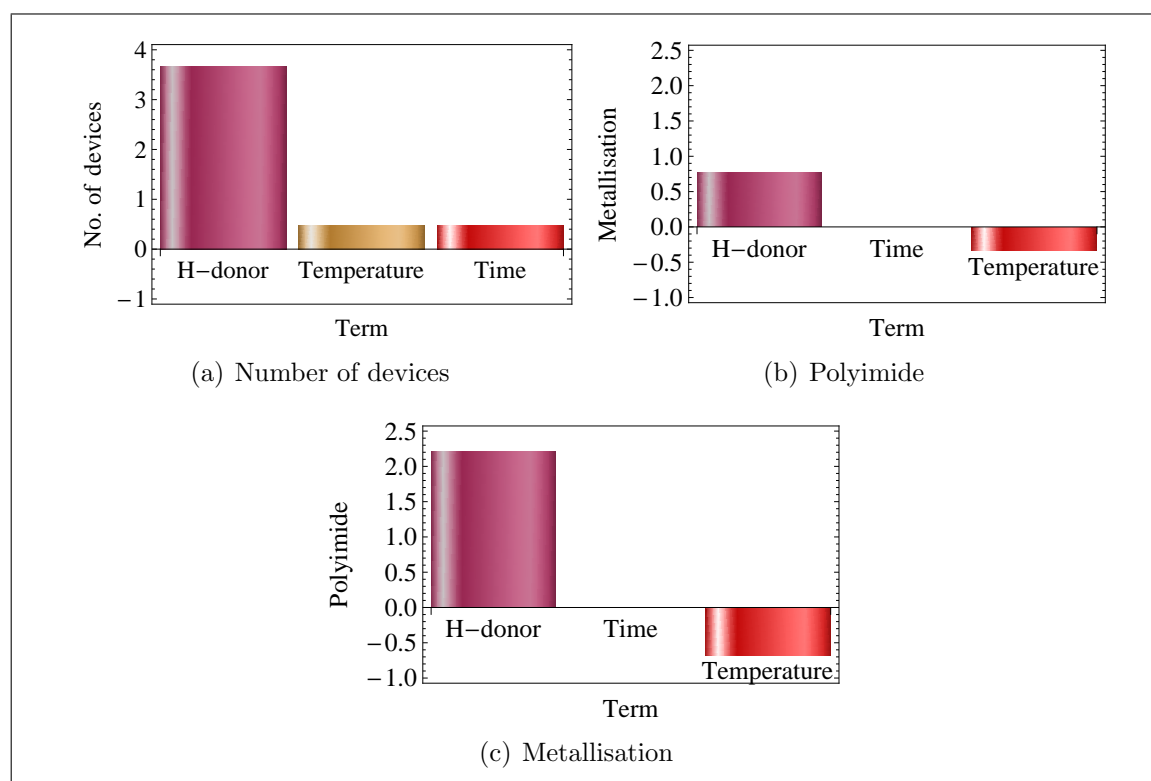


Figure 4.14.: Effects Pareto charts for the HPA hydrogenolysis and aminolysis series

#### 4.3.2.3. Parr Pressure Vessel

For all experiments a total volume of 50 mL solvent was used. If not stated differently the mixture ratio was always 50:50 volume percent (vol%). 70 bar nitrogen load was added before heating to 523 K. After 10 h and cooling over night the mould compound was manually removed, which required only very little if no force at all, as

#### 4. Experimental Setup and Results

in some cases the mould compound was already removed during the reaction itself. The devices were cleaned with acetone and dried with a stream of gaseous nitrogen.

9,10-Dihydroanthracene (DHA) could not be used at all during the Parr pressure vessel series, as it tends to sublime inside cavities and feed lines of the vessel during cool down and cleaning is nearly impossible.

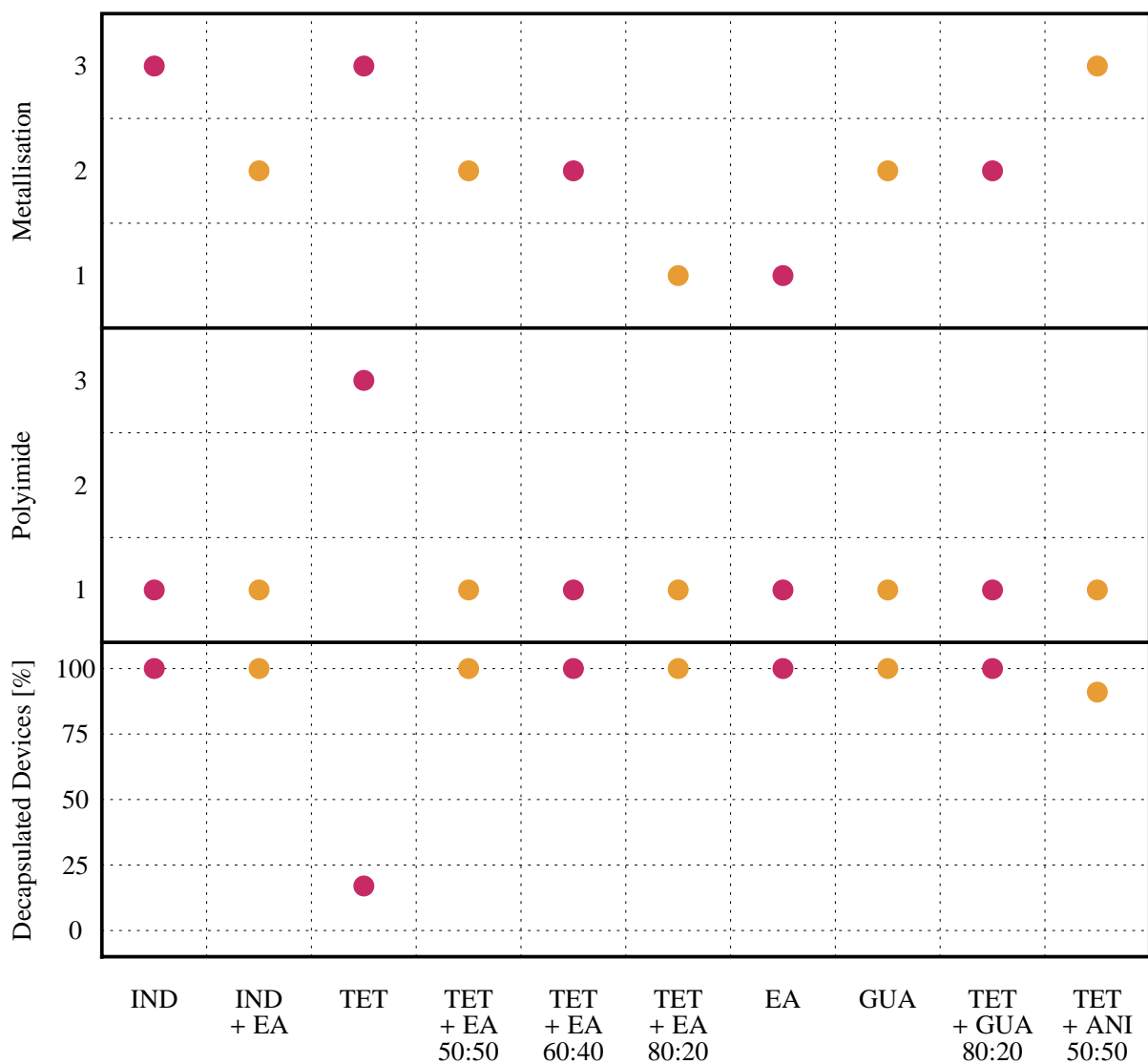


Figure 4.15.: Results of the transfer hydrogenolysis and aminolysis combination runs at 523 K

The pure hydrogen donors showed the same outcome as in the previous experiments,

#### 4. Experimental Setup and Results

where indoline always showed a good swelling behaviour (see figure 4.16) and tetraline was the opposite and did not show any effect at all.

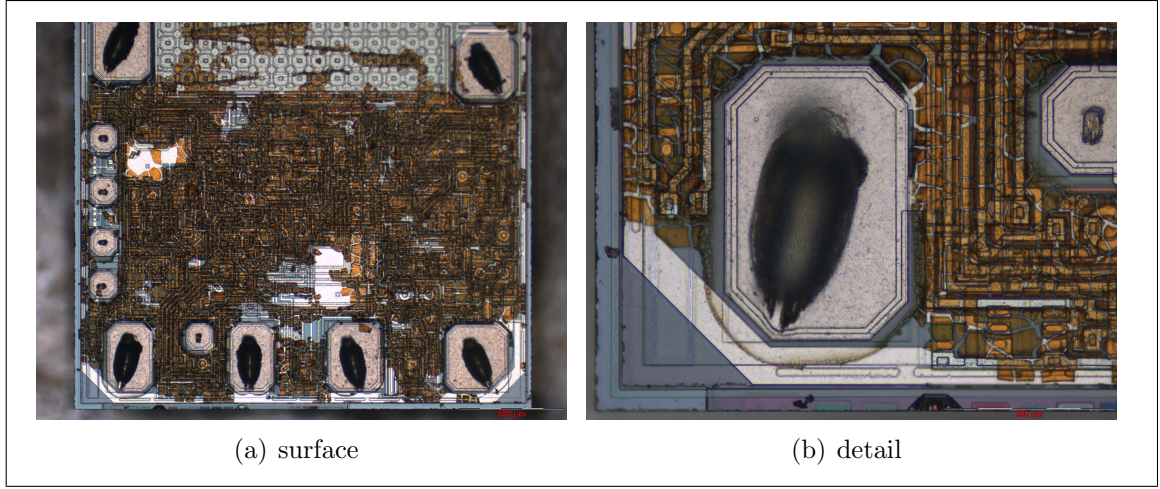


Figure 4.16.: Reflected-light micrographs of a device decapsulated with pure IND. The polyimide shows a giraffe like structures, which is due to temperature caused tightening.

The first amine which was used for a series of combination was ethanolamine (EA), a primary amine postulated to have a magnifying effect in combination with tetraline. It showed a high increase in the percentage of decapsulated devices, but the metallisation was harmed (see figure 4.17). This effect was attributed to decomposition of the amine, for example to ammonia.

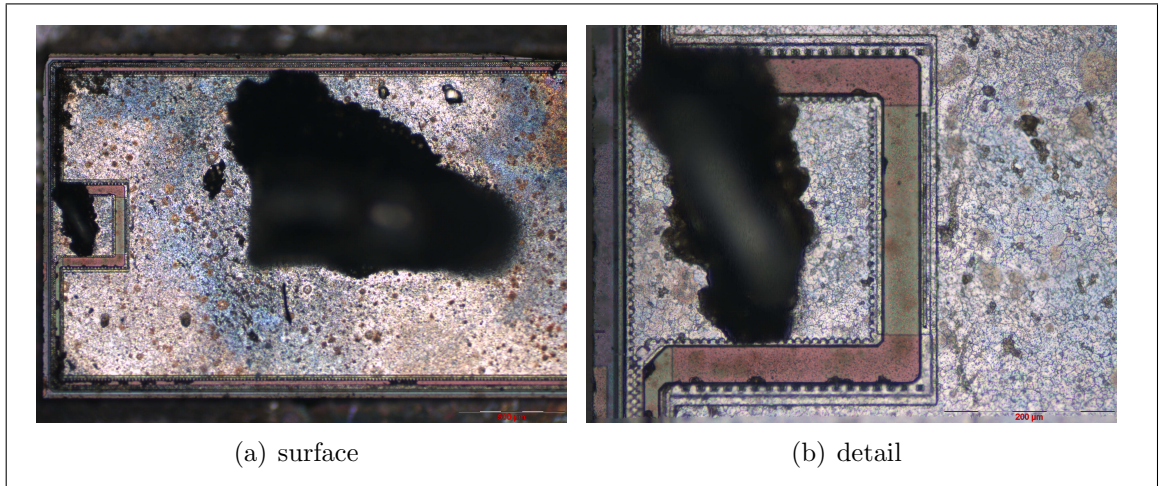


Figure 4.17.: Reflected-light micrographs of a device decapsulated with TET in combination with EA. Attack of the aluminium metallisation is visible.



#### 4. Experimental Setup and Results

It was expected, that to exclude decomposition, secondary or tertiary amines, which have an increased stability at higher temperatures, could be used to gain an advantage during transfer hydrogenolysis. 1,1,3,3-Tetramethylguanidine (GUA) and aniline (ANI) were used for this purpose as they were already available. GUA showed only little discolouration and a better outcome as EA, but still it was not satisfying. ANI, which although a primary amine, is more stable, showed a positive influence on the swelling behaviour and the metallisation was in a perfect condition (see figure 4.18. This was first evidence, that more stable amines could lead to better results without harming the metallisation.

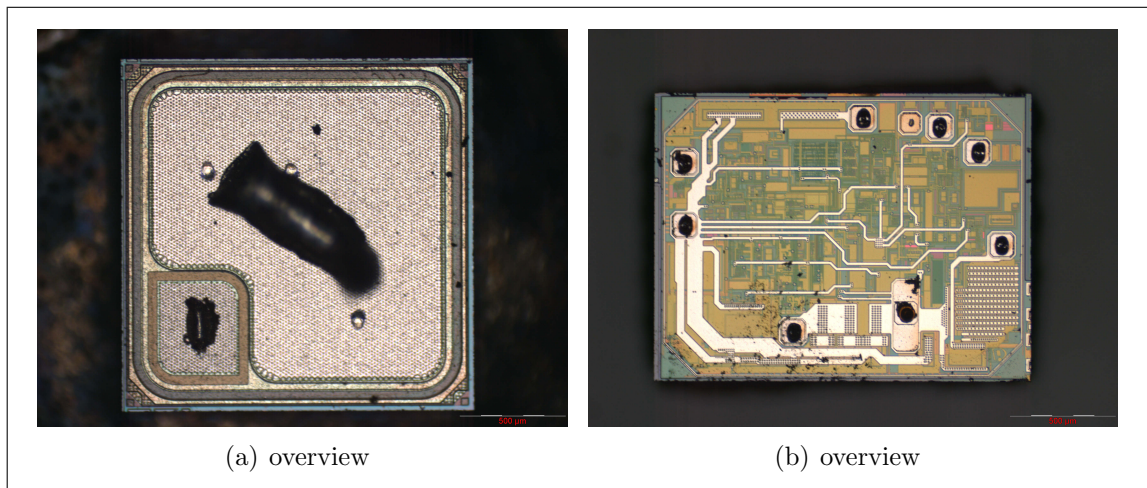


Figure 4.18.: Reflected-light micrographs of devices decapsulated with a mixture of TET and ANI. The metallisation is in perfect shape and only little mould compound residues can be seen.

In general all amines showed not swelling alone, but also a reaction with the mould compound at the surface of the devices. These were the first cases of a physical effect combined with a chemical reaction (aminolysis).

A series of combinations of indoline (IND) with the solvents from the solvolysis experiments was performed in order to get some information on possible increasing effect on the mould compound (see figure 4.19 for the results). The same experimental setup as for the previous series was used and in case of triple combination, like IND + DETA/DMF, the ratio was 50:25:25 vol%.

#### 4. Experimental Setup and Results

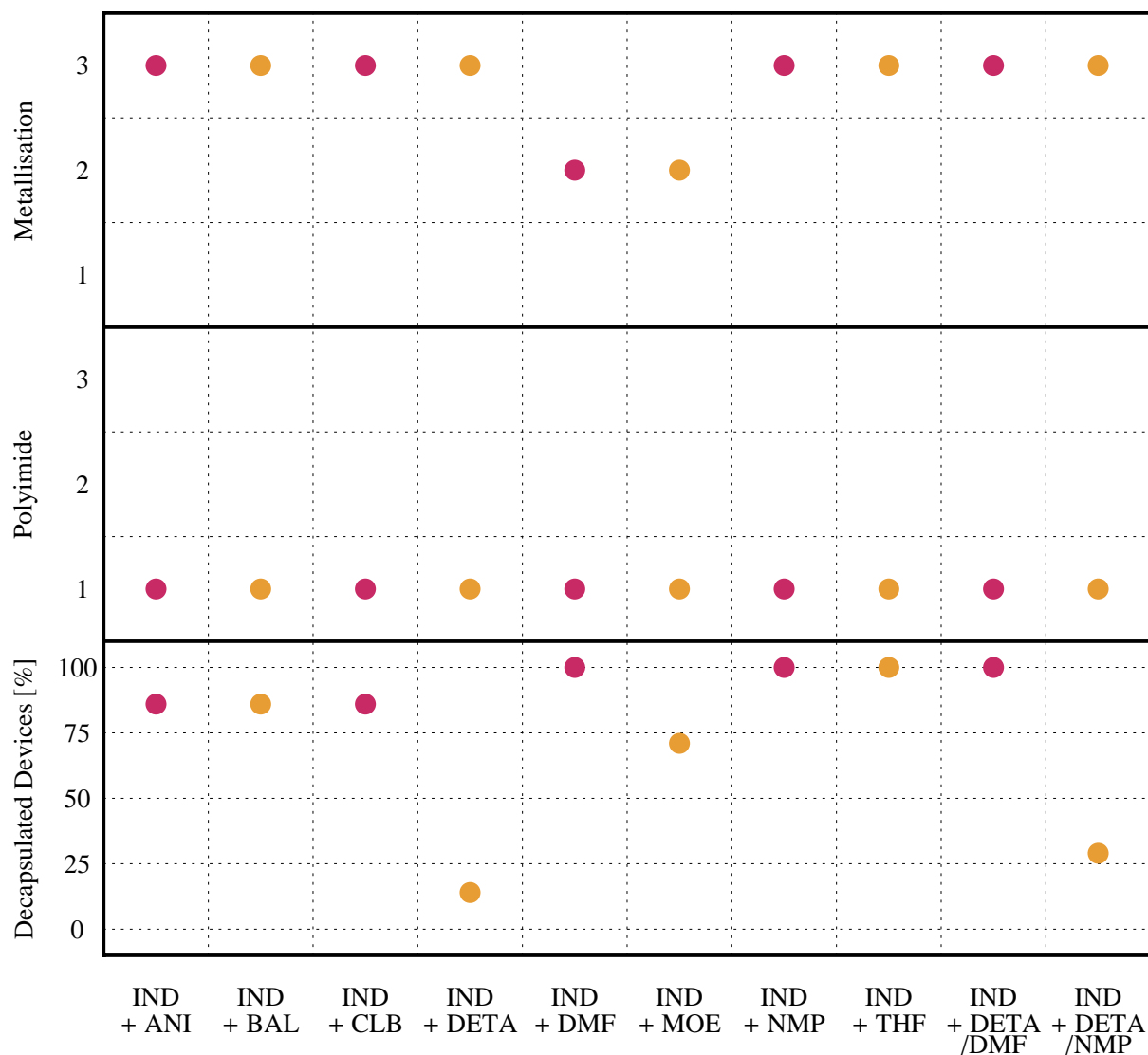


Figure 4.19.: Results of the indoline combination runs at 523 K

The outcome for most of the solvents was nearly the same as for the pure solvents (compare with figure 4.9), although the swelling effect was slightly larger and the mould compound was more easily removed. Only N,N-diethyl-m-toluamide (DETA) showed an unexplainable behaviour. With pure DETA the percentage of decapsulated devices sank to a minimum, but using a DETA/DMF combination it was at 100 %.

IND and DMF showed slight discolourations and mould compound residues, but in a triple combination with DETA the result was better and no discolourations could be observed (see figure 4.20).

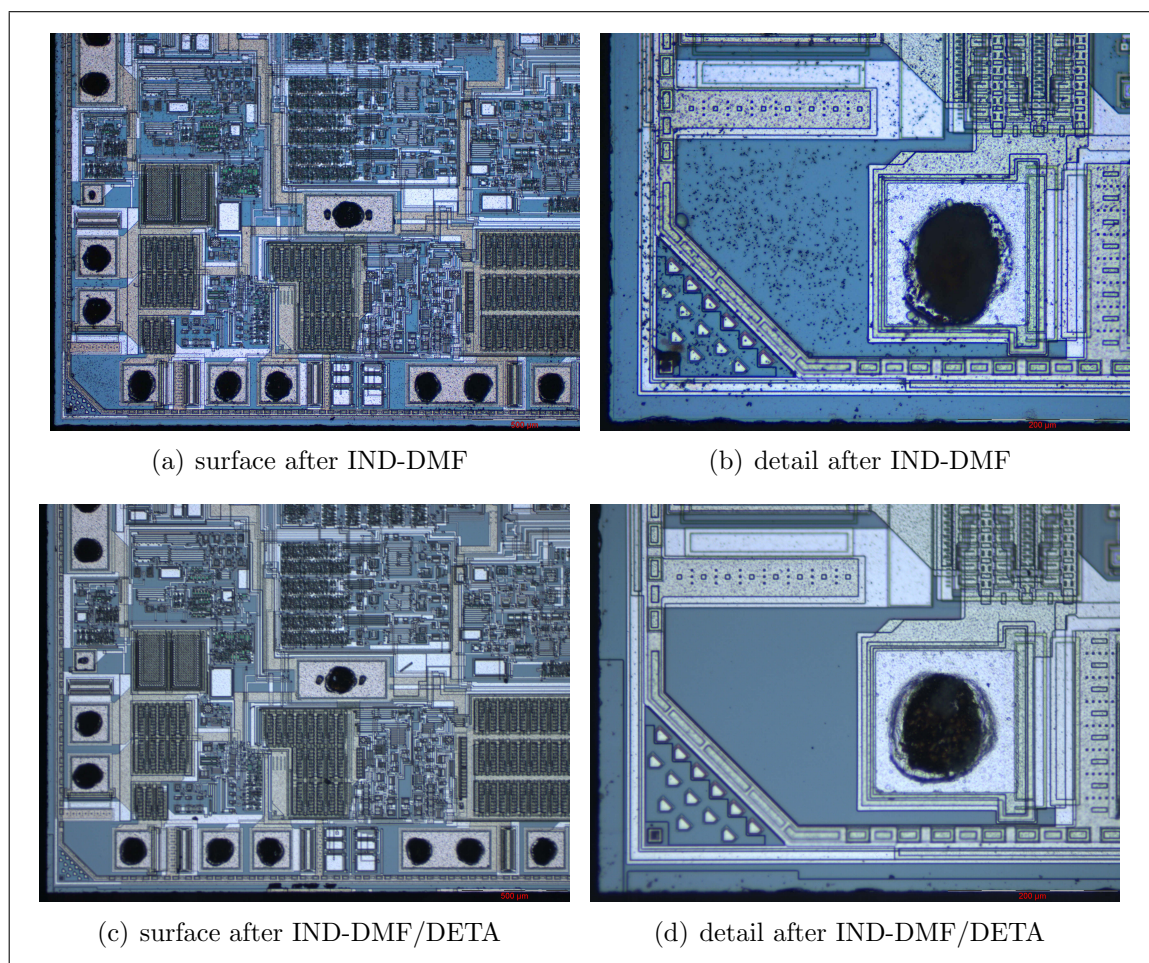


Figure 4.20.: Reflected-light micrographs after preparation with IND-DMF or IND-DETA/DMF.

### 4.3.3. Sub- and Supercritical Solvents

#### 4.3.3.1. Parr Pressure Vessel

In all reactions the solvent amount was increased to 100 mL in total (from 50 mL as used in the solvolysis/transfer hydrogenolysis experiments). This is necessary as it is believed that in this cases the solvent volume becomes limiting quite quickly. Only deionised water was used.

The first series was water at two different temperatures and in combinations with a possible catalyst (sodium carbonate  $\text{Na}_2\text{CO}_3$ ). Also three reaction experiments similar to supercritical water oxidation (SCWO) were conducted with  $\text{H}_2\text{O}_2$  as main

#### 4. Experimental Setup and Results

oxidizing agent, but the reaction temperature was only 523 K. Both  $\text{Na}_2\text{CO}_3$  and  $\text{H}_2\text{O}_2$  were added in weight per cent (w%) ratios. No nitrogen load was added, as water itself has a very high vapour pressure.

After 10 h and cooling over night the mould compound was manually removed if possible. As water does not show a swelling effect, but makes the devices brittle the manual removal was difficult. After all reactions, which involved water, the devices were cleaned using deionised water and tetrahydrofuran, and afterwards dried with a stream of nitrogen.

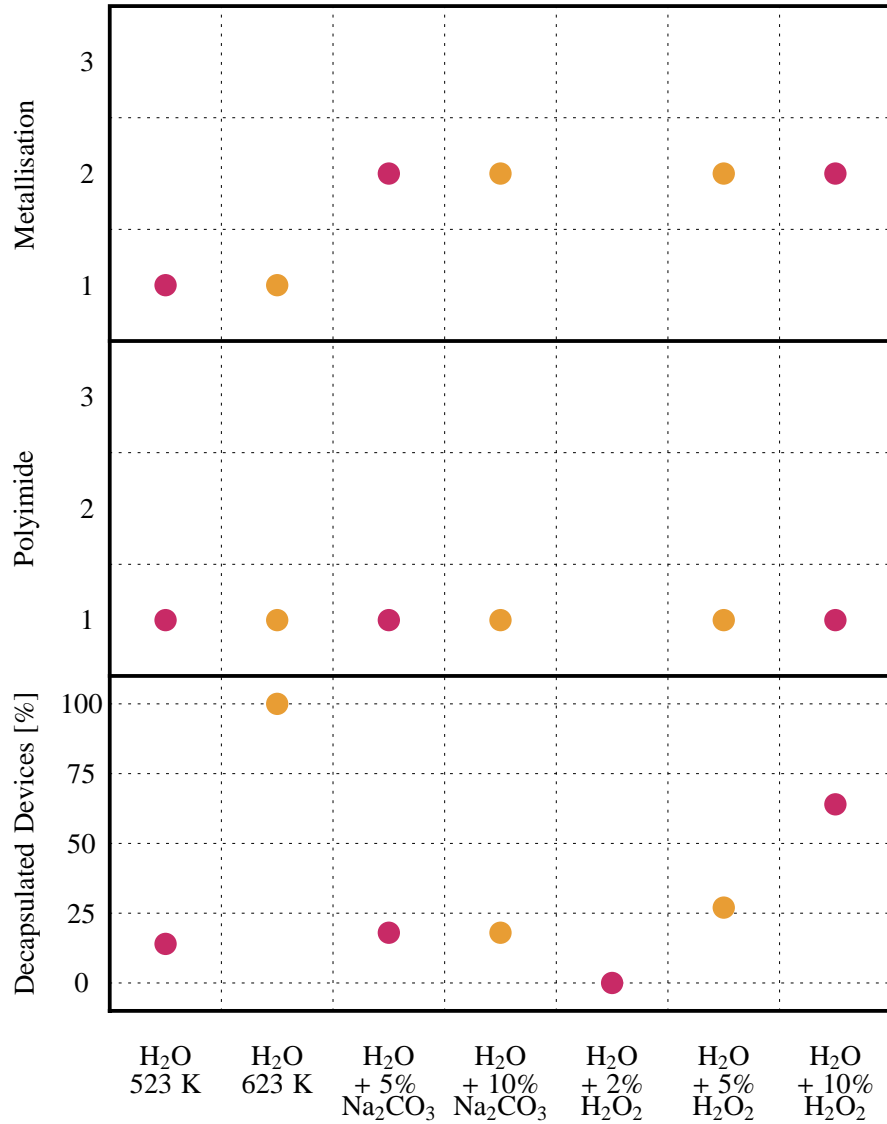


Figure 4.21.: Results of the subcritical water runs in combination with salt or hydrogen peroxide at 523 K (except for one  $\text{H}_2\text{O}$  run at 623 K)



#### 4. Experimental Setup and Results

The results in figure 4.21 show that especially pure water showed a severe attack on all metal parts, and the devices were severely damaged. Decapsulation was possible and the mould compound was completely disintegrated at 623 K. Only the filler particles remained on the device. At 523 K the reaction occurred only at the surface and was not sufficient enough to decapsulate a sufficient number of devices.

$\text{Na}_2\text{CO}_3$  showed only little catalysing effect, but the metallisation showed less artefacts as after use of pure water, although it was severely polluted with mould compound and solvent residues (see figure 4.22).

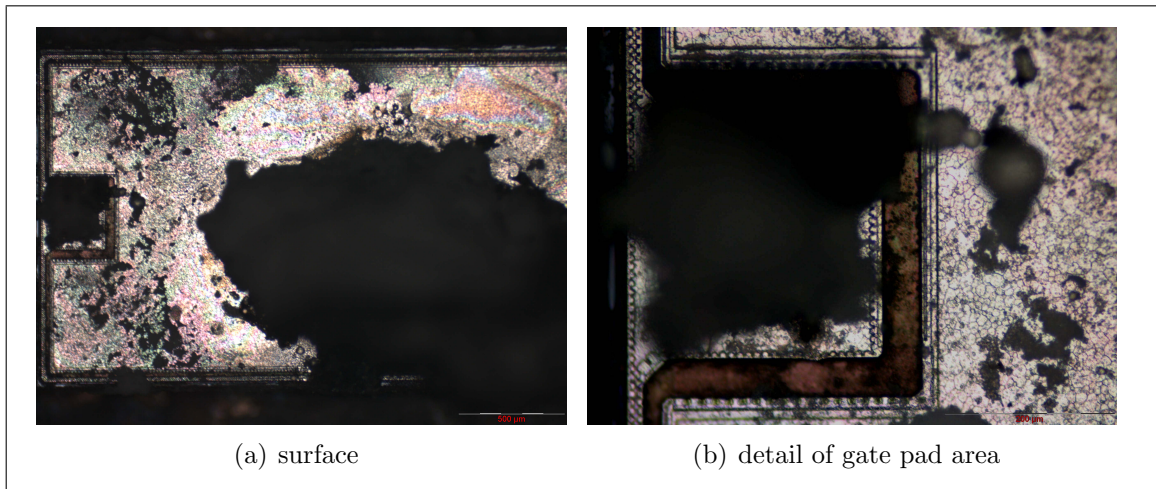


Figure 4.22.: Reflected-light micrographs of a device decapsulated with a mixture of deionised water with 1 w%  $\text{Na}_2\text{CO}_3$

An increased amount of  $\text{H}_2\text{O}_2$  led to an increase in the percentage of decapsulated devices. The metallisation showed discolourations independent of the amount of hydrogen peroxide in use (see figure 4.23).

#### 4. Experimental Setup and Results

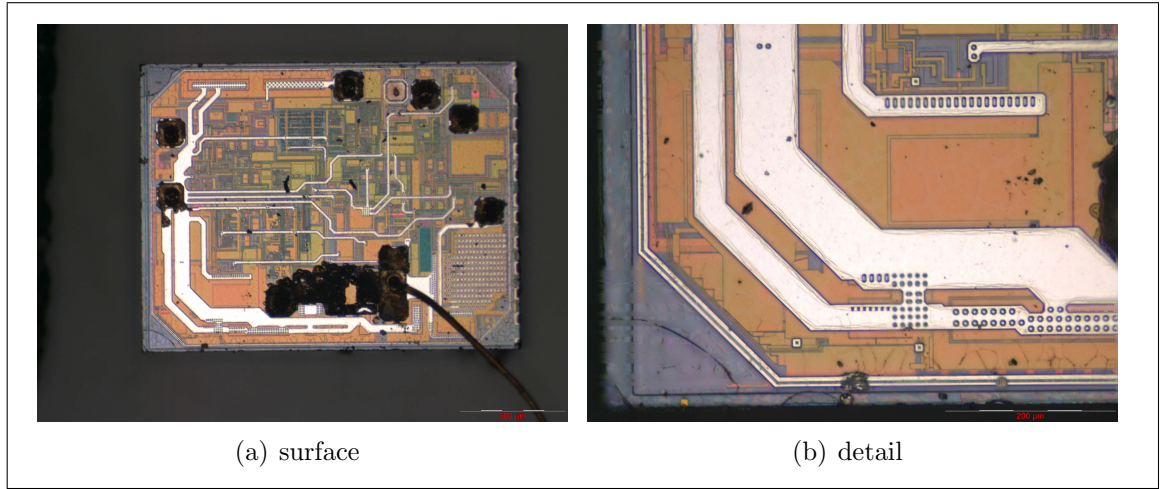


Figure 4.23.: Reflected-light micrographs of a decapsulated device using deionised water with 10 w% hydrogen peroxide.

Subcritical water was also used for some combinations with other solvents or reagents from previous experiments. For these experiments 75 mL of water and 25 mL of reagent were used. The other experimental settings were the same as in the previous water series.

#### 4. Experimental Setup and Results

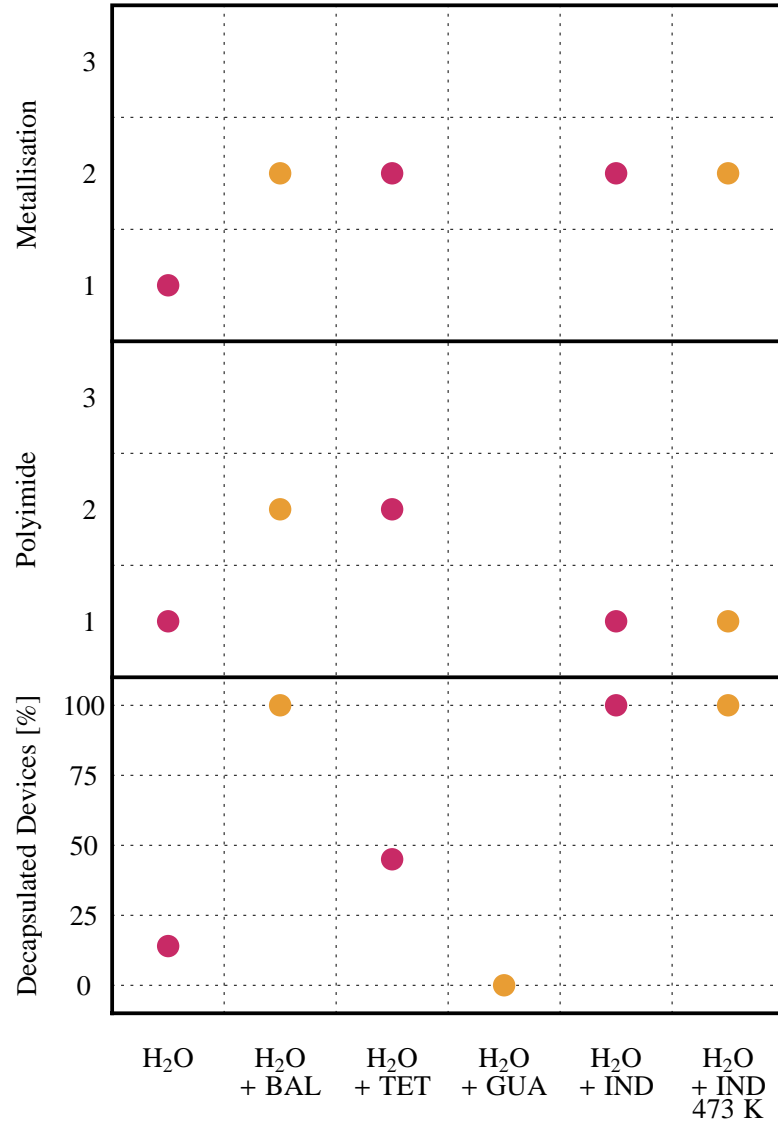


Figure 4.24.: Results of the subcritical water runs in combination with other solvents/reagents at 523 K (except for H<sub>2</sub>O+IND at 473 K)

BAL, TET, and IND in combination with water all showed an increase in metallisation quality after decapsulation (compare with figure 4.24, see figure 4.25 for an example). GUA in combination with water could not help to decapsulate the devices at all, because it completely disintegrated.

#### 4. Experimental Setup and Results

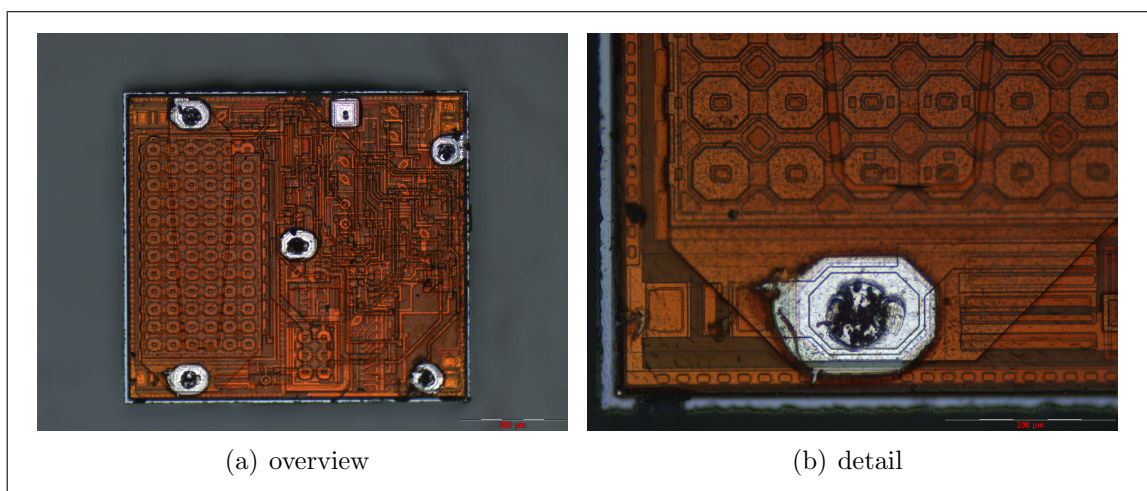


Figure 4.25.: Reflected-light micrographs of a device decapsulated using a mixture of deionised water and BAL. The polyimide remained on the die surface.

The combination of water with indoline showed such extreme swelling that hardly any mechanical forces were needed to remove the mould compound. Some of the packages showed an increase in the volume of the mould compound of about 300 %. Because of this immense swelling capability a run at 473 K was performed, which also showed a large effect (see figure 4.26 for examples). This was the only experiment in which the reaction temperature could be reduced to the wished-for 473 K. This is also an important starting point for further investigations.

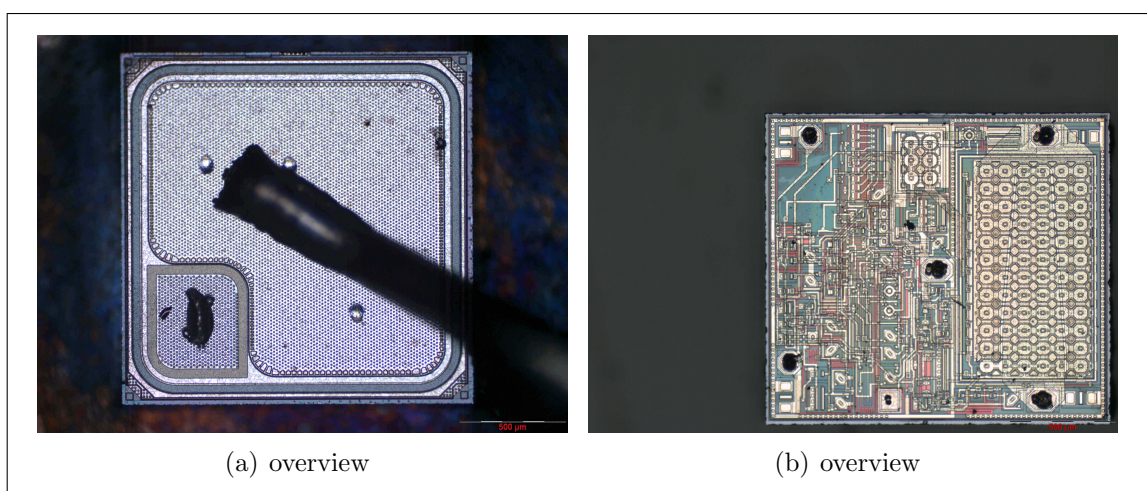


Figure 4.26.: Reflected-light micrographs of two devices decapsulated with a mixture of deionised water and indoline at 473 K.

Supercritical methanol was also used in volumes of 100 mL. After 10 h and cooling

#### 4. Experimental Setup and Results

over night the mould compound was manually removed using tweezers. The cleaning was further enhanced in comparison to the previous experiments as now a combination of tetrahydrofuran, followed by deionised water, and again tetrahydrofuran was used. After each step the devices were dried with a stream of nitrogen. This improved the cleaning performance immensely.

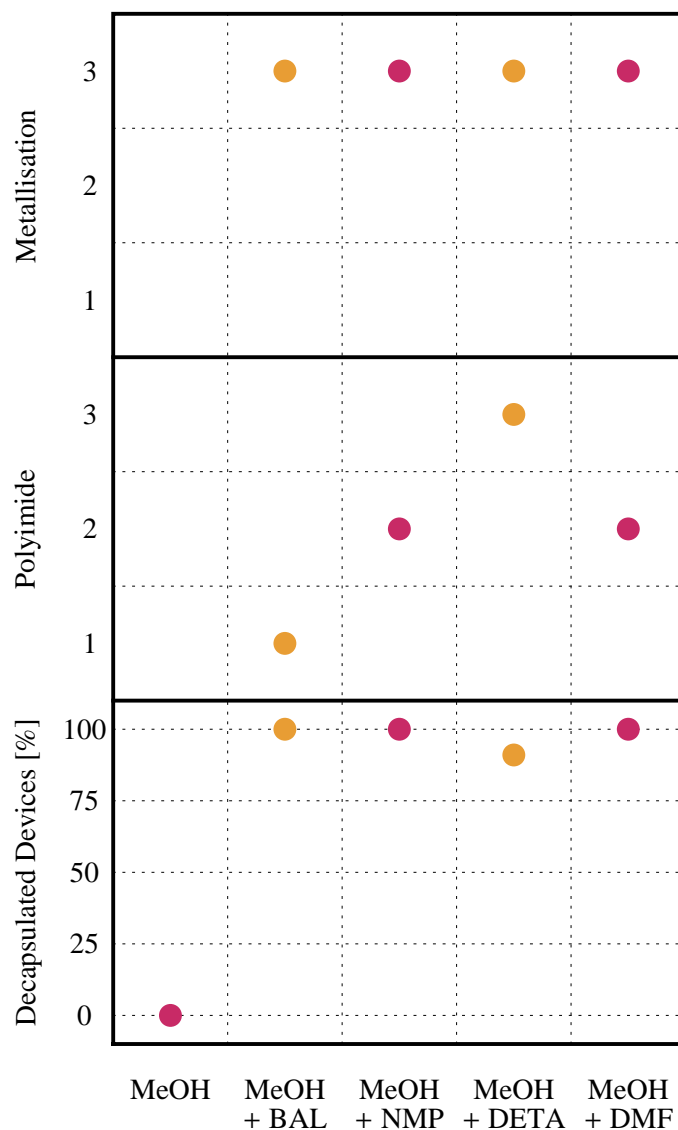


Figure 4.27.: Results of the subcritical methanol runs in combination with other solvents/reagents at 523 K

Methanol (MeOH) alone did not show any observable effect on the mould compound (see results in figure 4.27). But in combination with other solvents all used devices could be decapsulated. The mould compound was very easy to remove and soft, and



the metallisation was in perfect condition. Especially interesting is the combination of MeOH and N,N-diethyl-m-toluamide (DETA). When used alone none of the two shows any interaction with the device, but in combination there was a huge effect (compare with figure 4.9 and see figure 4.28 for an example).

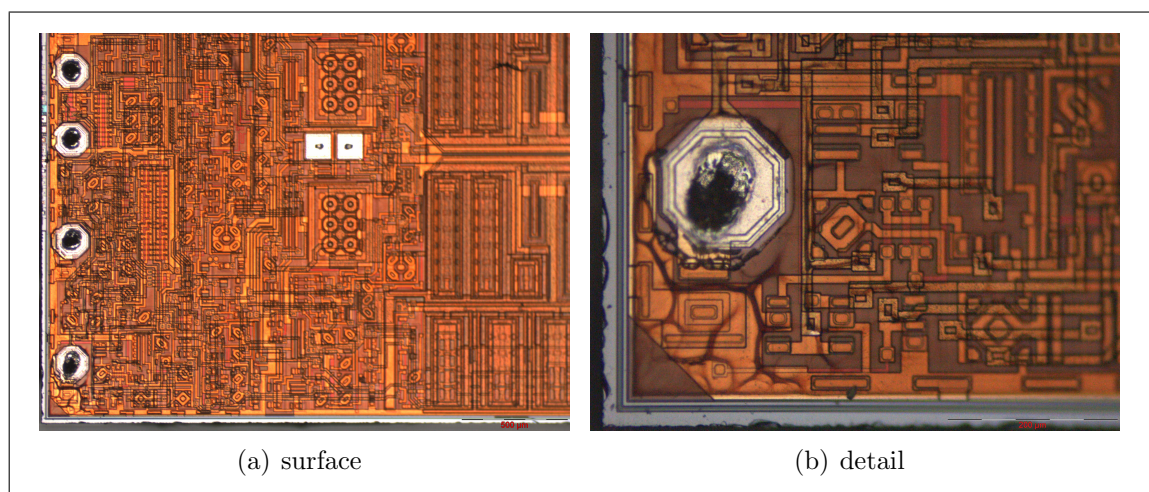


Figure 4.28.: Reflected-light micrograph of a device decapsulated using a mixture of MeOH and DETA. The polyimide layer remained on the die surface.

### 4.3.4. Glycolysis

#### 4.3.4.1. Parr Pressure Vessel

For the glycolysis experiment a weight ratio of 20:100 device : diethylene glycol (DEG) was used. The amount of titanium (IV) n-butoxide (TBT) catalyst was altered between 0,1 and 0,5 weight per cent (w%). No nitrogen pressure load was added, but the vessel was purged with nitrogen before starting the heating cycle to a maximum temperature of 523 K. This temperature was kept for 14 h and afterwards the vessel was cooled to room temperature over night. The devices were cleaned with tetrahydrofuran, followed by deionised water, and again tetrahydrofuran. After each step the devices were dried with a stream of nitrogen.

No observable effect could be seen on the devices. It is believed that the TBT reacted with the extracted additives of the moulding compound before it had a chance to react sufficiently with the resin. Due to safety reasons the amount of catalyst could not be increased, as it is highly inflammable.

## **4.4. Analytical Methods**

### **4.4.1. Analysis of Devices**

In general all devices were inspected using stereoscopic and reflected-light optical microscopy after preparations. In some cases scanning electron microscopy (SEM) was used in order to gain more detailed information.

In order to inspect possible changes to the moulding compound, embedded cross section investigations were conducted.

#### **4.4.1.1. Optical Microscopy**

The optical micrographs of the devices were taken with a Nikon Eclipse L200 reflected light microscope.

#### **4.4.1.2. Scanning Electron Microscopy**

Two different field emission scanning electron microscopes were in use, namely a Hitachi S-4700 (coupled with a EDAX DX-4 system) and a Hitachi S-4800. The samples were positioned on a carbon pad on a specimen holder. To gain the necessary degree of conductivity all devices were connected to the carbon pad using conductive silver (Acheson Silver Electrode 1415M) and sputtered with different amounts of gold using a Cressington 208HR high resolution sputter coater coupled with a MTM-20 high resolution thickness controller. The thickness of the gold is in general lower for EDX analysis (about 2 nm) and higher for surface analysis (up to 4 nm).

#### **4.4.1.3. Focused Ion Beam**

A FEI Helios Nanolab DualBeam system was used for the focused ion beam (FIB) preparations. Gallium ions are used to mill cavities into the sample surface at a working distance of 4 mm. No process gas was added.

### 4.4.1.4. **Scanning Acoustic Microscopy**

A Sonoscan D-9000 in C-SAM scan mode, which is a reflection mode, was used to generate the shown micrographs. For the "front through die" micrographs the copper backside of the device were removed combining chemical etch and mechanical grinding.

### 4.4.2. **Analysis of the Reaction Solutions**

In order to obtain more information about the reaction progress and possible reaction types, different analytical methods were used.

#### 4.4.2.1. **UV-Vis Spectroscopy**

A Varian Cary 50 UV-Vis spectrophotometer was used to measure two reaction solutions from the High Pressure Asher experiments, namely N-diethyl-m-toluamide (DETA) and 2-methoxyethanol (MOE). Those samples were compared to the pure solvents. Data was collected in a range between 800 to 450 nm at a scan rate of 24000 nm/min. and a data interval of 5 nm. The obtained data can be seen in figures 4.29 and 4.30.



#### 4. Experimental Setup and Results

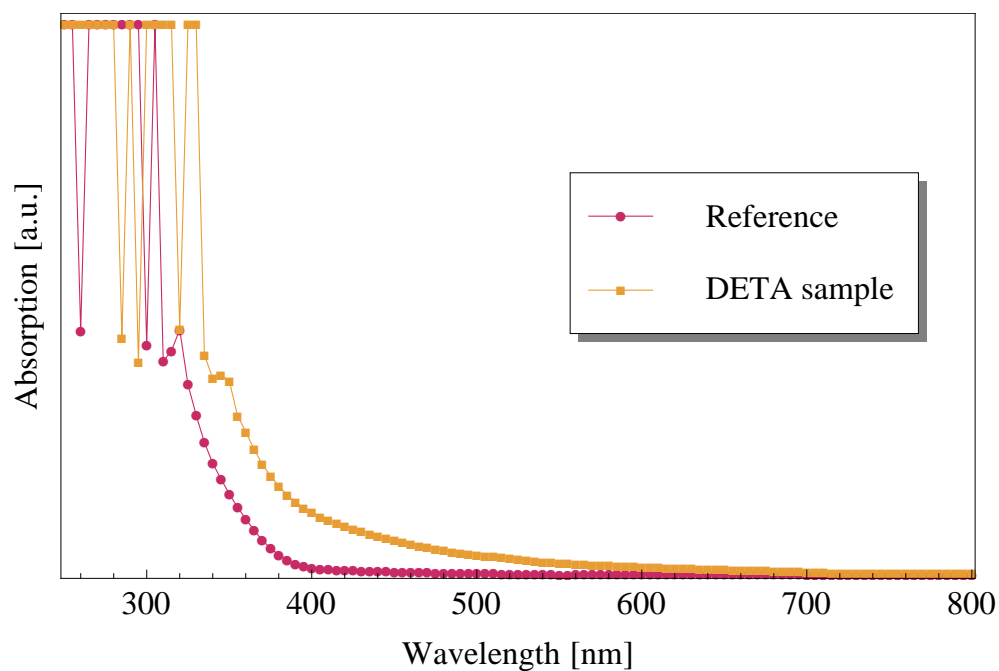


Figure 4.29.: UV-Vis spectra of a HPA DETA sample and a pure solvent reference

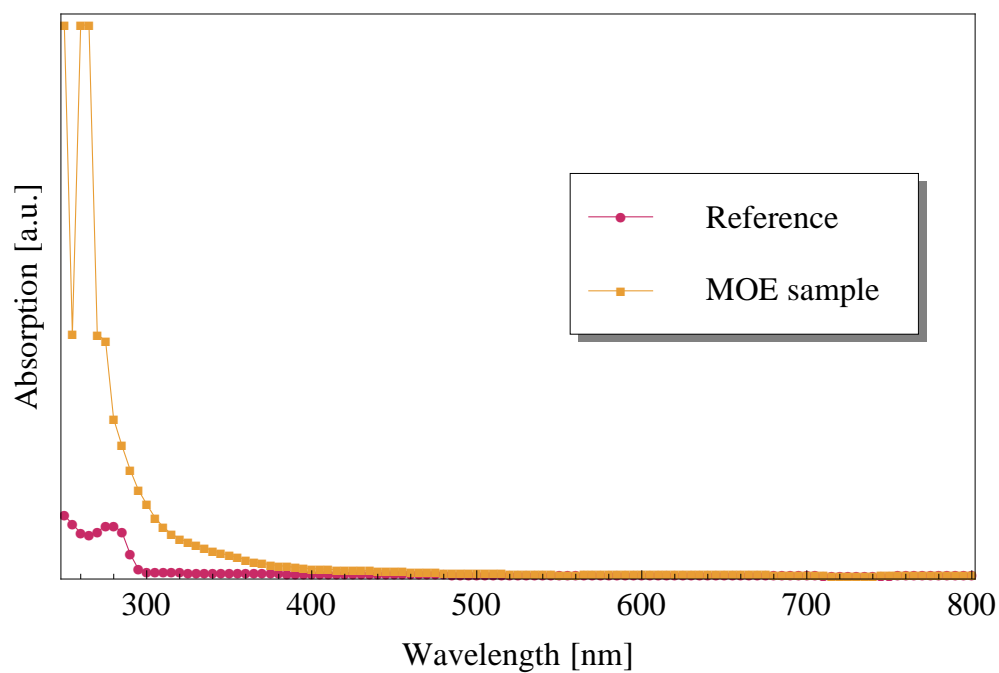


Figure 4.30.: UV-Vis spectra of a HPA MOE sample and a pure solvent reference

The spectra showed an increase of absorption in the solvents after usage, which proved the existence of low molecular species, but did not give any information

about their nature. This is the reason why only two of the solvents used in the HPA series were analysed as it was believed that the outcome of all the solvents would be similar. Hence other analytical methods were necessary to gain more information.

### 4.4.2.2. High Performance Liquid Chromatography

A high performance liquid chromatography (HPLC) setup (HPLC 1100 by Agilent) was used to analyse the liquids after processing devices in the High Pressure Asher (HPA). The method informations are given in table 4.9. The goal was to search for low-molecular species which could afterwards be further investigated with a GC-MS system. For these measurements, runs R3 and R5 from the HPA series were used (see table 4.1 for more information), because they did not show too severe reactions and could be analysed easily. The liquid samples were diluted 1:10 with tetrahydrofuran except for two samples of run R5 (using aniline and methoxyethanol), which were diluted 1:50 with tetrahydrofuran.

Table 4.9.: HPLC method information

parameter	setting
column	PLgel 5 $\mu$ 100 Å(L=600 mm, I.D.=7,7 mm)
column flow	1 ml/min
time	35 min
solvent	80% tetrahydrofuran and 20% methanol (isocratic)

In all nine samples low-molecular species could be found using HPLC coupled with a diode array detector. The chromatograms are given in figures A.2 to A.10 in the appendix. Again information about the specific nature of the species could not be obtained.

### 4.4.2.3. Gas Chromatography coupled with a Mass Spectroscopy Detector

A HP 5890 gas chromatograph (GC) coupled with a mass spectroscopy (MS) detector was used. The solvent samples were centrifuged for 5 minutes and thereafter filtered using a hydrophilic Acrodisc 13 mm Syringe filter with a 0,2  $\mu$ m GHP membrane by Pall. The solutions were diluted 1:1000 with methanol before injected into

the GC system.

A method by Braun et al. was adjusted for the settings of the GC system [30]. The injector temperature was set to 573 K and the injector split ratio was 1:20 and the gas flow was measured using a bubble meter to adjust the right split. A gas flow rate of 2.2 ml/min and a capillary column with 30 m length and a diameter of 0,32 mm was used. The column temperature began at 373 K followed by a slow heating ramp at 1.5 K/min to a temperature of 433 K. Then another ramp at 15 K/min to a maximum temperature of 573 K was performed.

Due to problems with the volatility of the solvents no reproducible results were attained.

### 4.4.2.4. Fourier Transformation Infrared Spectroscopy

In order to gain information about the reaction progress, a transmission Fourier Transformation Infrared (FTIR) of the reaction solvents was performed. A Mattson 3000 FTIR spectrometer with WinFirst software was used and the liquid samples were applied on different substrates to get a uniform layer. Teflon or nitrocellulose filters showed very poor results and hence couldn't be used. The best choice were non doped silicon wafers without thermal oxide, which have a favorable transmission over a large area (see figure A.11 in the appendix).

Spin coating was used to deposit and gain a uniform liquid layer of the solvent. 500  $\mu$ L of the solvents were pipetted on the wafer pieces, which were cleaned with acetone prior to use. The speed during spin coating was at 1000 rpm (round per minute), which was held for 20 seconds. An acceleration rate of 1000 rpm in 3 seconds was employed. After spin coating the samples were dried using an infrared lamp.

It was very difficult to attain uniform layers due to the difficulty to vaporise, and the surface tension of the solvents. The problems during sample preparation made it impossible to gain reliable results.

## 5. Case Studies

In this chapter some special case studies are described, which all incorporate new copper technologies. For none of them a suitable decapsulation method was known.

### 5.1. Devices with Bare Copper Metallisation and Soldered Top Die

The semiconductor devices in question (SiC JFET technology) are a typical example which face severe problems during decapsulation with inorganic acids due to their copper metallisation. The last metallisation layer is bare copper with no coating and in addition to that a soldered top chip with aluminium metallisation is present. Because of the presence of a top chip it is not possible to laser decapsulate as far as needed during standard decapsulation procedure. During the manual chemical etching, which follows laser ablation, over etching occurs since the mould compound thickness is uneven.

The used moulding compound for the devices was an ortho cresole novolac (OCN) with a phenol novolac (PN) hardener. The package type is a PG-TO220-3-1 (see figure 5.1) with a heat sink.

## 5. Case Studies

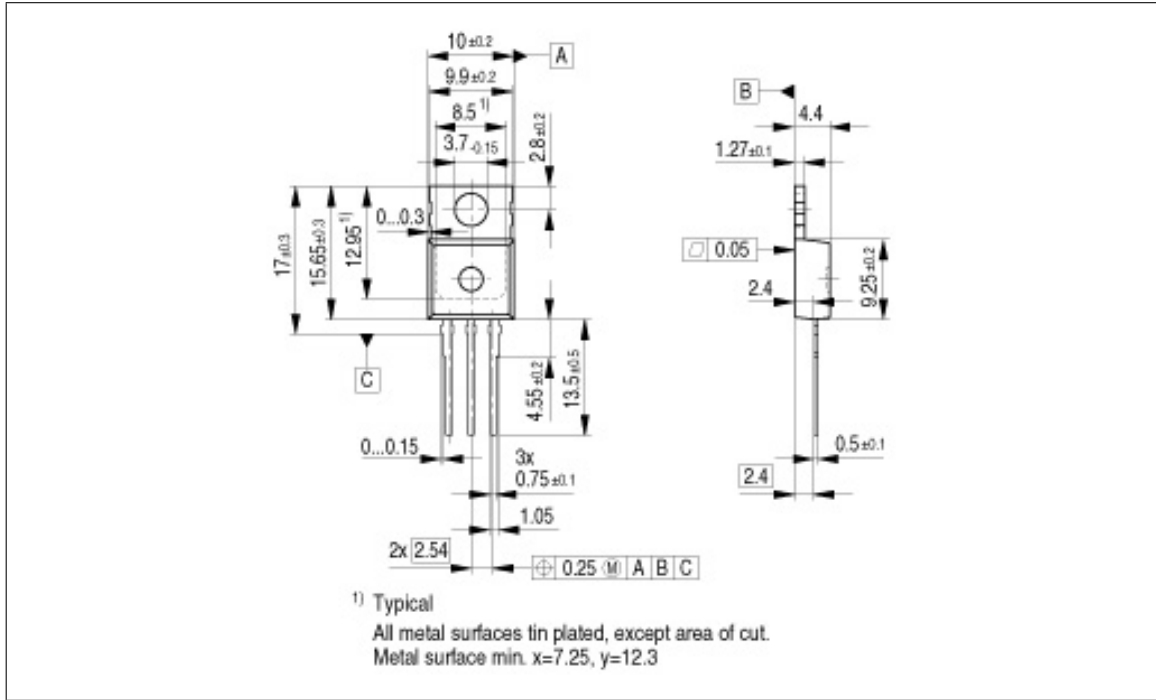


Figure 5.1.: Package Outline of a PG-TO220-3-1. All dimension given in mm. [69]

Two devices were prepared for the first test in different ways. One was prepared by a special laser decapsulation and the other was manually grinded until the wires were cut (see subsection 4.2.1 for more detailed explanation and figure 5.2 for micrographs after preparation). In case of both devices the outstanding leads were cut off, and the solder at the heat sink of the device was removed by grinding until the copper was exposed. After mechanical preparation the devices were immersed into 50 mL of N-diethyl-m-toluamide and refluxed for 9 hours using the standard reflux equipment (see subsection 4.1.1 for the tool description). The mould compound could be removed with some mechanical effort and thereafter the devices were cleaned using acetone and dried with a stream of nitrogen.

## 5. Case Studies

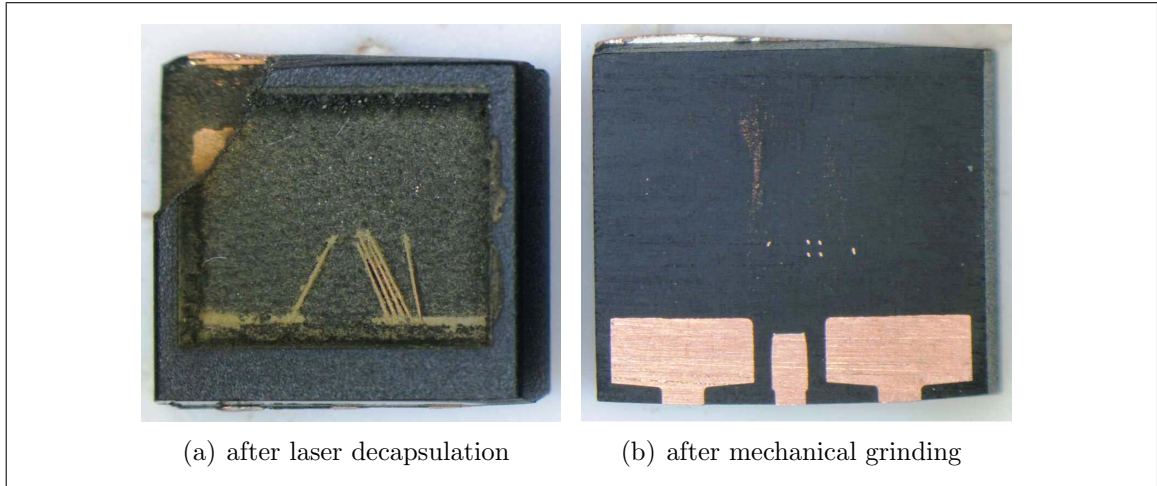


Figure 5.2.: Bare copper devices after preparation prior to solvolysis experiment using N-diethyl-m-toluamide

After the solvolysis preparation the devices were investigated using reflected-light microscopy and scanning electron microscopy (SEM Hitachi S-4700) with an energy dispersive X-ray detector (EDX). The chosen sputtered gold layer had 2 nm thickness.

The results were very similar independent of the prior preparation. In both cases the copper and aluminium metallisation as well as the polyimide could be preserved. Some of the ball bonds remained on the bond pad. In some areas of the devices moulding compound remains could not be avoided.

The copper metallisation appeared to be discoloured after preparation. To gain information whether this was a serious artefact a SEM analysis with EDX was performed, which showed that a layer of copper oxide occurred. This did not limit the microscopical assessment of the copper surface structure, as the thin oxide functions as a passivation layer, and the copper is not harmed (see figures 5.3 to 5.4). The occurrence of copper oxide was also seen on a variety of other devices, so it is not a feature of this bare copper metallisation alone.

## 5. Case Studies

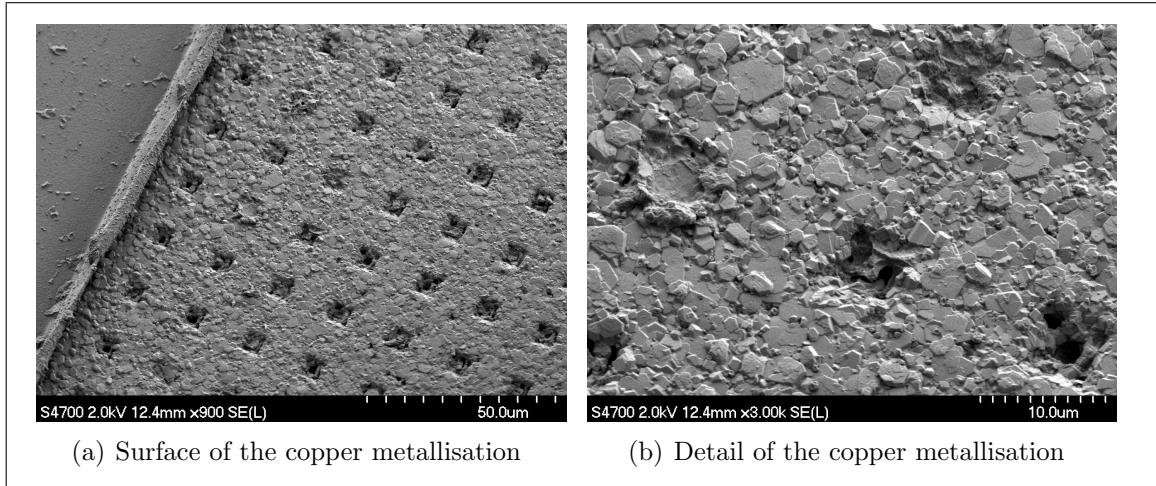


Figure 5.3.: SEM micrographs of the copper metallisation at the base die

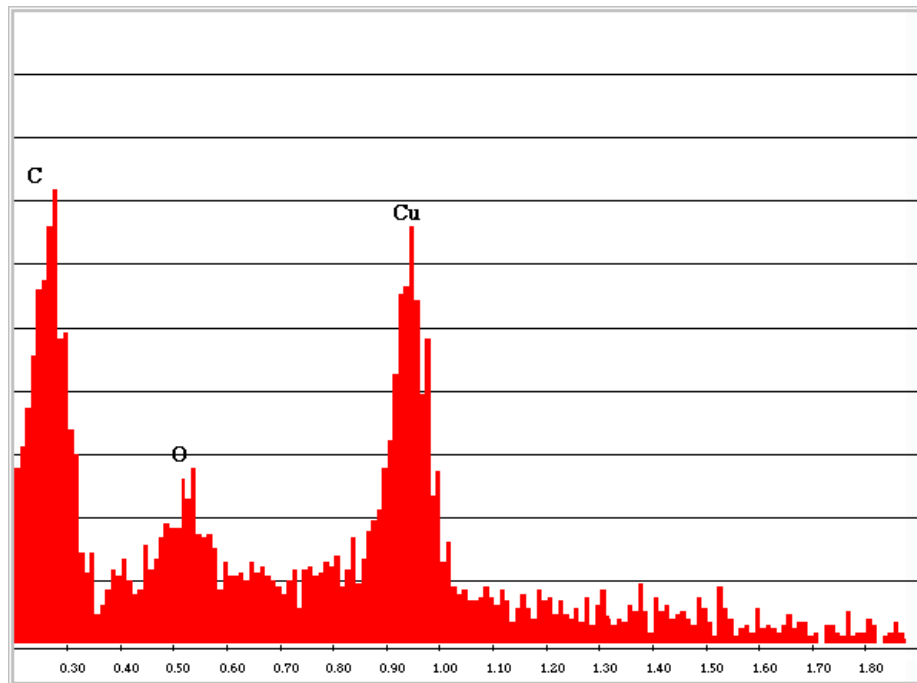


Figure 5.4.: EDX result at the copper metallisation of the base die (excitation energy: 2 kV). The carbon peak results from organic contaminations.

Figure 5.5 shows two decapsulated devices, one using the conventional laser ablation/wet chemical etch (with a mixture of 3 parts fuming nitric acid and 1 part sulfuric acid) combination, and one using the described method involving solvents.

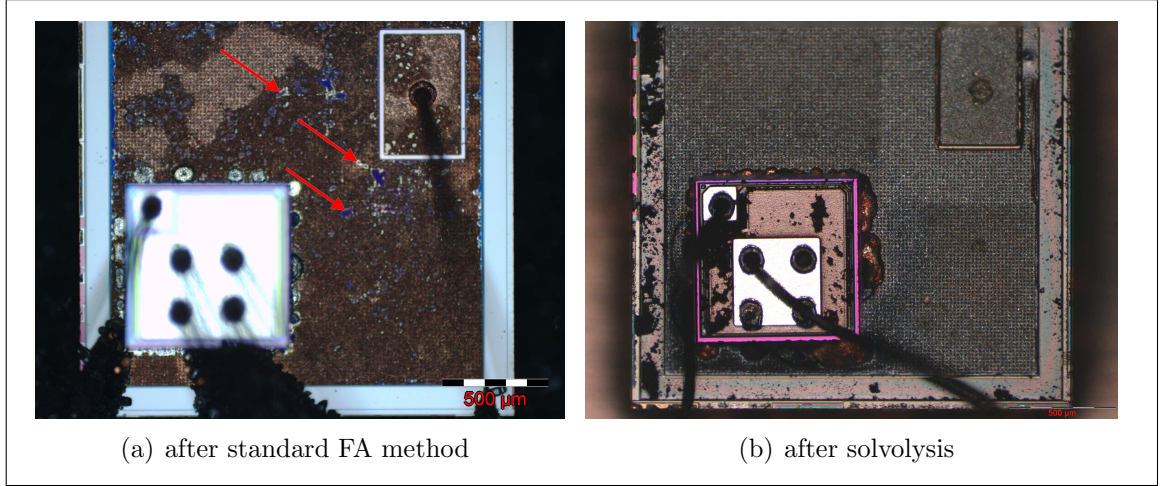


Figure 5.5.: Comparison of decapsulated dies using two different methods, namely laser ablation combined with wet chemical etch and solvolysis

The conventionally decapsulated devices show severe attack of the copper including complete removal at some points (see red arrows in figure 5.5(a)). The new solvolysis method did not show any artefacts on the die surface, and in addition the polyimide layer of the top die was preserved.

## 5.2. Devices with Sputtered Bare Copper Metallisation

In the SFET5 technology a sputtered copper metallisation is used and for the experimental runs such devices in a PG-TDSON-8-5 package were used. The devices for the solvolysis experiments were immersed in a 50:50 volume per cent (vol%) mixture of N-diethyl-m-toluamide (DETA) and N-methylpyrrolidone (NMP) with a total volume of 50 mL, and placed inside the Parr tool (see section 4.1.3 for tool setup). 70 bar nitrogen was adjusted to gain the desired reaction pressure. After the preparation the mould compound was removed with little effort and the devices were cleaned with NMP and acetone, and dried with a stream of nitrogen.

Thereafter reflected-light microscopy was done and it showed two different noticeable changes (see figure 5.6). First of all the copper surface seemed rougher, especially at the edges of the die. And second the copper metallisation was missing at the gate pad area and only the underlying aluminium remained.



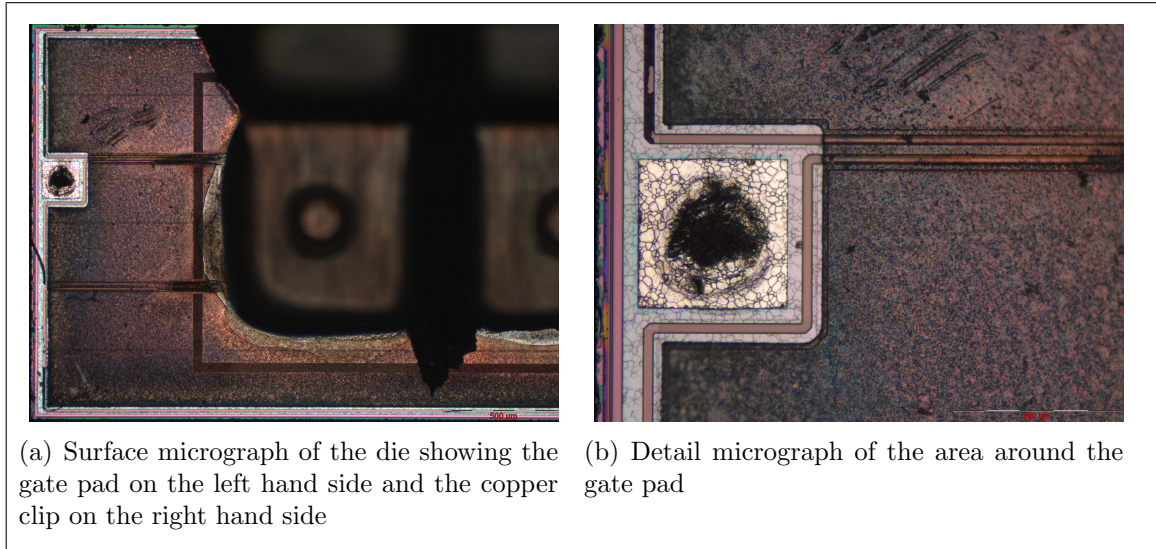


Figure 5.6.: Reflected-light micrographs of the die surface after solvolysis treatment with DETA-NMP

In order to gain more information on both observations a SEM analysis was conducted on the sample and a previously unpackaged reference device, which was cut directly out of a lead frame. In order to gain the needed conductivity of the samples for the SEM analysis, a 3,5 nm gold layer was sputtered on the surface. In case of the missing copper it could be shown, that the intermetallic layer between the underlying aluminium metallisation and the copper layer above only started to grow at the grain boundaries of the aluminium and directly under the ball bond, but not on the grains themselves (see figure 5.7). Due to that reason no sufficient adhesion could be obtained. In the further process development it was necessary to add a temper step in order to anneal both metallisations better.

## 5. Case Studies

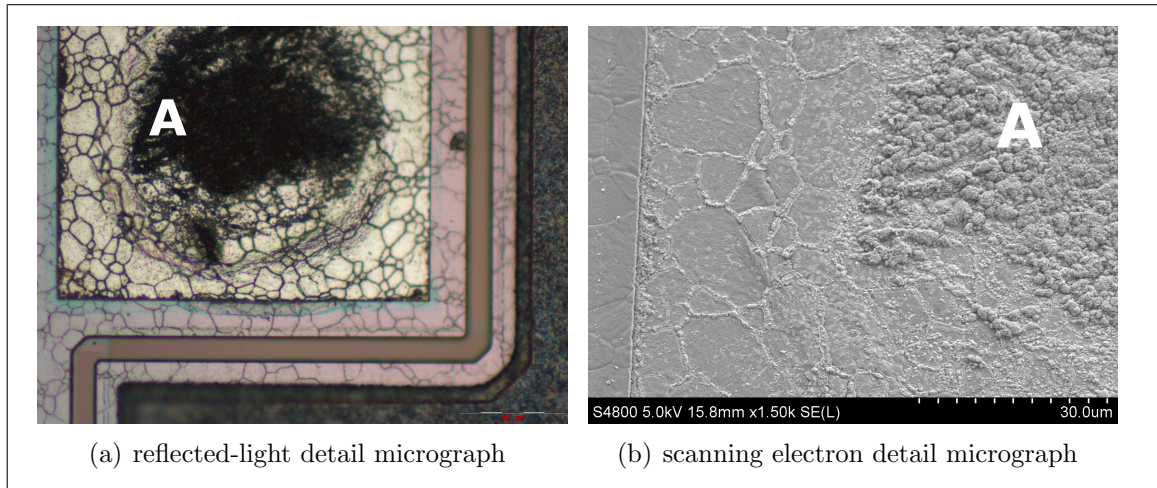


Figure 5.7.: Surface at the gate pad area of a SFET5 device after decapsulation with DETA-NMP (A... ball bond area with intermetallic phase)

Regarding the rough die surface it could be shown that the reason for this was, that the copper recrystallised. Sputtered copper is disordered to a great extent and has smaller crystal grains. The temperatures and pressures in use during decapsulation caused the small crystal fragments to recrystallise into larger ones which leads to an increased roughness.

In order to exclude that the effect had some connection to the use of the solvents themselves, a HTS (high temperature storage) test on unpackaged reference parts was done for 3, 6, and 10 hours at 250°C. The devices were again analysed using scanning electron microscopy.

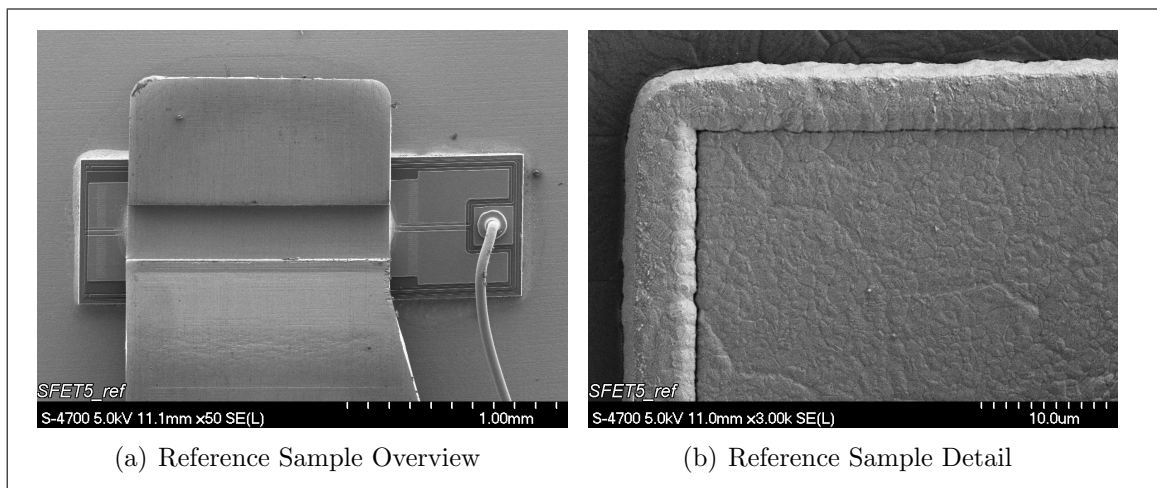


Figure 5.8.: Scanning electron micrographs of a non-moulded reference device before temperature storage

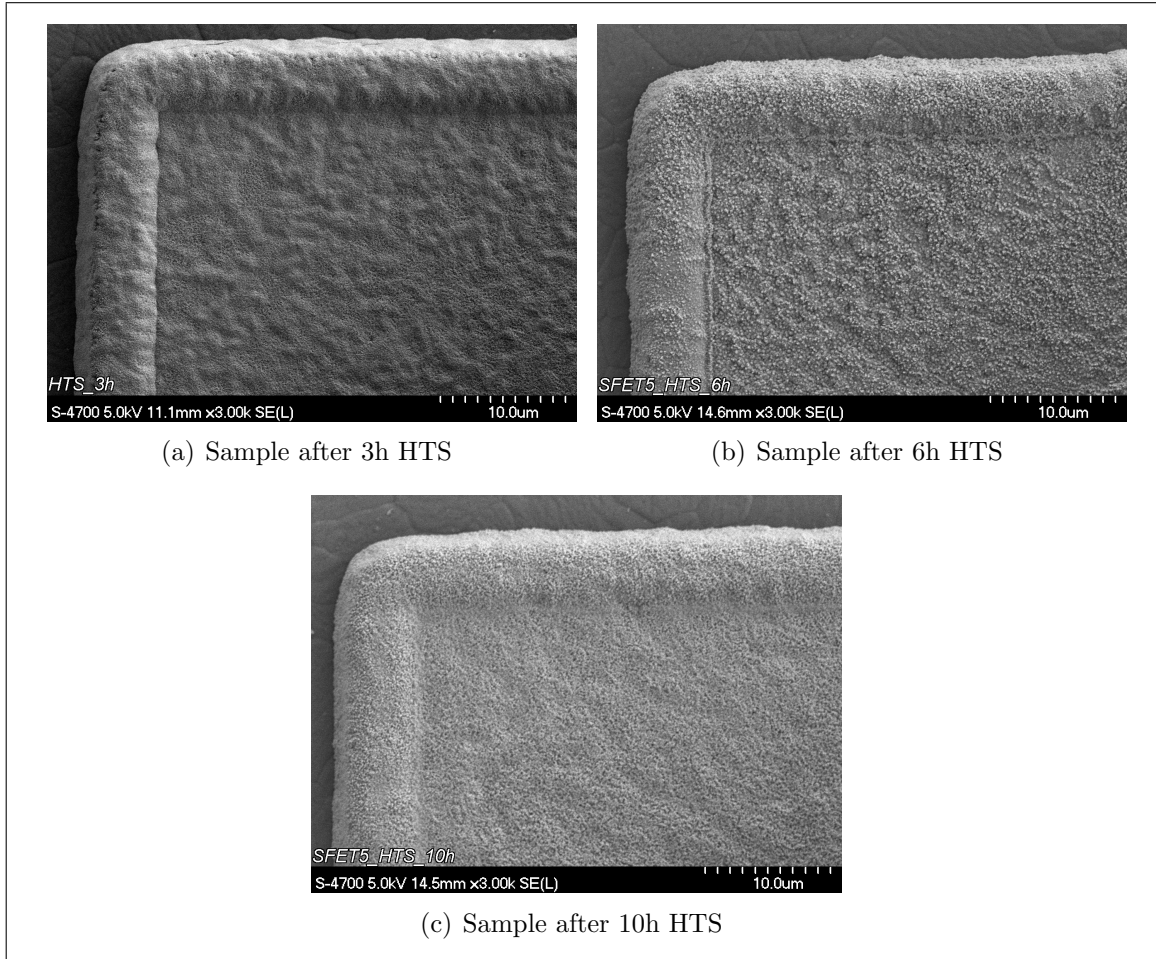


Figure 5.9.: Scanning electron micrographs of the gate pad on non-moulded devices after HTS

Although the observed results were different, all tests showed recrystallisation of the sputtered copper metallisation. The reason for this difference in the formed copper crystals after solvolysis, could be the addition of pressure, which can influence the structure.

### 5.3. Next Generation Packages

In next generation packages (NGPs) instead of a mould compound a composite of glass fibre mats soaked in resin is used. The wire connections are replaced by copper vias. Those vias are manufactured by laser cutting through the glass fibre mats followed by electrochemical deposition. Due to the ablation of the resin, the

## 5. Case Studies

fibres break, but remainders are left which point inside the cavity. These remainders cause a very strong connection between the composite and the copper as they act like barbs. The underlying die has a bare copper metallisation as top layer. Figure 5.10 shows a schematic cross section of a NGP device, showing all relevant components.

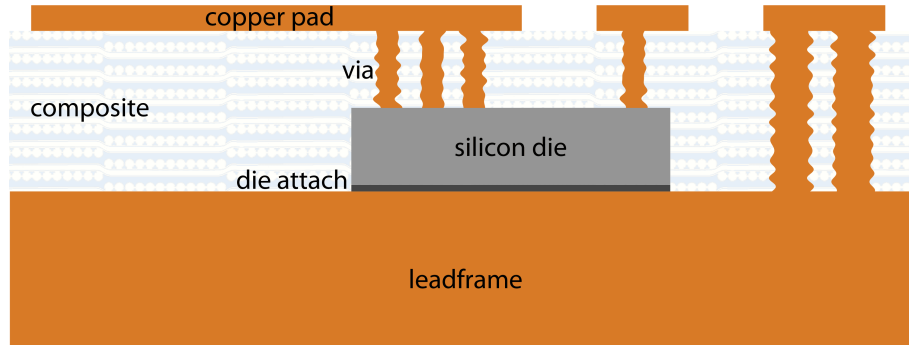


Figure 5.10.: Schematic cross section of a next generation package

This new construction makes wet chemical decapsulation very difficult. Even with the best attuned method the acid severely attacks the copper, because it takes a long time to dissolve the resin and the copper vias to an extend, which allows the removal of the glass fibre mats.

A new approach incorporating solvolysis treatment was found. Before solvolysis the devices were parallel polished until approximately one fibre mat layer remained above the die (see figure 5.11(b)). Then the devices were immersed in 50 mL aniline (ANI) and heated to 523 K for 10 h using the Parr pressure vessel. A nitrogen load of 50 bar was added. Afterwards the devices were removed from the solvent and in all cases the fibre mat (see figure 5.11(d)) was already separated from the die and leadframe (see figure 5.11(c)) and did not need to be removed manually. Both parts were cleaned using tetrahydrofuren and carefully dried with a stream of nitrogen.



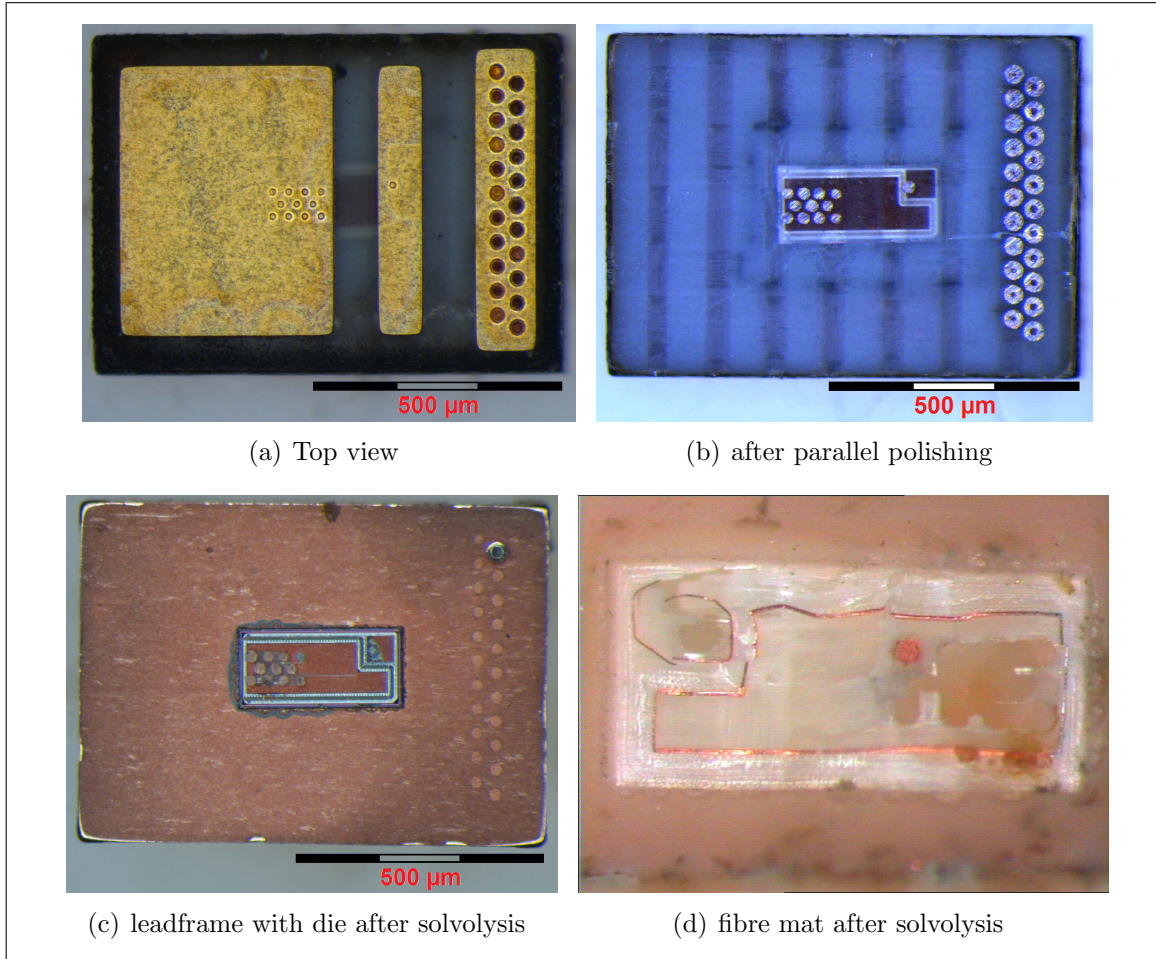


Figure 5.11.: Stereo micrographs of different stages of NGP preparation

The major problem are remaining parts of fibre glass between the densely positioned vias. They could not be removed manually without harming the copper die surface. Except for this small area the die surface could be assessed completely using reflected-light microscopy.

In addition a weak spot of the device could be shown. In the reflected-light micrograph of the glass fibre mat (see figure 5.11(d)) copper residues were observed, which had the outline of the copper metallisation of the die. This copper was removed from the die during solvolysis, because the adhesion of the copper to the underlying layers on the die was not sufficient. This layout problem was already known and the present method confirmed it.

## 5.4. Devices with Power Copper Metallisation

Power copper metallisation is a metallisation stack, which has a thick layer of copper and in most cases a NiMoP (nickel molybdenum phosphor) coating on top. The inspected device is a SMART6 die encapsulated in a PG-DSO-14-40 package. It consists of a logic part and two large DMOS (double-diffused metaloxidesemiconductor) transistors (see overview in figure 5.12).

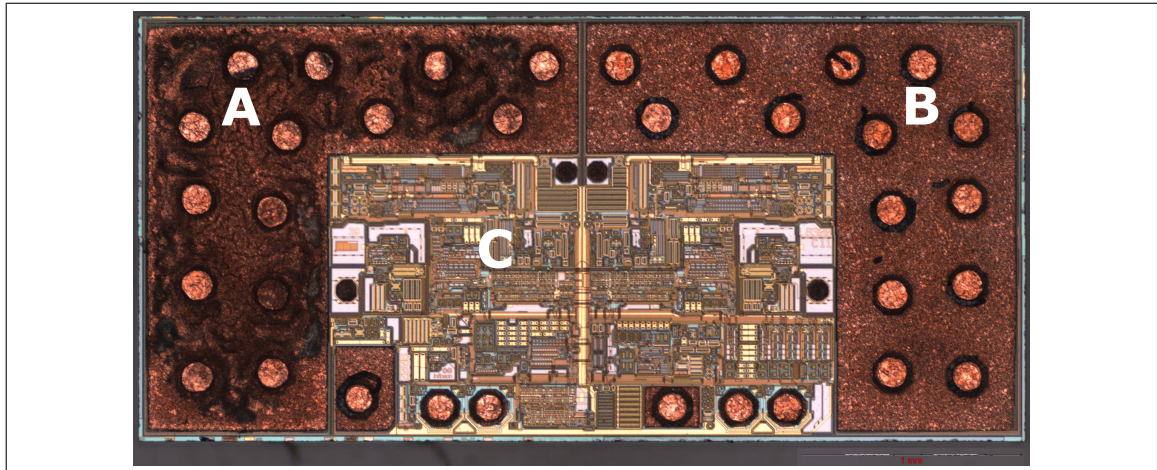


Figure 5.12.: Reflected-light micrograph of a SMART6 die decapsulated using ANI (A... electrically stressed DMOS, B... unstressed DMOS, C... logic part)

The copper and polyimide structures and interactions are of high importance for this product. Some failure mechanisms are still not fully understood, which is why a reliable decapsulation method is so important. During inorganic acid decapsulation the polyimide as well as the metallisation is always severely damaged or removed and assessment is hardly possible (see figure 5.13).

## 5. Case Studies

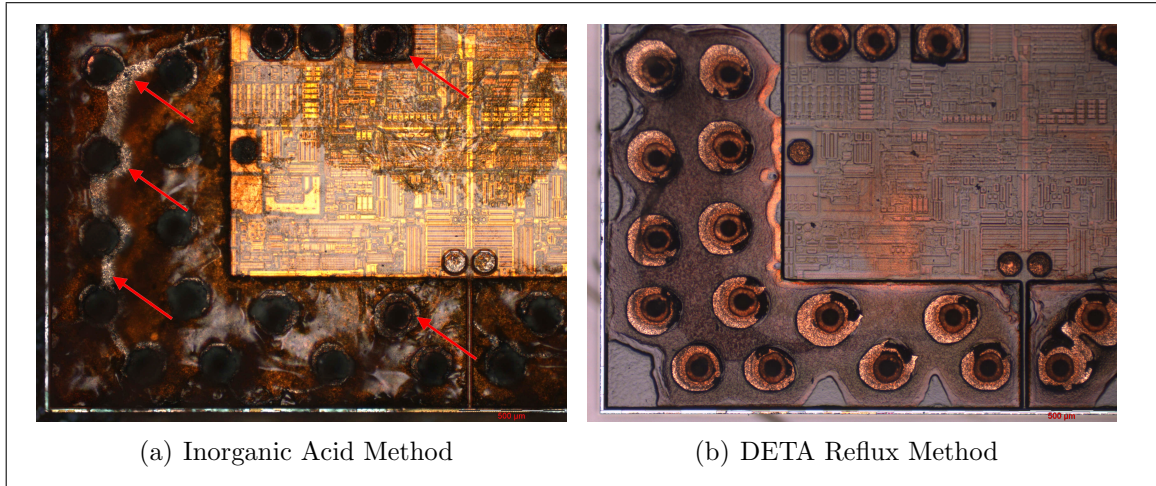


Figure 5.13.: Reflected light micrographs of decapsulated devices using different methods

Initial (unstressed) devices were used in the Parr experimental series and here a special case will be described in which electrically stressed devices were decapsulated. In the SMART6 devices only one of the two DMOS transistors had been electrically stressed, which allowed direct comparison between initial and stressed condition.

First a scanning acoustic microscopy (SAM) analysis was performed, which showed signs of damage and degradation in the stressed transistor. This can be seen as dark lines and apparently enlarged ball bonds (see figure 5.14).

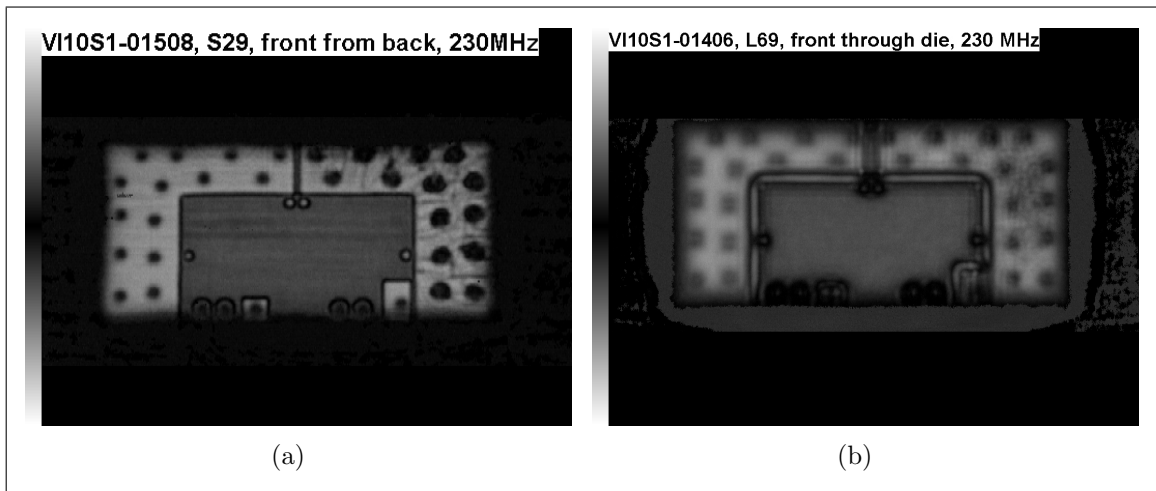


Figure 5.14.: Scanning acoustic micrographs of partly stressed SMART6 devices (mirrored images).

One device was prepared using parallel polishing before treatment with benzyl al-



## 5. Case Studies

cohol in the Parr pressure vessel. After preparation a stereo micrograph was taken (see figure 5.15). In this picture the stressed DMOS is on the left side (opposite to the SAM pictures, because now we look at the device from the front).

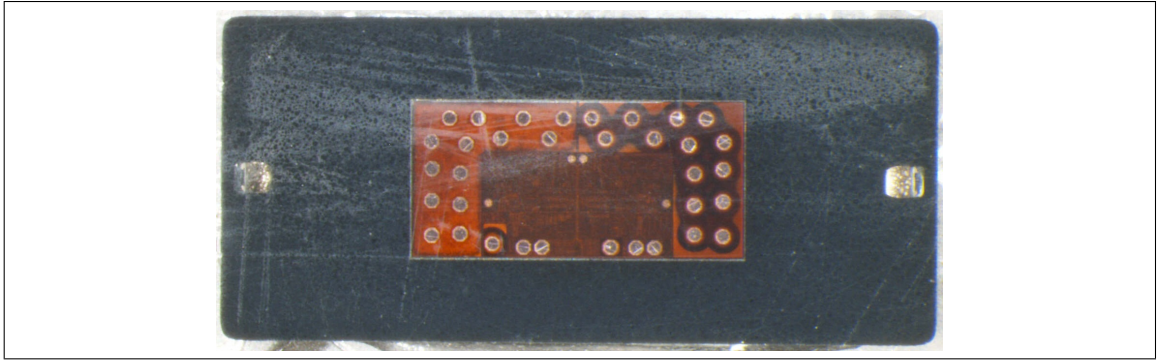


Figure 5.15.: Stereoscopic micrograph of a partly stressed device after parallel grinding.

It was believed that the thinning of the mould compound would help to remove it more quickly, but the handling of the device became very difficult and the last layer of moulding compound could not be removed after solvolysis with BAL. Therefore the devices were immersed in ANI and as it dissolves the polyimide the last layer of mould compound fell off by itself. After cleaning with tetrahydrofuran and drying with a stream of nitrogen, the surface could be inspected and the cracks and bumps on the copper could be seen (see figure 5.16).

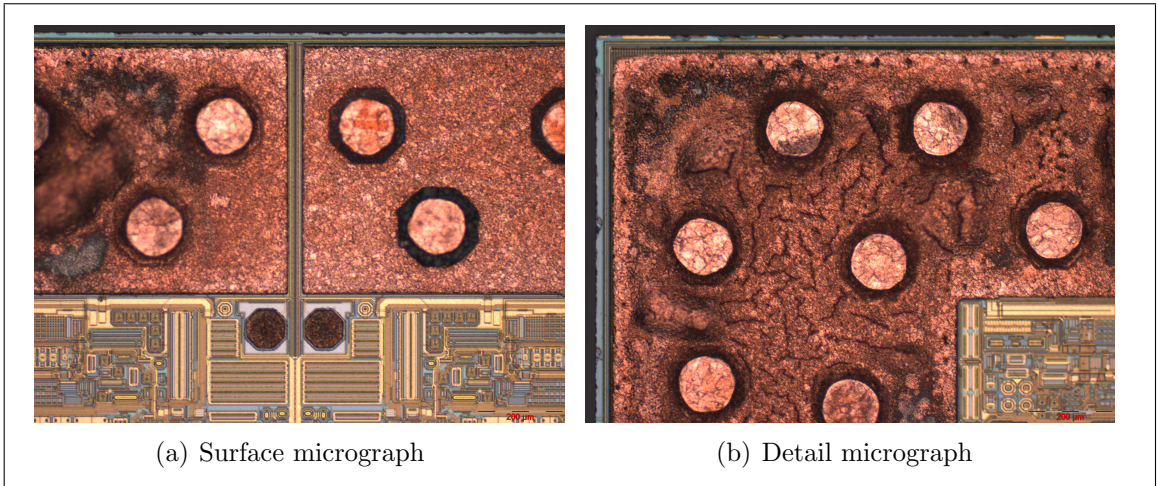


Figure 5.16.: Reflected light micrograph of a SMART6 device after preparation with ANI

For closer inspection of the defects a SEM analysis was performed, where the cracks and bumps could be confirmed (see figure 5.17).



## 5. Case Studies

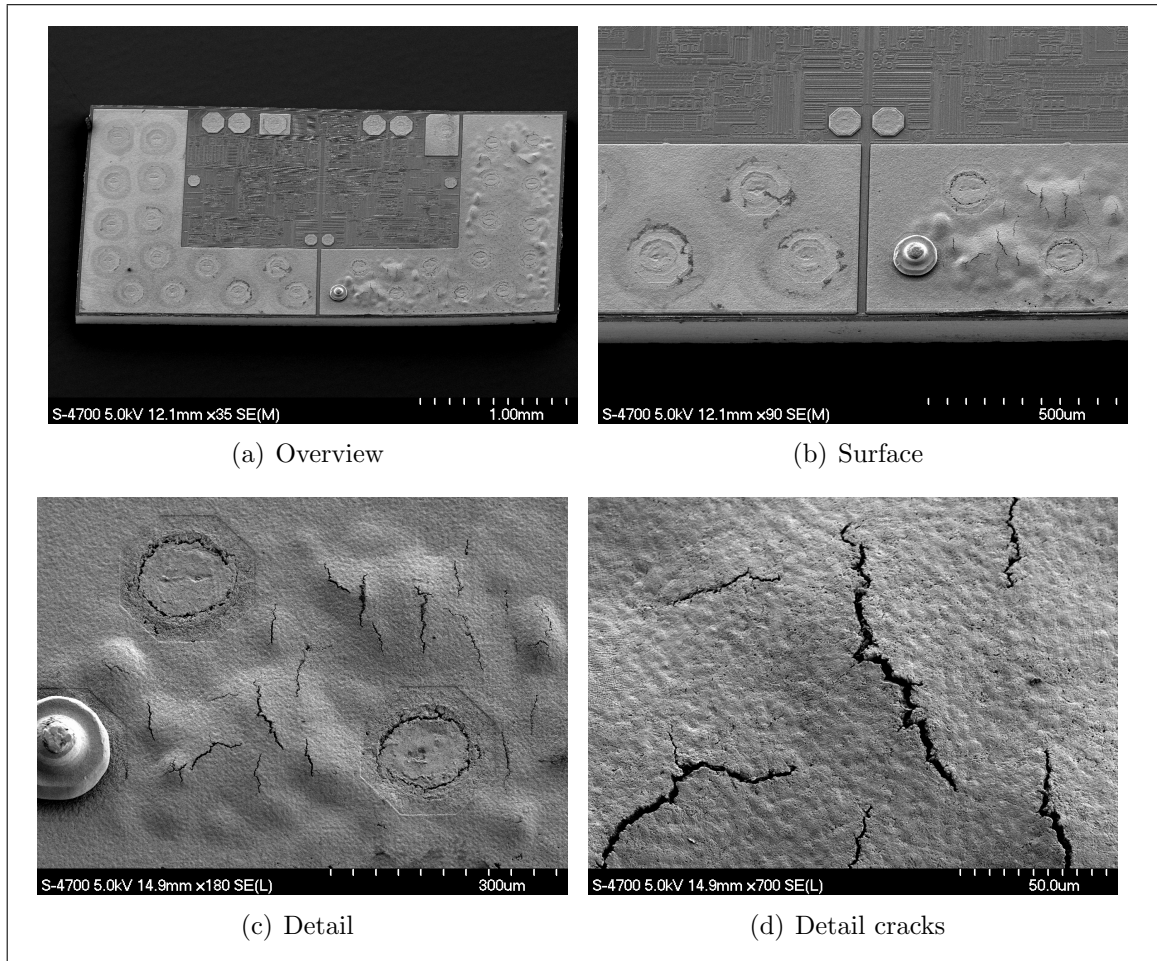


Figure 5.17.: SEM micrographs of a SMART6 device after preparation with ANI

The next question was how deep the cracks descend, which is a major characteristic to decide upon the severeness of the problem. To find an answer to this question a focused ion beam (FIB) cross section was performed. Three cross sections were positioned at the location of different cracks (see figure 5.18).

## 5. Case Studies

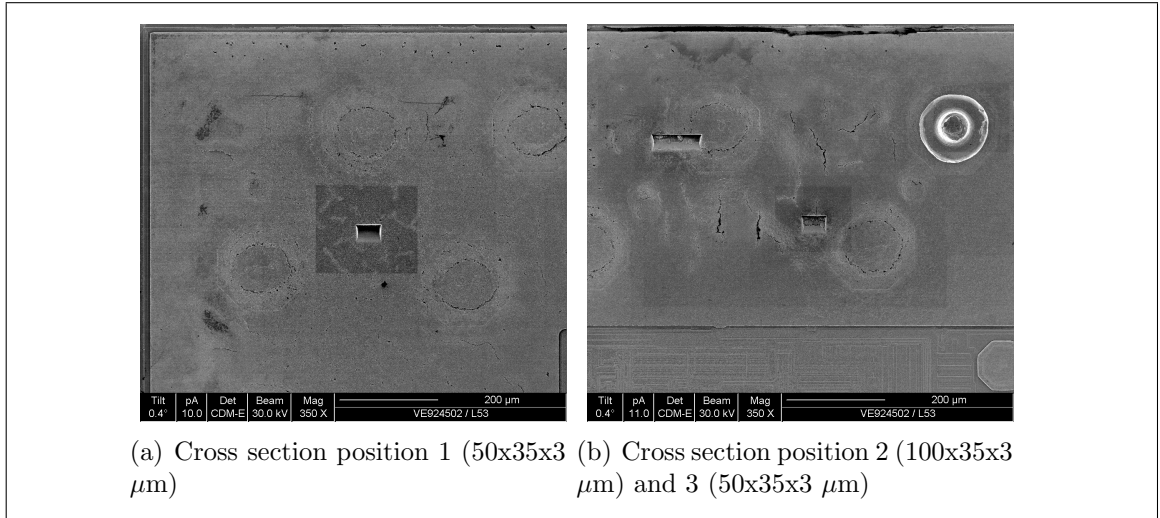


Figure 5.18.: Micrographs showing the FIB cutting positions on the stressed transistor of a SMART6 device

All cracks went through the complete copper metallisation and then ran along above the underlying layer (see figure 5.19).

## 5. Case Studies

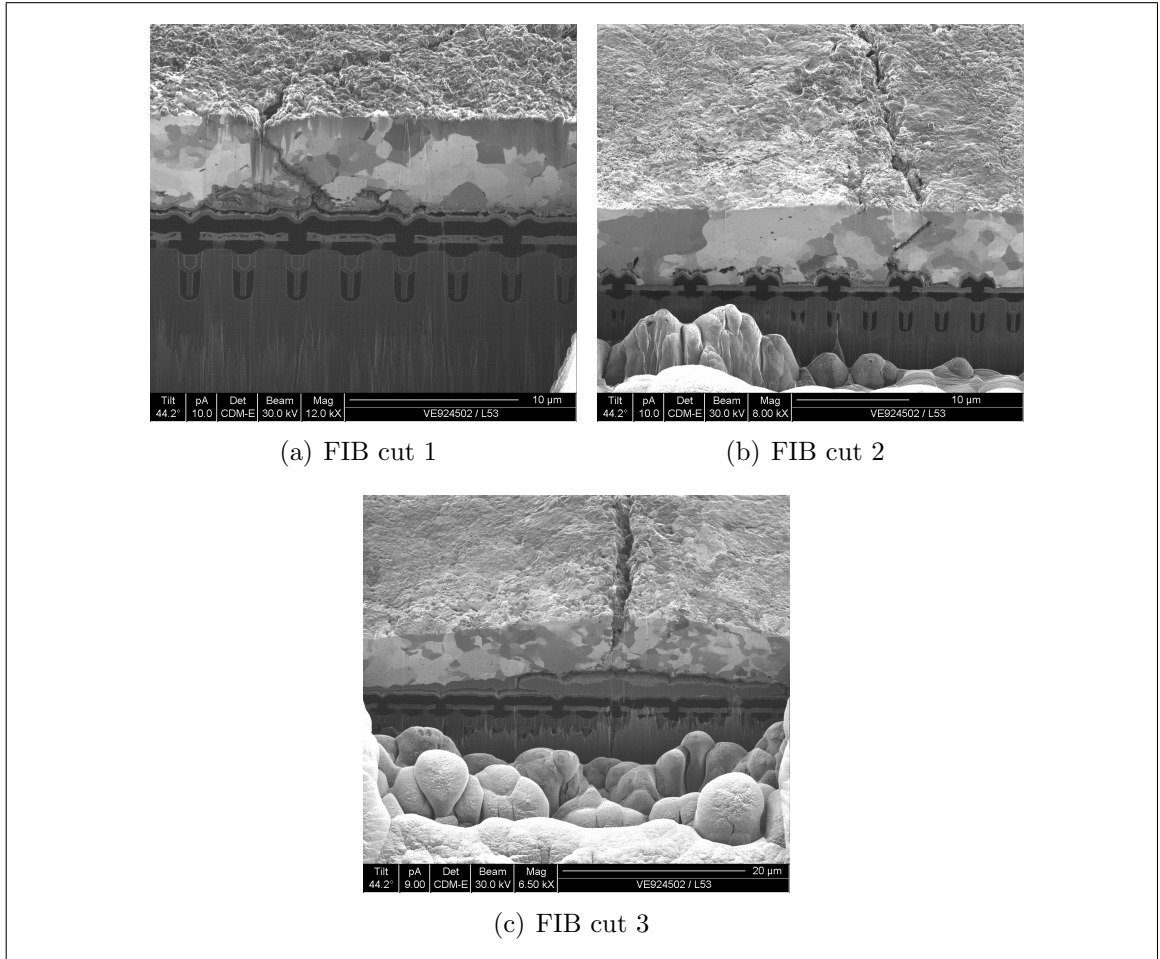


Figure 5.19.: FIB cuts

Using the standard inorganic acid decapsulation method the present defects would have been severely altered (artefacts), a distinction between stressed and unstressed transistor would have been hardly possible, and some of the defects might have not been found. This analysis clearly shows, that the present solvolysis methods are capable of providing accurate results, which are consistent in comparison with other established standard analysis methods.

## 6. Conclusion

In this thesis it could be shown, that it is possible to decapsulate an integrated device using organic solvent systems. Although the moulding compounds are complex systems, which cause major problems during decapsulation, a practicable method was invented. It is now possible to analyse devices including new and fragile copper technologies without creating artefacts. The decapsulation results are consistent with other standard examination methods like SAM, SEM, and FIB.

Further improvements are the possibility to decapsulate a device without harming the polyimide layer and to show possible adhesion problems at interfaces inside the device.

Not only swelling behaviour was observed, but also disintegrating tendencies in some solvent systems. The major concern at the beginning was the reaction temperature, which did not seem to be reducible to the maximum allowable 473 K. In the end even this goal could be reached using a mixture incorporating subcritical media.

A constraint is that it is a total decapsulation method, which makes inspection of the wire connections and the die attach difficult, and can involve some mechanical forces at the device. Furthermore it is not an easy method when it comes to operator handling, but it is certainly less complex than other new decapsulation attempts, e.g. plasma etch.

For further improvement of the method it is vital to gain more information on the moulding compounds used. This is a rather difficult task, but could be solved using FT-IR investigations on mould compound pellets.

The Parr pressure vessel could be improved by adding a second valve to purge the reactor, a injection valve for addition of catalysts or additional reactants during the ongoing reaction, and a shaker underneath the vessel heater to accomplish better contact between the solvent and the devices. Also quenching of the reactions, in-

## 6. Conclusion

stead of a slow cool down phase, could help to improve the practicability.

An increased usage of physically and electrically stressed devices for decapsulation experiments could help to gain more information about the interaction between solvents and the devices.

Several links to further investigations could be shown, like using more stable amines, mixtures incorporating even more different subcritical media, and experimental series to achieve the best possible reaction conditions at 473 K.

Against all odds the thesis showed a new way to decapsulate semiconductor devices with reasonable effort and constraints. The method could already be used for standard analysis of the newest technologies.

# A. Appendix

Table A.1.: Characteristics of the solvents for the primary screening

solvent	bp <sup>1)</sup> [K]	$\rho$ <sup>2)</sup> [g/cm <sup>3</sup> ]	M <sup>3)</sup> [g/mol]	supplier and quality
N,N-Diethyl-m-toluamide	568	0,996	191,28	Alfa Aesar, 97%
N,N-Dimethylformamide	426	0,949	73,10	Merck, LAB
1,1,2-Trichloroethylene	360	1,460	131,79	Merck, reinst
Chlorobenzene	405	1,107	112,56	Merck, zur Synthese
Aniline	457	1,022	93,13	Merck, zur Synthese
Tetrahydrofuran	338	0,885-0,895	72,11	Merck, p.A., ACS
Dimethyl sulfoxide	462	1,101-1,103	78,13	Merck, p.A., ACS
Benzyl alcohol	478	1,045	108,14	Merck, zur Synthese
2-Pyrrolidone	523	1,111	85,11	Merck, zur Synthese
2-Methoxyethanol	398	0,965-0,970	76,10	Merck, p.A., ACS

<sup>1)</sup> bp... boiling point, <sup>2)</sup>  $\rho$ ... density, <sup>3)</sup> M... molecular weight

Table A.2.: Characteristics of the hydrogen donors

substance	bp <sup>1)</sup> [C]	$\rho$ <sup>2)</sup> [g/cm <sup>3</sup> ]	M <sup>3)</sup> [g/mol]	supplier and quality
Tetralin	200-209	0,969	132,21	Merck, zur Synthese
Indoline	220-221	1,06	119,17	Alfa Aesar, 99%
9,10-Dihydroanthracene	312	0,88	180,25	

<sup>1)</sup> bp... boiling point, <sup>2)</sup>  $\rho$ ... density, <sup>3)</sup> M... molecular weight

## A. Appendix

Table A.3.: Antoine constants (A,B,C) and their temperature range for different solvents in use (taken from the NIST Chemistry WebBook [2])

solvent	A [-]	B [-]	C [-]	temperature [K]
ANI	4,34541	1661,858	-74,048	304-457
BAL	4,47713	1738,9	-89,559	395-479
MOE	5,06386	1853,556	-30,838	329-397
DMF	3,93068	1337,716	-82,648	303-363
THF	4,12118	1202,942	-46,818	296-373
TCE	3,55346	974,538	-85,811	291-360
CLB	4,11083	1435,675	-55,124	335-405
TET	4,12671	1690,912	-70,229	367-479
H <sub>2</sub> O	3,55959	643,748	-198,043	379-573

## A. Appendix

Workflow for Experimental Series with Parr Pressure Vessel (PV) 4766	<ul style="list-style-type: none"> <li>Vent pressure vessel (under closed fuming hood, wait for 2 min)</li> <li>Open pressure vessel (unscrew the 6 cap screws, loosen the drop band, remove the lid)</li> <li>Remove glass liner</li> <li>Transfer the solvent from the glass liner into a storage vial</li> <li>Clean the PV using acetone (bottom of the lid including temperature probe, stainless steel vessel, glass liner, gasket)</li> <li>In case of solid residues on the glass liner: cleaning with a few mL of fuming nitric acid and/or hydrochloric acid (afterwards rinse with water + acetone)</li> <li>Clean nitrogen load valve at PV and recesses in the lid with Q-tips and little acetone</li> <li>Rinse the devices with tetrahydrofuran (THF), allow excess solvent to drip off on a clean room wiper and remove the MC if necessary. Rinse with THF, water, THF and dry with a stream of nitrogen after each step.</li> </ul>	Clean room wipers Solvent storage Chemical waste containers Acetone Tetrahydrofuran Nitric acid HNO <sub>3</sub> (fuming) Hydrochloric acid HCl (32%)
	<ul style="list-style-type: none"> <li>Inspection of the tool (Gasket, gas lines, screws, high-temperature grease)</li> <li>If necessary lubricate the screw fittings and remove bumps of the PTFE gasket with a scalpel</li> <li>Inspection of the nitrogen gas bottle (condition of the valves)</li> </ul>	Wrench (9/16") High-temperature grease scalpel
	<ul style="list-style-type: none"> <li>Immerse solvent in glass liner: prepare solvent first in a beaker, then transfer desired amount with a suitable measuring pipette</li> <li>Add the devices</li> <li>Assembly and sealing of the pressure vessel (drop band followed by the cap screws)</li> </ul>	Solvents Devices Measuring pipette
	<ul style="list-style-type: none"> <li>Add nitrogen load to the PV               <ol style="list-style-type: none"> <li>Close fume hood</li> <li>PV valve open, white valve open, reduction valve closed, green ventilation valve closed</li> <li>Open main valve</li> <li>Open reduction valve: continuous control of the actual pressure in the vessel</li> <li>Close PV valve</li> <li>Close main valve</li> <li>Open green ventilation valve slowly</li> <li>Close green ventilation valve, Close reduction valve</li> <li>Remove nitrogen feed line and cover the coned pressure fitting with a glove (protection from harmful lab environment)</li> </ol> </li> </ul>	
	<ul style="list-style-type: none"> <li>Control pressure after 5 min waiting time (leak tightness)</li> <li>Connect power plug and temperature probe</li> <li>Start temperature controller and heater (default setting is 250°C)</li> <li>Control temperature and pressure after 15 and 30</li> </ul>	
	<ul style="list-style-type: none"> <li>Turn off heater after max. 10 h reaction time</li> <li>Coolin to room temperature (over night)</li> <li>Turn off temperature controller</li> <li>Disconnect temperature probe</li> <li>Disconnect power plug</li> <li>Record experiment in the tool journal</li> </ul>	Tool journal

Figure A.1.: Workflow of the Parr pressure vessel series



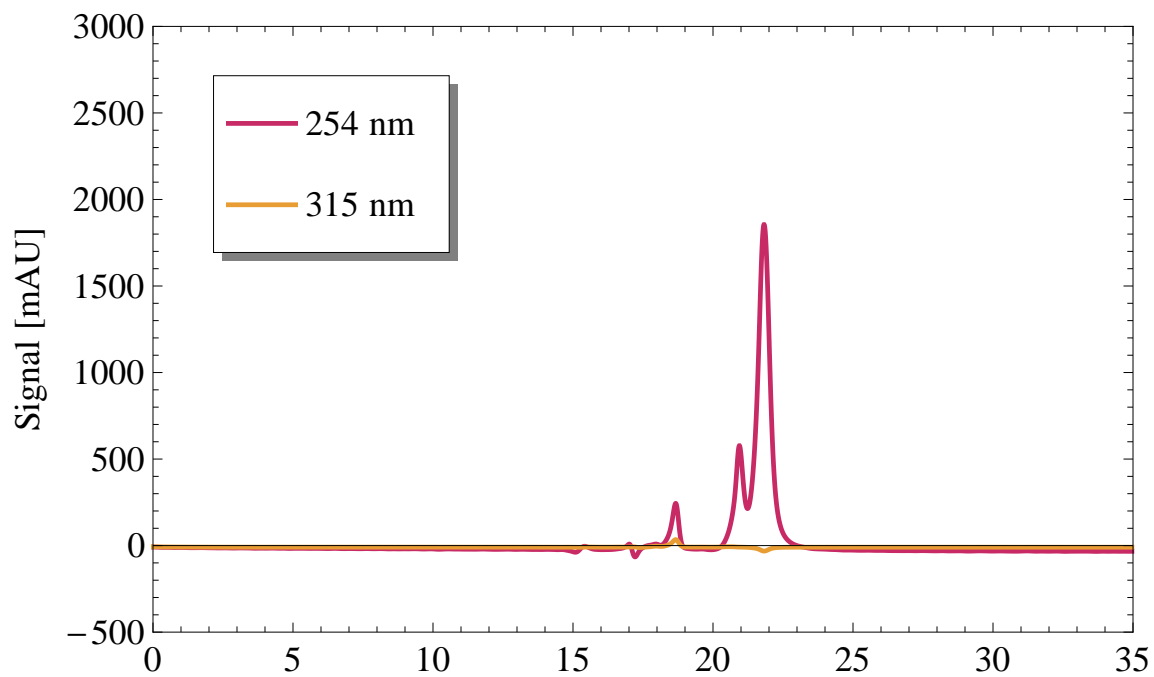


Figure A.2.: HPLC chromatogram of HPA run R3 using 9,10-dihydroanthracene

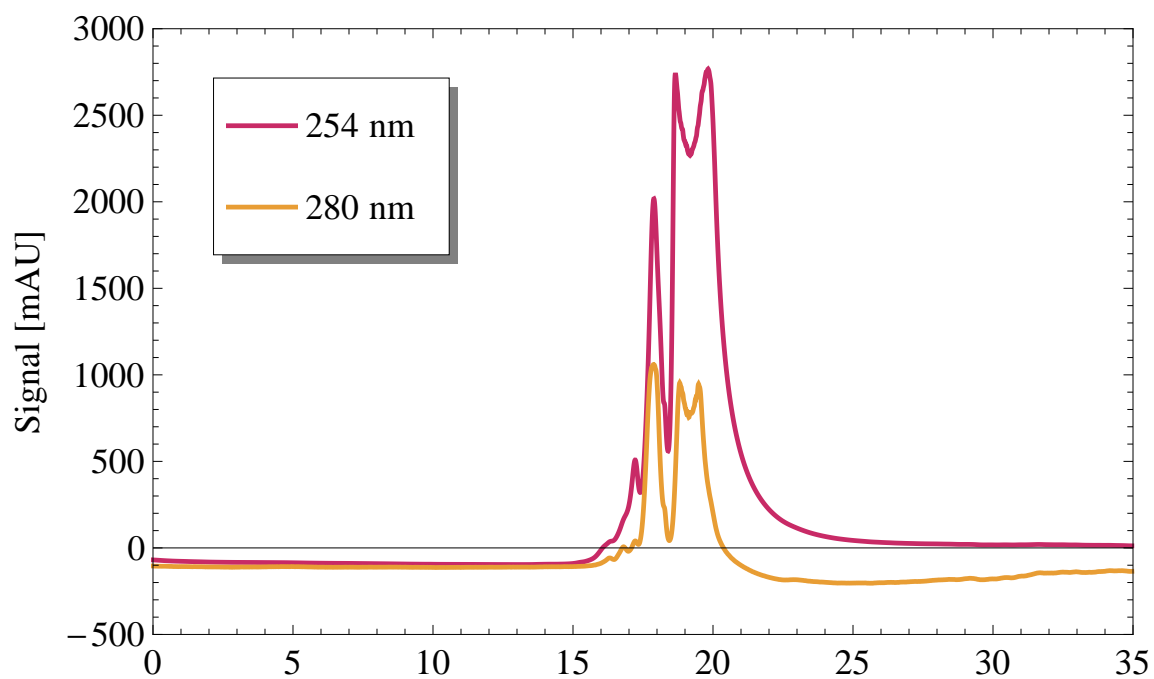


Figure A.3.: HPLC chromatogram of HPA run R3 using indoline

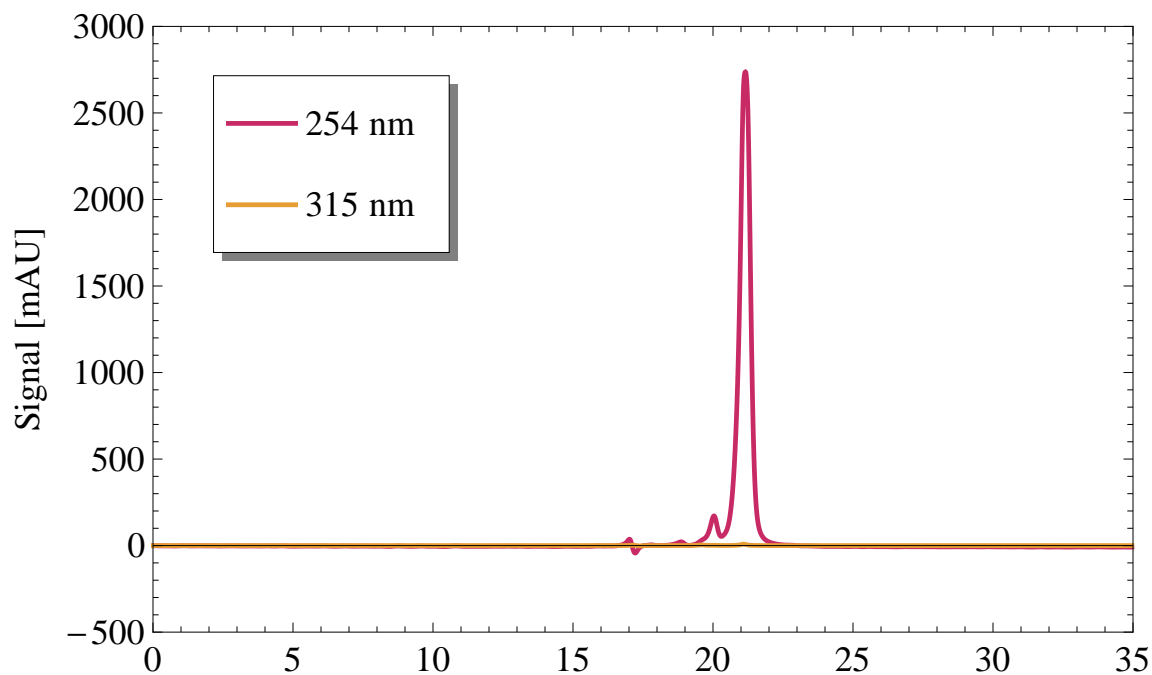


Figure A.4.: HPLC chromatogram of HPA run R3 using tetralin

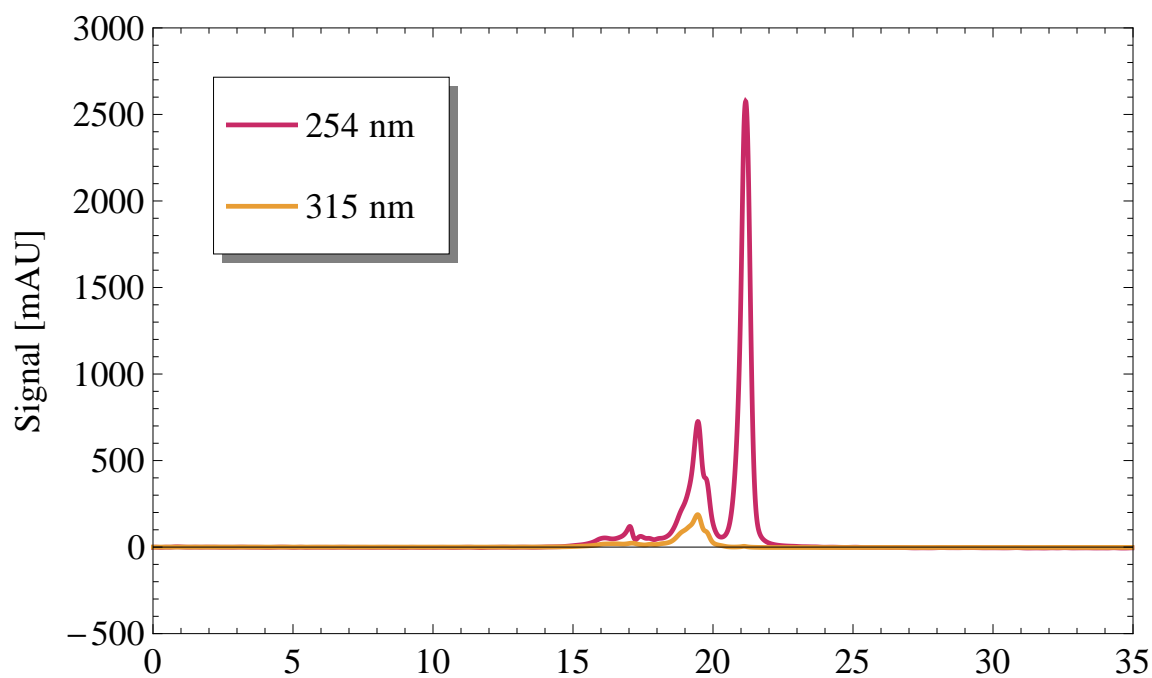


Figure A.5.: HPLC chromatogram of HPA run R3 using a mixture of tetralin and ethanolamine (1:1 v/v, upper phase)

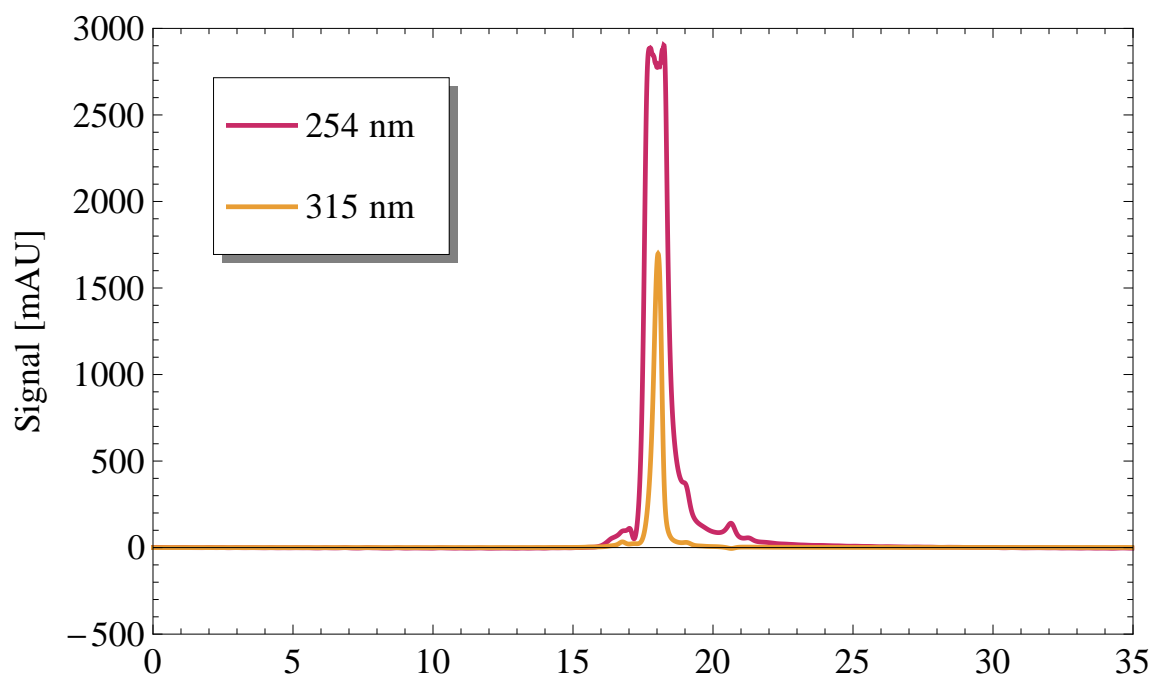


Figure A.6.: HPLC chromatogram of HPA run R5 using aniline

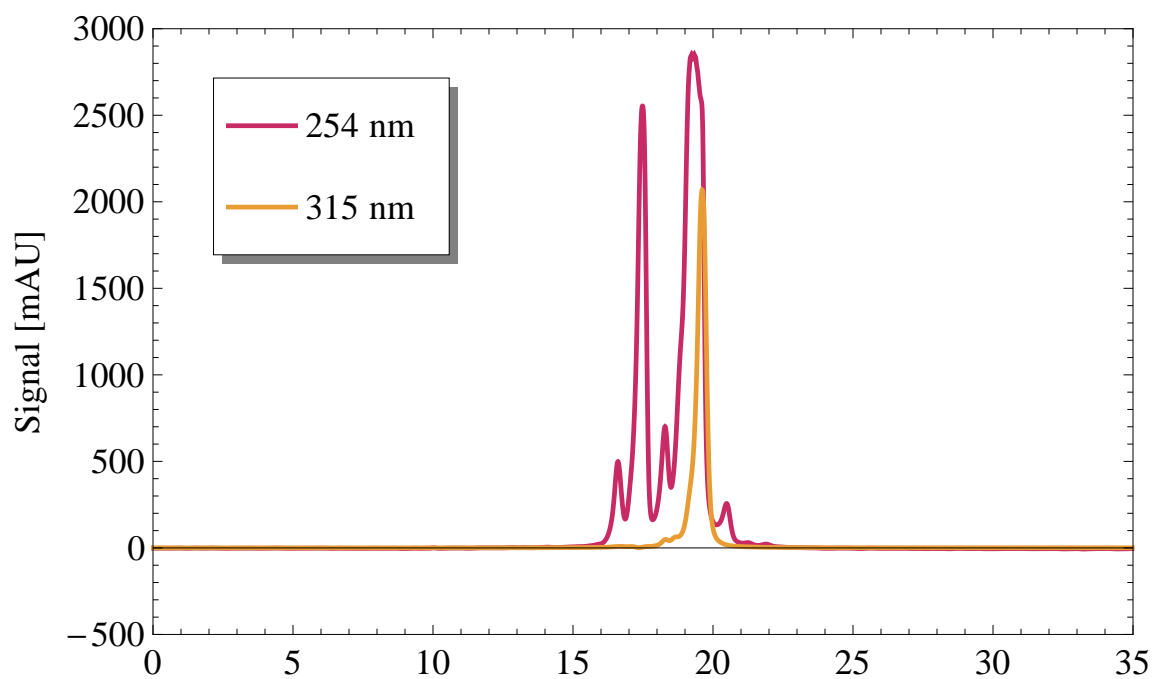


Figure A.7.: HPLC chromatogram of HPA run R5 using benzyl alcohol

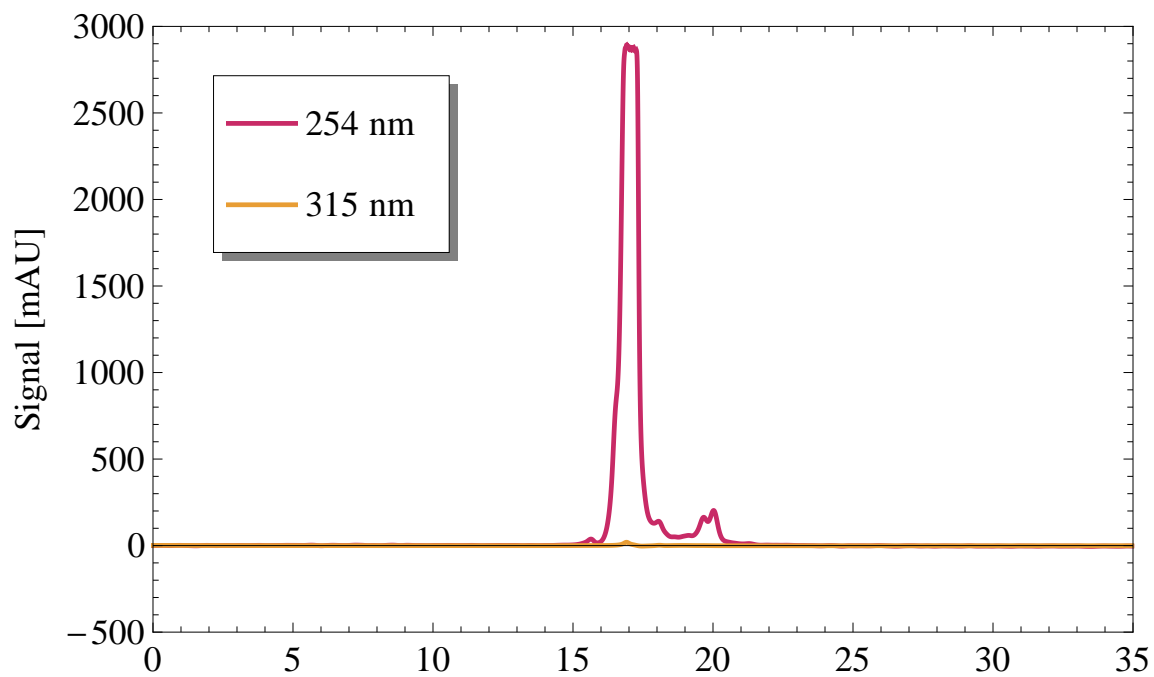


Figure A.8.: HPLC chromatogram of HPA run R5 using N,N-diethyl-m-toluamide

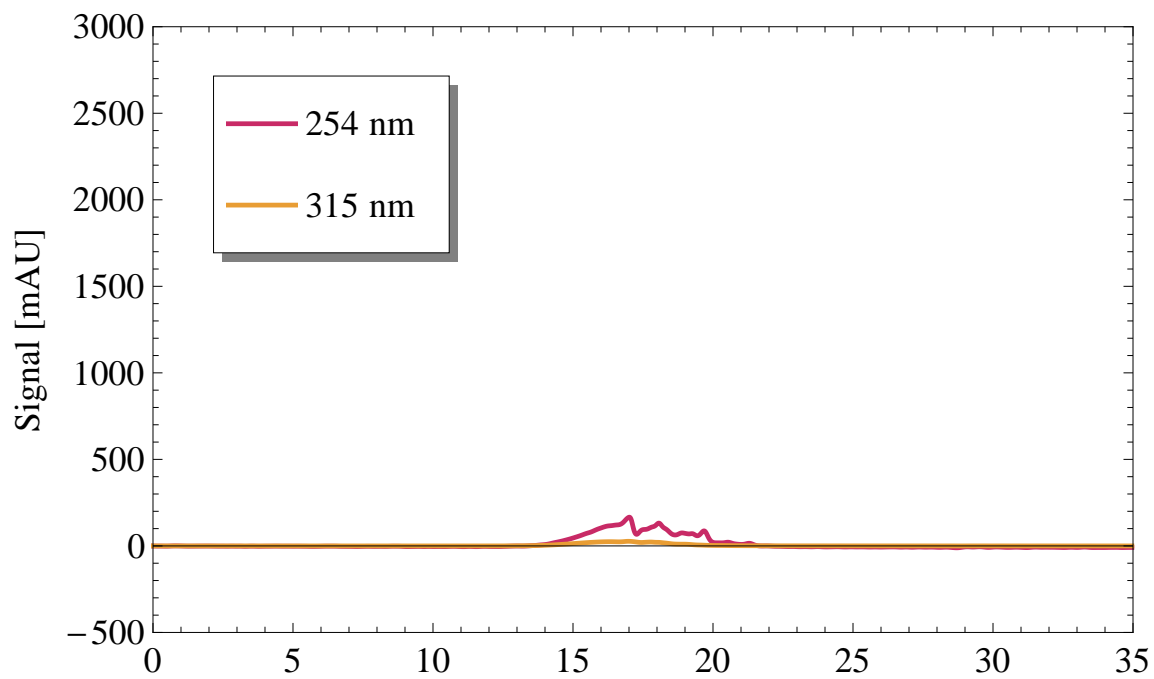


Figure A.9.: HPLC chromatogram of HPA run R5 using 2-methoxyethanol

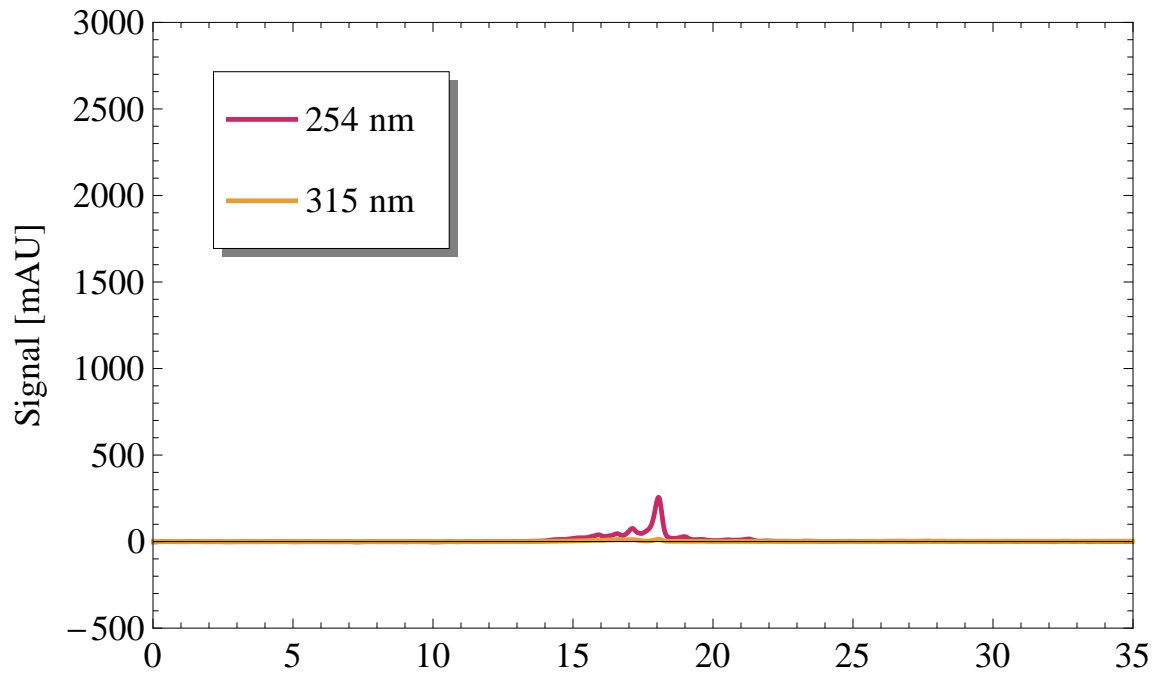


Figure A.10.: HPLC chromatogram of HPA run R5 using 2-pyrrolidone

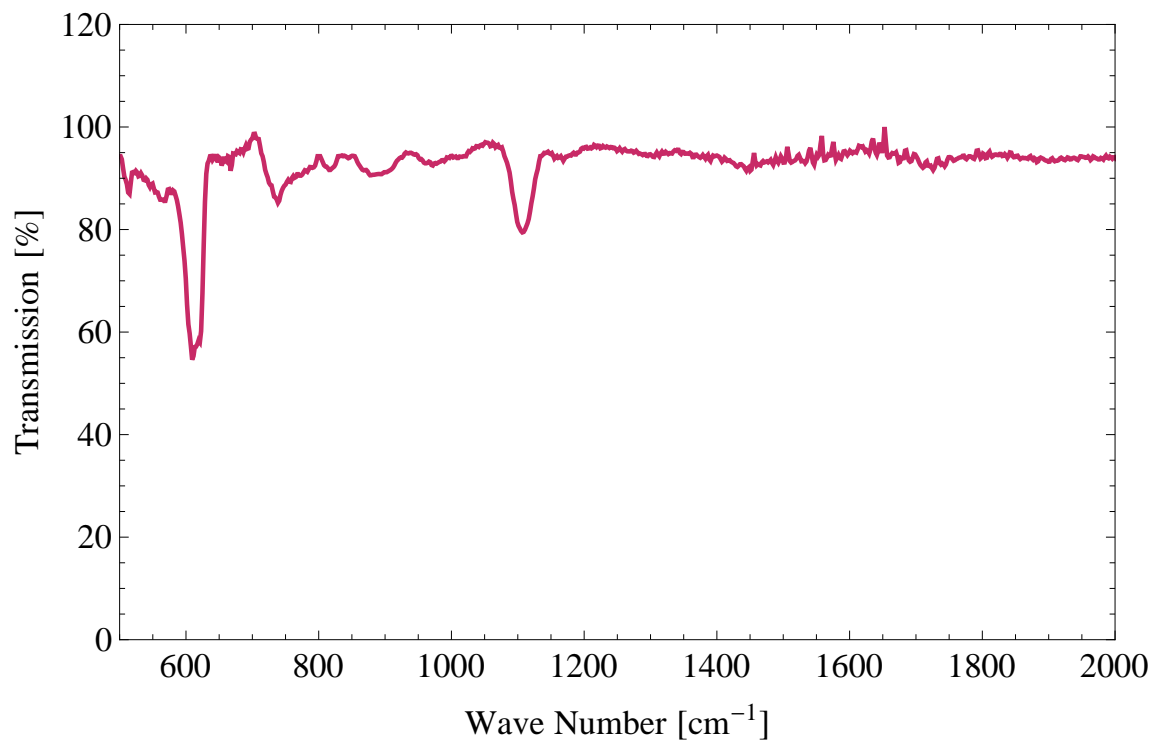


Figure A.11.: Background of the wafer used as substrate for the FT-IR analysis

# Glossary

**aminolysis**

Special type of solvolysis. An amine acts as the specific solvent reagent.

**ball bond**

Ball-shaped electrical connection of a wire to the die. Ball bonds are mainly used for gold or aluminium bonds.

**cohesion energy**

Negative molar internal energy. Used in the solubility parameter concept.

**cohesion parameter**

synonym for solubility parameters.

**critical point**

In thermodynamics the point where the phase boundary between the liquid and the gas phase is no longer existent.

**curing**

Polymerisation and cross-linking of a polymer in order to harden it. The cross-linking can be done through heat, irradiation, or chemical reactions.

**curing agent**

see hardener.

**Debye interaction**

Dipole-induced dipole interactions, which occur between a molecule with permanent dipole and a neighbouring molecule, which can be polar or not.

**decapsulation**

Process in which the moulding compound is partially or completely removed from a semiconductor device.

**die**

Small part of a wafer, on which an integrated circuit is located.

**die attach**

Part of the semiconductor package which attaches the die to the leadframe. Adhesives or solders are used.

**die pad**

Part of the leadframe, on which the die is attached (see die attach).

**dielectric**

Substances with low or none electrical conductivity. They are primarily used as isolating or protective layers on the semiconductor device. Most common are silicon dioxide and silicon nitride.

**diode array detector**

A detector for UV-Vis spectroscopy which simultaneously detects all wave length at a time by using an array of most commonly 512 photo diodes.

**epoxy resin**

Are thermosets which are formed during the polyaddition reaction between an epoxide oligomer and a hardener.

**equation of state**

A mathematical correlation between thermodynamic properties of a system (pressure, temperature, volume) and the amount of substance.

**failure analysis**

Is the process of determining the reason a semiconductor device has failed. It also includes determining the present failure mechanism and possibilities to avoid it in the future.

**filler**

Inert particles, which are part of the moulding compound, mostly silicon dioxide.

**gas chromatography**

Analytical method to separate compounds which are volatile. A gas functions as mobile phase.

**Hansen Solubility Parameter (HSP)**

Possibility to predict solubility of one material in a given solvent. Developed by Charles Hansen.

**hardener**

Used to cross link an epoxide oligomer during curing.

**heat sink**

Non-packaged metal part of a device used to dissipate large amounts of heat especially in power ICs.

**high performance liquid chromatography**

Analytical method to separate, and in combination with a detector identify, compounds using a solvent as mobile phase which passes through a column (stationary phase).

**hydrogenolysis**

Special type of solvolysis. Hydrogen acts as the specific solvent reagent.

**integrated circuit**

Is an miniaturised electronic circuit based on a single semiconductor substrate.

**Keesom interaction**

Orientation effects result from dipole-dipole interactions. They occur only between molecules which have permanent dipole moments.

**lead**

Part of the leadframe, which is the electrical connection from the die to the exterior.

**leadframe**

Metallic frame, which provides mechanical support to the die. It consists of the die pad and the leads.

**London force**

Induced dipole-induced dipole interactions between adjacent pairs of molecules. Weakest intermolecular forces.

**mass spectroscopy**

Analytical method for elemental analysis. Often in combination with gas chromatography.

**metallisation**

A metal layer (if not stated otherwise) on the die.

**moulding compound**

Composite materials used to encapsulate semiconductor devices.

**oligomer**

Chain of some monomer units.



**package**

Carrier or container for an integrated circuit that can be made of plastics, ceramics or metals.

**pad**

Open metal area on a die used to contact wires or probe needles.

**Polar force**

Interactions between molecules, divided into orientation and induction effects (see Keesom and Debye interaction).

**polyimide**

A polymer used as a protective coating on many semiconductor devices.

**resin**

Epoxide oligomer used in combination with a hardener/curing agent to form an epoxy thermosetting polymer.

**scanning electron microscopy**

A microscopic technique where instead of light a focused electron beam is used, which scans the surface of a sample and generates a micrograph.

**semiconductor**

A material which has an electric conductivity which lies between conductors and insulators. Doped silicon is the most widely used semiconductor for commercial applications.

**solubility**

Property of a substrate to dissolve in a solvent to form a homogeneous solution.

**solute**

minority can be more than one substance.

**solvent**

majority substance.

**solvolysis**

Reaction, where the solvent acts as a reagent.

**surface mounted device**

Devices which are mounted directly onto the surface of printed circuit boards using solderable contact areas.

**thermoset**

Polymers which are three-dimensional cross linked and can't be deformed after cure.

**via**

Vertical connection between different metallisation layers in a semiconductor device.

**wafer**

Substrate for semiconductor devices. Most commonly thin disc of defect-free silicon.

**wedge bond**

Wedge-shaped electrical connection of a wire to the die. Wedge bonds are mainly used for aluminium bonds.

# Acronyms

AN	ANnna
ANI	Aniline
BAL	Benzyl alcohol
BER	Biphenyl Epoxy Resin
CF <sub>4</sub>	Tetrafluoromethane
CLB	Chlorobenzene
DCPD	Dicyclopentadienyl Resin
DDM	diamino diphenyl methane
DDM <sub>e</sub>	tetraethyl derivative of diamino diphenyl methane
DDS	diamino diphenyl sulfone
DETA	N-Diethyl-m-toluamide
DGEBA	Diglycidyl ether of bisphenol A
DHA	9,10-Dihydroanthracene
DMF	N,N-Dimethylformamide
DMOS	double-diffused metaloxidesemiconductor
DMSO	Dimethylsulfoxid
DOE	Design of Experiments
EA	Ethanolamine
ECN	Epoxy Cresole Novolak
EDX	Energy Dispersive X-Ray Spectroscopy
EPN	Epoxy Phenol Novolak
FA	Failure Analysis
FIB	Focused Ion Beam
FTIR	Fourier Transformation Infrared Spectroscopy
GC	gas chromatography
GUA	N,N,N',N'-Tetramethylguanidine
H <sub>2</sub> O <sub>2</sub>	Hydrogen peroxide
HPA	High Pressure Asher
HPLC	High Performance Liquid Chromatography
HSP	Hansen Solubility Parameter
HTS	High Temperature Storage
HTW	high temperature water
IC	Integrated Circuit
IND	Indoline
JFET	junction gate field-effect transistor

## *Acronyms*

LMW	Low Molecular Weight Resin
LWA	Low Water Absorption Hardener
MAR	Multiaromatic Resin
MAWL	Maximum Allowable Water Loadling
MC	Mould/Moulding Compound
MeOH	Methanol
MFR	Multifunctional Resin
MOE	Methoxyethanol
MS	Mass Spectroscopy
Na <sub>2</sub> CO <sub>3</sub>	Sodium carbonate
NGP	Next Generation Package
NiMoP	nickel molybdenum phosphor
NIST	National Institute of Standards and Technology
NMP	N-Methylpyrrolidone
OCN	Ortho Cresole Novolak
PN	Phenolic Novolak Hardener
PTFE	polytetrafluoroethylene, Teflon
PYR	2-Pyrrolidone
SAM	Scanning Acoustic Microscopy
SCW	Sub- or Supercritical Water
SCWO	Sub- or Supercritical Water Oxidation
SEM	Scanning Electron Microscopy
SFET	see JFET
SiC	silicon carbide
SMD	Surface mounted device
TCE	Trichloroethylene
TET	Tetralin
TGAP	triglycidyl derivative of amino phenol
THF	Tetrahydrofuran
Via	Vertical interconnect access

# List of Symbols

$a$	equation of state specific parameter
$A_0$	equation of state specific parameter
$\alpha$	equation of state specific parameter
$\alpha_i$	polarisability for molecule $i$
$b$	equation of state specific parameter
$B_0$	equation of state specific parameter
$C_0$	equation of state specific parameter
$ced$	cohesive energy density
$\delta$	Hildebrand solubility parameter
$\delta_d$	Hansen solubility parameter for dispersion bonds
$\delta_h$	Hansen solubility parameter for hydrogen bonds
$\delta_p$	Hansen solubility parameter for polar bonds
$\delta_t$	total Hansen solubility parameter
$e$	Euler's constant
$\varepsilon_0$	vacuum permittivity
$F_i$	Group molar contributions
$\gamma$	equation of state specific parameter
${}_l\Delta_g H$	enthalpy of vaporisation
$I_i$	ionisation potential for molecule $i$
$k_B$	Boltzmann constant
$M$	molecular mass
$\mu_i$	permanent dipole moment for molecule $i$
$n$	amount of substance
$\omega$	acentric factor
$p$	pressure
$p_c$	critical pressure
$\pi$	mathematical constant
$\pi_p$	internal pressure
$R$	universal gas constant
$r$	separation distance
$R_1$	radius of the solute sphere of solubility
$R_{12}$	solubility parameter distance
$RED$	relative energy difference
$\rho$	density
$T$	temperature

## *List of Symbols*

$T_c$	critical temperature
$T_R$	reduced temperature
$U$	molar internal energy
$U_{coh}$	cohesive energy
$U_d$	dispersive energy
$U_h$	hydrogen bonding energy
$U_p$	polar energy
${}_l\Delta_g U$	molar energy of vaporisation
$V$	volume
$f_i$	fractional Hansen Solubility Parameter for compound $i$
$V_c$	critical volume
$V_m$	molar volume
$w$	amount of substance

# Bibliography

- [1] Allan F. M. Barton. *CRC handbook of solubility parameters and other cohesion parameters*. CRC Press, 1991.
- [2] <http://webbook.nist.gov/chemistry/>, last visited 05th of june 2010.
- [3] Parr Instrument Company. Pressure vessel catalog.
- [4] Friedrich Beck. *Integrated Circuit Failure Analysis. A Guide to Preparation Techniques*. John Wiley & Sons, 1998.
- [5] A. Aubert, L. Dantas de Moraes, and J.-P. Rebrass. Laser decapsulation of plastic packages for failure analysis: Process control and artefact investigations. *Microelectronics Reliability*, 48:1144–1148, 2008.
- [6] M. Krueger, J. Krinke, K. Ritter, B. Zierle, and M. Weber. Laser-assisted decapsulation of plastic-encapsulated devices. *Microelectronics reliability*, 43:1827–1831, 2003.
- [7] H. Qiu, H.Y. Zheng, X.C. Wang, and G.C. Lim. Laser decapsulation of molding compound from wafer level chip size package for solder reflow. *Materials Science in Semiconductor Processing*, 8:502–510, 2005.
- [8] P. Schwindenhammer, H. Murray, P. Descamps, and P. Poirier. Determination of temperature change inside ic packages during laser ablation of molding compound. *Microelectronics reliability*, 48:1263–1267, 2008.
- [9] T. J. Lett. Laser decapsulation of electronics packages. *SIMTech Technical Report*, 2000.
- [10] P. E. Paranal. Localized die metallization damage induced during laser-marking of a semiconductor package. *International Symposium for Testing and Failure Analysis*, 33, 2007.
- [11] V. Bhide. Decapsulation of silicone-epoxy copolymer packages. *IEEE Proc. International Reliability Physics Symposium*, 20:156–162, 1982.

## Bibliography

- [12] W. Byrne. Three decapsulation methods for epoxy novalac type packages. *IEEE International Reliability Physics Symposium*, 18:107–109, 1980.
- [13] H. Schafft. Failure analysis of wire bonds. *IEEE Reliability Physics Symposium*, 11:98–104, 1973.
- [14] D. Platteter. Basic integrated circuit failure analysis techniques. *Annual Reliability Physics Symposium*, 14:248–255, 1976.
- [15] W. Dang, M. Kubouchi, and S. Yamamoto. Decomposition mechanism of epoxy resin in nitric acid for recycling. *2nd International Symposium on Environmentally Conscious Design and Inverse Manufacturing*, 2:980–985, 2001.
- [16] S. Murali and N. Srikanth. Acid decapsulation of epoxy molded ic packages with copper wire bonds. *IEEE Transactions on electronics packaging manufacturing*, 29(3):179–183, July 2006.
- [17] Q. Li, C. Beenakker, and C. Vath. A novel decapsulation technique for failure analysis of integrated circuits. *IEEE International Conference on Electronics Packaging Technology*, 7:1–5, 2006.
- [18] D. Wilson and J. Beall. Decapsulation of epoxy devices using oxygen plasma. *Reliability Physics Symposium*, 15:82–84, 1977.
- [19] K. Dusek, editor. *Epoxy Resins and Composites II*, volume 75 of *Advances in Polymer Science*. Springer, 1985.
- [20] K. Dusek, editor. *Epoxy Resins and Composites I*, volume 72 of *Advances in Polymer Science*. Springer, 1985.
- [21] K. Dusek, editor. *Epoxy Resins and Composites IV*, volume 80 of *Advances in Polymer Science*. Springer, 1985.
- [22] <http://www.hansen-solubility.com/>, last visited 05th of june 2010.
- [23] F. Gharagheizi, M. Sattari, and M. Angaji. Effect of calculation method on values of hansen solubility parameters of polymers. *Polymer Bulletin*, 57:377–384, 2006.
- [24] D.L. Ho and C.J. Glinka. New insights into hansen’s solubility parameters. *Journal of Polymer Science: Part B: Polymer Physics*, 42:4337–4343, 2004.
- [25] V. Bellenger, E. Morel, and J. Verdu. Solubility parameters of amine-crosslinked aromatic epoxies. *Journal of Applied Polymer Science*, 37:2563–2576, 1989.



## Bibliography

- [26] H. Launay, C. Hansen, and K. Almdal. Hansen solubility parameters for a carbon fiber/epoxy composite. *Carbon*, 45:2859–2865, 2007.
- [27] G. Curran, R. Struck, and E. Gorin. Mechanism of the hydrogen-transfer process to coal and coal extract. *I&EC Process design and development*, 6(2):166–173, 1967.
- [28] Y. Sato, Y. Kodera, and T. Kamo. Effect of solvents on the liquid-phase cracking of thermosetting resins. *Energy & Fuels*, 13:364–368, 1999.
- [29] Arnd-Peter Rudolf. *Hydrierende Spaltung von vernetzten Polymeren*. PhD thesis, Technische Universitt Darmstadt, 2000.
- [30] D. Braun, W. von Gentzkow, and A.P. Rudolf. Hydrogenolytic degradation of thermosets. *Polymer Degradation and Stability*, 74:25–32, 2001.
- [31] R. Pinero-Hernanz, C. Dodds, J. Hyde, J. Garca-Serna, M. Poliakoff, E. Lester, M. Cocero, S. Kingman, S. Pickering, and K. Hoong Wong. Chemical recycling of carbon fibre reinforced composites in nearcritical and supercritical water. *Composites: Part A*, 39:454–461, 2008.
- [32] H. Tagaya, Y. Shibsaki, C. Kato, J.-I. Kadowaka, and B. Hatano. Decomposition reactions of epoxy resin and polyetheretherketone resin in sub- and supercritical water. *Journal of Material Cycles and Waste Management*, 6(1):1–5, 2004.
- [33] Y. Suzuki, H. Tagaya, T. Asou, J. Kadokawa, and K. Chiba. Decomposition of prepolymers and molding materials of phenol resin in subcritical and supercritical water under an ar atmosphere. *Industrial & Enigineering Chemistry Research*, 38:1391–1395, 1999.
- [34] Y. Shibasaki, T. Kamimori, J. Kadokawa, B. Hatano, and H. Tagaya. Decomposition reactions of plastic model compounds in sub- and supercritical water. *Polymer Degradation and Stability*, 83:481–485, 2004.
- [35] Y.-C. Chien, H. P. Wang, K.-S. Lin, and Y. W. Yang. Oxidation of printed circuit board wastes in supercritical water. *Water Research*, 34(17):4279–4283, 2000.
- [36] N. Akiya and P.E. Savage. Roles of water for chemical reactions in high-temperature water. *Chemical Reviews*, 102:2725–2750, 2002.
- [37] R. W. Shaw, B. Thomas, A. C. Anthony, and A. E. Charles E. U. Franck.

- Supercritical water - a medium for chemistry. *Chemical Engineering News*, 1991.
- [38] X. Wang, L. U. Gron, and M. T. Klein. The influence of high-temperature water on the reaction pathways of nitroanilines. *The Journal of Supercritical Fluids*, 8:236–249, 1995.
  - [39] A. J. Belsky, P. G. Maiella, and T.B. Brill. Spectroscopy of hydrothermal reactions 13. kinetics and mechanisms of decarboxylation of acetic acid derivatives at 100-260c under 275 bar. *Journal of Physical Chemistry A*, 103:4253–4260, 1999.
  - [40] J.-I. Ozaki, S. K. Ingwang Djaja, and Asao Oya. Chemical recycling of phenol resin by supercritical methanol. *Industrial and Engineering Chemistry Research*, 39:245–249, 2000.
  - [41] M. Genta, T. Iwaya, M. Sasaki, M. Goto, and T. Hirose. Depolymerization mechanism of poly(ethylene terephthalate) in supercritical methanol. *Industrial & Engineering Chemistry Research*, 44:3894–3900, 2005.
  - [42] G. Jiang, S.J. Pickering, E.H. Lester, T.A. Turner, K.H. Wong, and N.A. Warrior. Characterisation of carbon fibres recycled from carbon fibre/epoxy resin composites using supercritical n-propanol. *Composites Science and Technology*, 69:192–198, 2009.
  - [43] B. Z. Wan, C. Y. Kao, and W. H. Cheng. Kinetics of depolymerization of poly(ethylene terephthalate) in a potassium hydroxide solution. *Industrial & Engineering Chemistry Research*, 40:509–514, 2001.
  - [44] H. Tagaya, N. Komuro, Y. Suzuki, M. Karasu, and J. Kadokawa. The decomposition reaction of plastics and model compound of them in sub- and supercritical water. *Proc Int Symp Feedstock Recycl Plast*, 1:83–86, 1999.
  - [45] L.A. Torry, R. Kaminsky, M.T. Klein, and M.R. Klotz. The effect of salts on hydrolysis in supercritical and near-critical water: Reactivity and availability. *Journal of Supercritical Fluids*, 5:163–168, 1992.
  - [46] G.L. Huppert, B.C. Wu, S.H. Townsend, M.T. Klein, and S.C. Paspek. Hydrolysis in supercritical water: Identification and implications of a polar transition state. *Industrial & Engineering Chemistry Research*, 28:161–165, 1989.
  - [47] P. E. Savage, J. Yu, N. Stylski, and E. E. Brock. Kinetics and mechanism of methane oxidation in supercritical water. *Journal of Supercritical Fluids*, 12:141–153, 1998.

## Bibliography

- [48] F.-R. Xiu and F.-S. Zhang. Recovery of copper and lead from waste printed circuit boards by supercritical water oxidation combined with elektrokinetic process. *Journal of Hazardous Materials*, 165:1002–1007, 2009.
- [49] H. Tagaya, C Katoh, K. Katoh, and J. Kadokawa. The reaction of model compounds of plastics in sub- and supercritical d2o. *Proc Int Symp Feedstock Recycl Plast*, 1:281–284, 1999.
- [50] T.M. Hayward, I.M. Svishchev, and R.C. Makhija. Stainless steel flow reactor for supercritical water oxidation: corrosion tests. *Journal of Supercritical Fluids*, 27:275–281, 2003.
- [51] P. Kritzer. Corrosion in high-temperature and supercritical water and aqueous solutions. a review. *Journal of Supercritical Fluids*, 29:1–29, 2004.
- [52] M. Sun, X. Wu, Z. Zhang, and E.-H. Han. Oxidation of 316 stainless steel in supercritical water. *Corrosion Science*, 51:1069–1072, 2009.
- [53] F. Pardal and G. Tersac. Comparative reactivity of glycols in pet glycolysis. *Polymer Degradation and Stability*, 91:2567–2578, 2006.
- [54] F. Pardal and G. Tersac. Kinetics of poly(ethylene terephthalate) glycolysis by diethylene glycol. i. evolution of liquid and solid phases. *Polymer Degradation and Stability*, 91:2840–2847, 2006.
- [55] Francis Pardal and Gilles Tersac. Kinetics of poly(ethylene terephthalate) glycolysis by diethylene glycol. part ii: Effect of temperature, catalyst and polymer morphology. *Polymer Degradation and Stability*, 92:611–616, 2007.
- [56] K. El Gersifi, N. Destais-Orvoen, G. Durand, and G. Tersac. Glycolysis of epoxide-amine hardened networks. i. diglycidylether/aliphatic amines model networks. *Polymer*, 44:3795–3801, 2003.
- [57] K. El Gersifi, G. Durand, and G. Tersac. Solvolysis of bisphenol a diglycidyl ether/anhydride model networks. *Polymer Degradation and Stability*, 91:690–702, 2006.
- [58] N. Destais-Orvoen, G. Durand, and G. Tersac. Glycolysis of epoxide-amine hardened networks ii - aminoether model compound. *Polymer*, 45:5473–5482, 2004.
- [59] G. Soave. Improvement of the van der waals equation of state. *Chemical Engineering Science*, 39:357–369, 1984.

- [60] K.K. Shah and G. Thodos. A comparison of equations of state. *Industrial & Engineering Chemistry*, 57(3):30–37, 1965.
- [61] G. Soave. Equilibrium constants from a modified redlich-kwong equation of state. *Chemical Engineering Science*, 27:1197–1203, 1972.
- [62] D.-Y. Peng and D.B. Robinson. A new two-constant equation of state. *Industrial & Engineering Chemistry*, 15(1):59–64, 1976.
- [63] D.G. McFee, K.H. Mueller, and J. Lielmezs. Comparison of benedict-webb-rubin, starling and lee-kesler equations of state for use in p-v-t calculations. *Thermochimica Acta*, 54:9–25, 1982.
- [64] R. Span, E. W. Lemmon, R. T. Jacobsen, W. Wagner, and A. Yokozeki. A reference equation of state for the thermodynamic properties of nitrogen for temperatures from 63.151 to 1000 k and pressures to 2200 mpa. *Journal of Physical and Chemical Reference Data*, 29:1361–1433, 2000.
- [65] P. Nowak, R. Kleinrahm, and W. Wagner. Measurement and correlation of the (p,  $\rho$ , t) relation of nitrogen. i. the homogeneous gas and liquid regions in the temperature range from 66 k to 340 k at pressures up to 12 mpa. *Journal of Chemical Thermodynamics*, 29:1137–1156, 1997.
- [66] P. Nowak, R. Kleinrahm, and W. Wagner. Measurement and correlation of the (p,  $\rho$ , t) relation of nitrogen. ii. saturated-liquid and saturated-vapour densities and vapour pressures along the entire coexistence curve. *Journal of Chemical Thermodynamics*, 29:1157–1174, 1997.
- [67] C. L. Yaws and P. K. Narasimhan. *Thermophysical Properties of Chemicals and Hydrocarbons*. Elsevier Inc., 2009.
- [68] C. Nail. Applications for parallel grinding as an alternative to chemical decapsulation in preparing packaged samples for failure analysis. *International Symposium for Testing and Failure Analysis*, 33, 2007.
- [69] [http://www.infineon.com/cms/packages/leaded\\_and\\_through-hole/p-pg-to220/p-pg-to220-3-01.html](http://www.infineon.com/cms/packages/leaded_and_through-hole/p-pg-to220/p-pg-to220-3-01.html), last visited 05th of june 2010.
- [70] C. Özdemir and A. Güner. Solubility profiles of poly(ethylene glycol)/solvent systems, i: Qualitative comparison of solubility parameter approaches. *European Polymer Journal*, 43:3068–3093, 2007.
- [71] Y. Bai, Z. Wang, and L. Feng. Chemical recycling of carbon fibres reinforced

- epoxy resin composites in oxygen in supercritical water. *Materials and Design*, 31:999–1002, 2010.
- [72] Allan Barton. *CRC handbook of polymer-liquid interaction parameters and solubility parameters*. CRC Press, 1990. 0849335442, 9780849335440.
- [73] Allan Barton. Applications of solubility parameters and other cohesion parameters in polymer science and technology. *Pure & Appl. Chem.*, 57(7):905–912, 1985.
- [74] Allan Barton. *Handbook of Solubility Parameters*. CRC Press, 1983.
- [75] Friedrich Beck. *Integrierte Halbleiterschaltungen. Konstruktionsmerkmale, Fehlererscheinungen, Ausfallmechanismen*. VCH, 1993.
- [76] Friedrich Beck. *Präparationstechniken fr die Fehleranalyse an integrierten Halbleiterschaltungen*. VCH, 1988.
- [77] K. Camman. *Instrumentelle analytische Chemie: Verfahren, Anwendungen und Qualitätssicherung*. Spektrum Akademischer Verlag, 2001.
- [78] S. Canumalla and L. W. Kessler. Towards a nondestructive procedure for characterization of molding compounds. *IEEE International Reliability Physics Symposium. Annual Proceedings.*, 35:149–155, 1997.
- [79] R. W. Crain and R. E. Sonntag. Nitrogen constants for the benedict-webb-rubin equation of state. *Journal of Chemical and Engineering Data*, 12(1):73–75, 1967.
- [80] W. Dang, M. Kubouchi, H. Sembokuya, and K. Tsuda. Chemical recycling of glass fiber reinforced epoxy resin cured with amine using nitric acid. *Polymer*, 46:1905–1912, 2005.
- [81] H. Domininghaus, P. Elsner, P. Eyerer, and T. Hirth. *Kunststoffe. Eigenschaften und Anwendungen*. Springer, 2008.
- [82] M. Garcia, I. Gracia, G. Duque, A. de Lucas, and J. Rodriguez. Study of the solubility and stability of polystyrene wastes in a dissolution recycling process. *Waste Management*, 29:1814–1818, 2009.
- [83] J. Guo, J. Guo, and Z. Xu. Recycling of non-metallic fractions from waste printed circuit boards: A review. *Journal of Hazardous Materials*, 168:567–590, 2009.

## Bibliography

- [84] R.T. Jacobsen, R.B. Stewart, and M. Jahangiri. Thermodynamic properties of nitrogen from the freezing line to 2000 K at pressures to 1000 MPa. *J. Phys. Chem. Ref. Data*, 15(2):735–909, 1986.
- [85] Mike Jacques. The chemistry of failure analysis. *Annual Reliability Physics Symposium, 1979*, 17:197–208, 1979.
- [86] R. Mezzenga, L. Boogh, and J.-A. Manson. Evaluation of solubility parameters during polymerisation of amine-cured epoxy resins. *Journal of Polymer Science: Part B: Polymer Physics*, 38:1883–1892, 2000.
- [87] C. Panayiotou. Solubility parameter revisited: an equation-of-state approach for its estimation. *Fluid Phase Equilibria*, 131:21–35, 1997.
- [88] Thomas, Baer, Westby, Mattson, and Haring. A unique application of decapsulation combining laser and plasma. *2009 Electronic Components and Technology Conference*, 59:2011–2015, 2009.
- [89] H.Y. Ueng and C.Y. Liu. The aluminum bond-pad corrosion in small outline packaged devices. *Materials Chemistry and Physics*, 48:27–35, 1997.
- [90] Infineon Technologies AG, editor. *Semiconductors*. Publicis Corporate Publishing, 2004.
- [91] K. Dusek, editor. *Epoxy Resins and Composites III*, volume 78 of *Advances in Polymer Science*. Springer, 1985.